EXAMINATION OF CURING CRITERIA FOR COLD IN-PLACE RECYCLING

(Phase 3: Calibration of Moisture Loss Indices and Development of Stiffness Gain Model)

Final Report
December 2011

Sponsored by
Iowa Highway Research Board
TR-609

Conducted by
Hosin "David" Lee
Adam Woods
Yongjoo "Thomas" Kim

Public Policy Center
University of Iowa

Disclaimer Notice

The contents of this report reflect the views of the authors, who are responsible for the facts and the accuracy of the information presented herein. The opinions, findings, and conclusions expressed in this publication are those of the authors and not necessarily those of the sponsors. The sponsors assume no liability for the contents or use of the information contained in this document. This report does not constitute a standard, specification, or regulation. The sponsors do not endorse products or manufacturers. Trademarks or manufacturers' names appear in this report only because they are considered essential to the objectives of the document.

Non-discrimination Statement

Federal and state laws prohibit employment and/or public accommodation discrimination on the basis of age, color, creed, disability, gender identity, national origin, pregnancy, race, religion, sex, sexual orientation or veteran’s status. If you believe you have been discriminated against, please contact the Iowa Civil Rights Commission at 800-457-4416 or Iowa Department of Transportation's affirmative action officer. If you need accommodations because of a disability to access the Iowa Department of Transportation’s services, contact the agency's affirmative action officer at 800-262-0003.

1. REPORT NO.	2. GOVERNMENT ACCESSION NO.	3. RECIPIENT'S CATALOG NO.
IHRB Report TR-609		

4. TITLE AND SUBTITLE	5. REPORT DATE
Examination of Curing Criteria for Cold In-Place Recycling (Phase 3: Calibration of Moisture Loss Indices and Development of Stiffness Gain Model)	December 2011
	6. PERFORMING ORGANIZATION CODE

7. AUTHOR(S)	8. PERFORMING ORGANIZATION REPORT NO.
Hosin “David” Lee , Adam Woods and Yongjoo “Thomas” Kim	

9. PERFORMING ORGANIZATION NAME AND ADDRESS	10. WORK UNIT NO.
Public Policy Center University of Iowa 227 South Quadrangle Iowa City, IA 52242-1192	11. CONTRACT OR GRANT NO

12. SPONSORING AGENCY NAME AND ADDRESS	13. TYPE OF REPORT AND PERIOD COVERED
Iowa Highway Research Board Iowa Department of Transportation 800 Lincoln Way, Ames, IA 50010	Final Report
	14. SPONSORING AGENCY CODE

15. SUPPLEMENTARY NOTES

16. ABSTRACT

In the previous study, moisture loss indices were developed based on the field measurements from one CIR-foam and one CIR-emulsion construction sites. To calibrate these moisture loss indices, additional CIR construction sites were monitored using embedded moisture and temperature sensors. In addition, to determine the optimum timing of an HMA overlay on the CIR layer, the potential of using the stiffness of CIR layer measured by geo-gauge instead of the moisture measurement by a nuclear gauge was explored.

Based on the monitoring the moisture and stiffness from seven CIR project sites, the following conclusions are derived:

1. In some cases, the in-situ stiffness remained constant and, in other cases, despite some rainfalls, stiffness of the CIR layers steadily increased during the curing time.
2. The stiffness measured by geo-gauge was affected by a significant amount of rainfall.
3. The moisture indices developed for CIR sites can be used for predicting moisture level in a typical CIR project. The initial moisture content and temperature were the most significant factors in predicting the future moisture content in the CIR layer.
4. The stiffness of a CIR layer is an extremely useful tool for contractors to use for timing their HMA overlay.

To determine the optimal timing of an HMA overlay, it is recommended that the moisture loss index should be used in conjunction with the stiffness of the CIR layer.

17. KEY WORDS	18. DISTRIBUTION STATEMENT
cold in-place recycling, curing criteria, moisture content, curing time, moisture loss index, geo-gauge	No restrictions.

19. SECURITY CLASSIF. (of this report)	20. SECURITY CLASSIF. (of this page)	21. NO. OF PAGES	22. PRICE
None	None	140	N/A

Examination of Curing Criteria for Cold In-Place Recycling
(Phase 2: Measuring Temperature, Moisture, Deflection and Distress from CIR Test Section)

Final Report

December 2011

Principal Investigator

Hosin "David" Lee, Ph. D., P. E.

Professor

Public Policy Center, Department of Civil and Environmental Engineering,

University of Iowa

Researchers

Adam Woods

Graduate Research Assistant

Public Policy Center, Department of Civil and Environmental Engineering,

University of Iowa

Yongjoo "Thomas" Kim, Ph. D.

Postdoctoral Research Scholar

Public Policy Center, Department of Civil and Environmental Engineering,

University of Iowa

Sponsored by

Iowa Highway Research Board

Public Policy Center
University of Iowa
207 South Quadrangle
Iowa City, IA 52242-1192
http://ppc.uiowa.edu

Technical Advisory Committee

Bob Nady, Consultant, rmnady@midiowa.net
Bill Kahl, W.K. Construction, wkc@chorus.net
Bill Rosener, APAI, billr@apai.net
Greg Parker, Johnson County, gparker@co.johnson.ia.us
John Hinrichsen, Iowa DOT, John.Hinrichsen@dot.iowa.gov
Larry Mattusch, APAI, lmatt2@mchsi.com
Mark Haines, Koss Construction, mah@kossconstruction.com
Mike Heitzman, NCAT, mah0016@auburn.edu
Scott Schram, Iowa DOT, Scott.Schram@dot.iowa.gov
Steve Buckner, Flint Hills Resources, Steve.Buckner@fhr.com

Table of Contents

LIST OF TABLES

LIST OF FIGURES

1. INTRODUCTION

The current practice in Iowa simply controls the maximum moisture content in the cold in-place recycling (CIR) of 2.0 percent, whereas many CIR projects, struggling with unfavorable climate, have been overlaid successfully with higher amounts of moisture. The prior research was conducted to explore technically sound and more effective ways to identify minimum in-place CIR properties necessary to permit placement of the HMA overlay.

Moisture loss indices were developed based on the field measurements from one CIR-foam and one CIR-emulsion construction sites. To calibrate the moisture loss indices, six CIR construction sites that include two CIR-foam sites, two CIR-emulsion (CSS-1) sites and two CIR-emulsion (HFMS-2s) sites, were proposed to be monitored using embedded moisture and temperature sensors. However, due to the lack of available CIR-emulsion sites nearby, one CIR-HFMS-2S emulsion site and six CIR-foam sites were monitored.

The potential of using the stiffness measured by geo-gauge to supplement (or possibly replace) the moisture measurement by a nuclear gauge was explored in this study. A correlation between stiffness and moisture content was developed.

1.1 Objectives

The main objectives of the study are to: 1) measure the moisture contents and temperature throughout a CIR layer from six CIR project sites, 2) calibrate the developed moisture loss indies using the field measurement from six CIR project sites, and 3) develop stiffness/density gain model to supplement (or possibly replace) the moisture criteria.

1.2 Benefits of the Study

During the previous study, both moisture and temperature conditions were measured in the field by embedding the sensors in the CIR layer. Based upon the field measurements, moisture loss indices were developed as a function of initial moisture condition and cumulative pavement temperature per hour. However, it is necessary to calibrate the moisture loss indices so that they can be applied to various CIR construction projects in

Iowa. The results of the research are presented as more accurate and rational moisture loss indices for various types of CIR construction. The moisture loss index will be a truly useful tool for all pavement engineers, which can help them accurately determine an optimum timing of an overlay without continually measuring moisture conditions in the field using a nuclear gauge. The moisture loss indices will rationalize the way the quality of CIR layer is inspected for the optimum timing of an HMA overlay and significantly enhance the long-term performance of CIR pavements. In addition, the stiffness of CIR layer measured by the Geo-gage can be used to supplement (or possibly replace) the moisture measurement during a curing period.

2. SUMMARY FROM THE PREVIOUS STUDY

During phase 1 study, to represent the curing process of CIR layer in the field construction, three different laboratory curing procedures were examined: 1) uncovered, 2) semi-covered and 3) covered specimens. Indirect tensile strengths and moisture contents of the CIR specimens cured for various curing periods were measured. To predict the field performance of CIR pavements during the curing process, dynamic modulus and dynamic creep tests were conducted using Simple Performance Testing (SPT) equipment.

Upon completion of phase 1 study, the following conclusions were derived:

- The indirect tensile strength of CIR specimens in all three curing conditions did not increase during the early stage of curing but increased during a later stage of curing, usually when the moisture content fell below 1.5%.
- Dynamic modulus and flow number increased as a curing time increased and a moisture content decreased.
- Given the same curing time, CIR-foam specimens exhibited the higher tensile strength, dynamic modulus and flow number than CIR-emulsion. This might have been caused by the higher moisture content in the CIR-emulsion specimens than the CIR-foam for the equivalent curing time.
- The curing method, temperature and duration had a significant impact on indirect tensile strength, dynamic modulus, and flow number of the CIR mixtures.

During phase 2 study, to develop a set of moisture loss indices, the moisture contents and temperatures of one CIR-foam and one CIR-emulsion layers were monitored for five months. The moisture contents were measured by embedded capacitance moisture sensors at a midpoint and a bottom of the CIR layer and they were compared against the moisture content measured by a nuclear gauge. The modulus and stiffness were measured using a falling weight deflectometer (FWD) and a geo-gauge during the curing time. Moisture loss indices were developed based on the initial moisture content and temperature of CIR-foam and CIR-emulsion layers.

Upon completion of phase 2 study, the following conclusions were derived:

- The moisture condition of a CIR layer can be monitored accurately using a capacitance moisture sensor.
- The moisture loss index for a CIR layer is a viable tool in determining the optimum timing for an overlay.
- The modulus of a CIR layer back-calculated from deflection measured by FWD seemed to be in a good agreement with the stiffness measured by geo-gauge.
- The stiffness of a CIR layer increased as curing time increased. The layer stiffness seemed to be affected by the pavement temperature.
- The geo-gauge should be considered for measuring the stiffness of a CIR layer that can be used to determine the optimum timing of an overlay.

3. MOISTURE LOSS INDEX DEVELOPED BY PREVIOUS STUDY

To develop moisture loss index for CIR layer, as shown in Figure 3-1, the field moisture contents and temperature were measured from CIR-emulsion and CIR-foam layers in 2008 (Kim et al. 2011).

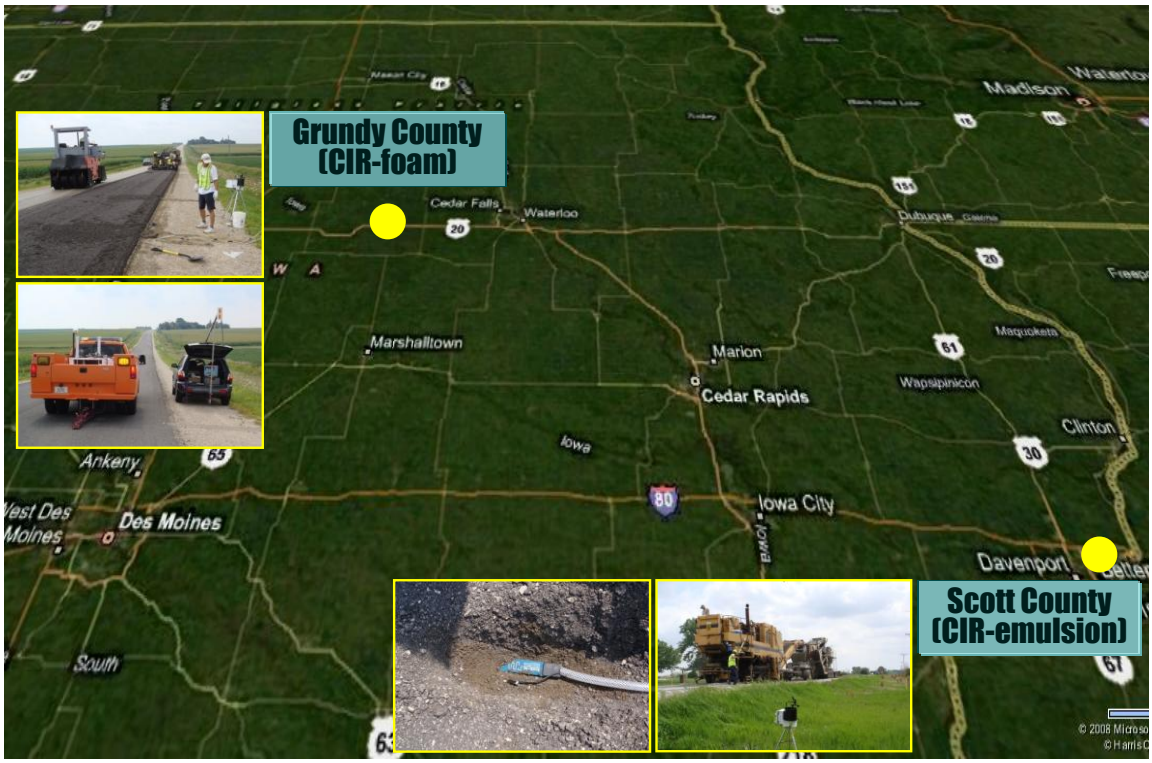

Figure 3-1. Locations of CIR-foam and CIR-emulsion project sites in Iowa

3.1 Moisture Content and Temperature of CIR-CSS-1-emulsion Layer

To measure the field moisture contents and temperature of CIR-emulsion layer, CIR with CSS-1 emulsified asphalt (CIR-CSS-1-emulsion) project site in Scott County was selected. The 2.5-mile section of County Road Y-40 was rehabilitated from Iowa Highway 22 in the town of Buffalo to Mayne Street in the town of Blue Grass, Iowa between June 5th and June 6th, 2008. The existing 10-cm thick Type B HMA layer on top of the concrete pavement was milled and mixed with CSS-1 emulsified asphalt to produce 4-inch thick CIR-CSS-1-emulsion layer. The 2-inch thick HMA intermediate course was overlaid on June 26th, 2008 followed by the 1.5-inch thick HMA wearing

course overlaid on July 3rd, 2008.

To monitor actual moisture contents and temperatures of the CIR-CSS-1-emulsion layer in the field, three ECH2O moisture sensors and two temperature sensors were installed at 3.5 inches from surface. A weather station was also installed to collect air temperature, humidity, and rainfall.

Figure 3-2 shows plots of moisture contents measured by three sensors along with dates and amounts of the fourteen rainfalls (with a total of 6.38 inches) measured during the curing period of 19 days. The moisture contents at the bottom of CIR-CSS-1-emulsion layer before the intermediate HMA overlay were measured as 9.4% from sensor A, 11.1% from sensor B, and 9.4% from sensor C. Despite the actual moisture content of CIR-CSS-1-emulsion layer being above 2.0%, the intermediate HMA overlay was constructed after 19 days of curing.

Figure 3-3 shows plots of temperatures measured by two sensors embedded in the CIR-CSS-1-emulsion layer against air temperatures from the weather station. This air-to-pavement temperature relationship was used to estimate the temperature of CIR-emulsion layer based on the air temperature.

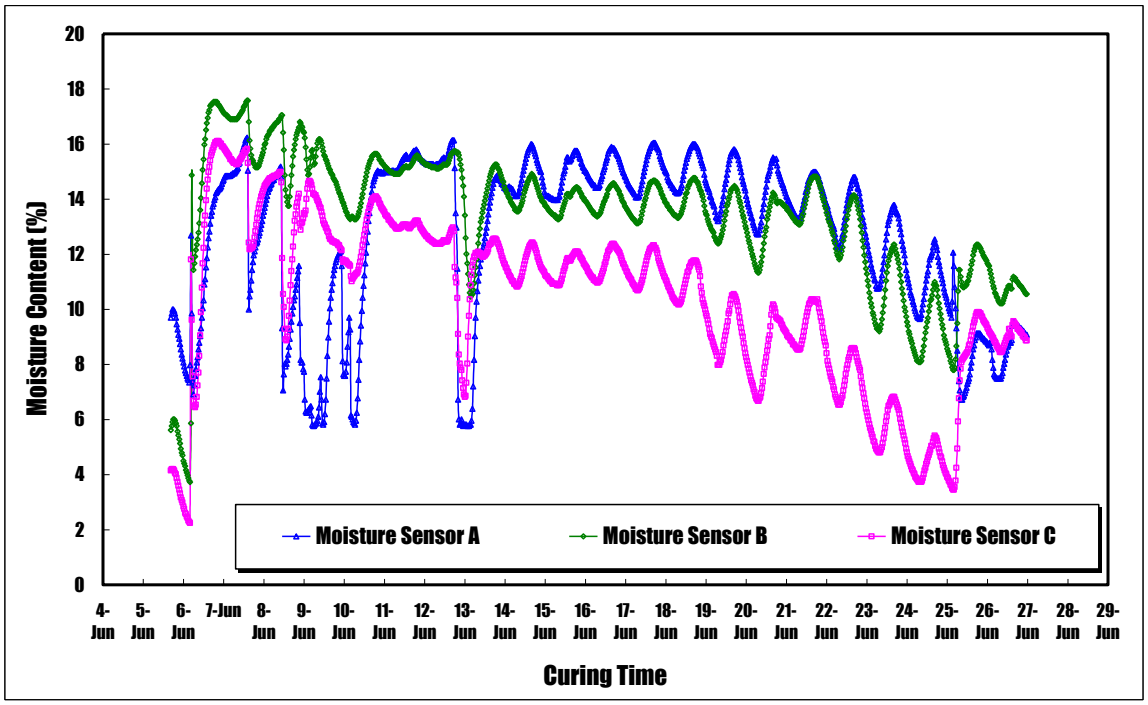

Figure 3-2. Plots of moisture contents against the curing time from three moisture sensors embedded in the CIR-CSS-1-emulsion layer

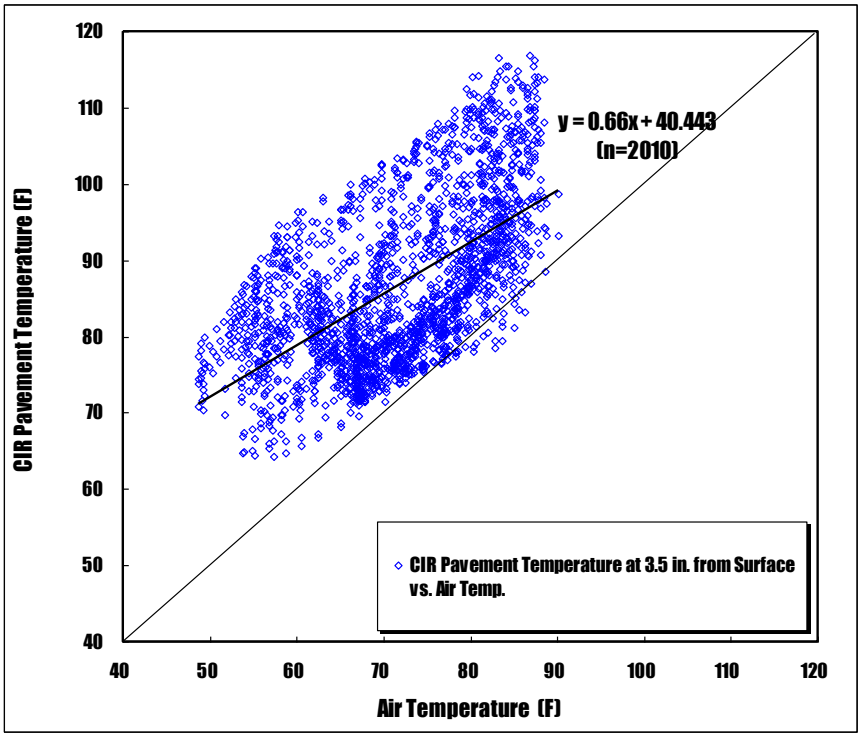

Figure 3-3. Plots of temperature from two sensors embedded in the CIR-CSS-1-emulsion layer against air temperature from weather

3.2 Moisture Content and Temperature of CIR-foam Layer

To measure the field moisture contents and temperature of CIR-foam layer, CIR with foamed asphalt (CIR-foam) project site in Grundy County was selected. The 6.5-mile section of County Road T 55 was rehabilitated from I-175 north to County Road D 25 starting on July 31, 2008. The top 3.5-inch of the existing 9-inch thick Type B HMA layer was milled and mixed with foamed asphalt to produce 3.5-inch thick CIR-foam layer. Upon completion of tack coating process on top of CIR-foam layer, the 1.5-inch thick HMA intermediate course was overlaid on August 22nd, 2008 followed by the 1.5-inch thick HMA wearing course overlaid on September 1st, 2008.

To monitor actual moisture contents and temperatures of the CIR-foam layer in the field, two ECH2O moisture sensors and one temperature sensor were installed at 3.5 inches from surface and one ECH2O moisture sensor and one temperature sensor were installed at 2 inches from surface. A weather station was also installed to collect air temperature, humidity, and rainfall.
Figure 3-4 shows plots of moisture contents measured by three sensors along with dates and amounts of the eleven rainfalls (with a total of 1.54 inches) measured during the curing period of 22 days. The moisture contents in the middle of the CIR-foam layer before the intermediate HMA overlay were measured as 12.1% from sensor A', 7.2% from sensor A at the bottom, and 14.5% from sensor B at the bottom. Despite the actual moisture contents of CIR-foam layer remaining above 2.0%, the intermediate HMA overlay was constructed after 22 days of curing.

Figure 3-5 shows plots of temperatures from two sensors embedded in the CIR-foam layer against air temperature from the weather station. This air-to-pavement temperature relationship was used to estimate the temperature of CIR-foam layer based on the air temperature.

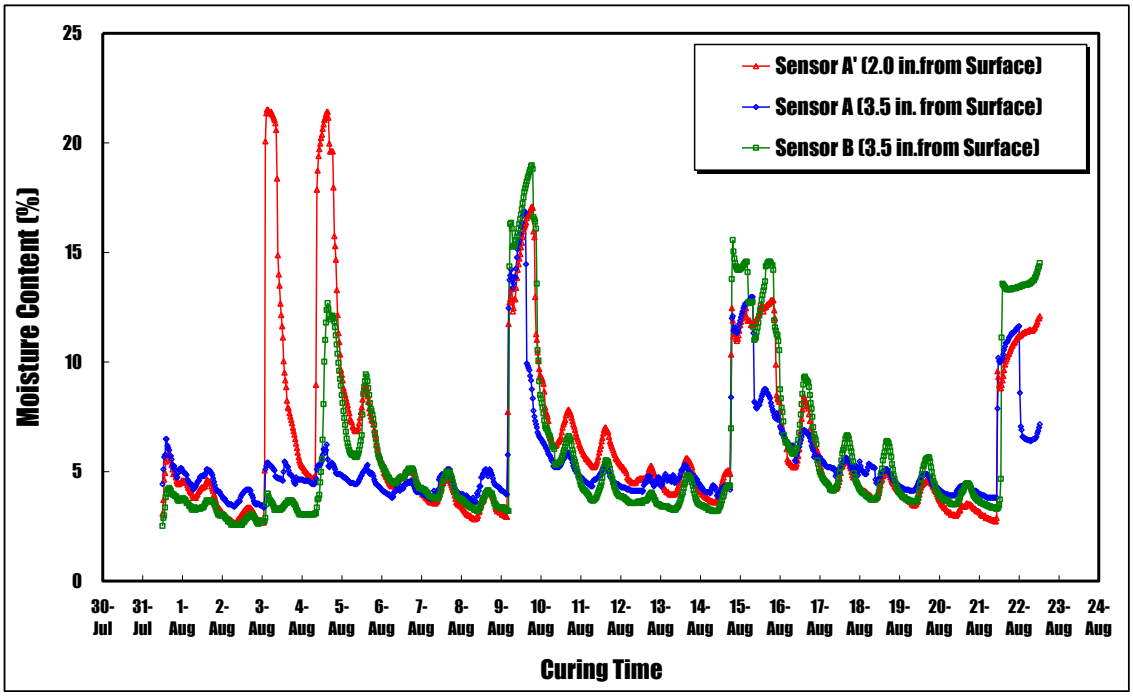

Figure 3-4. Plots of moisture contents against the curing time from three sensors embedded in the CIR-foam layer

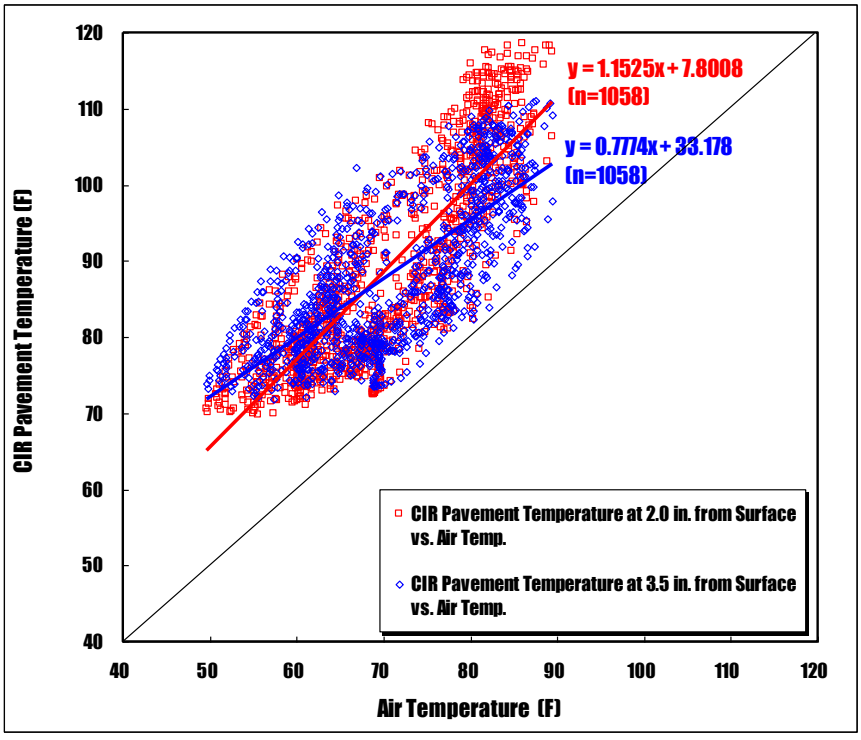

Figure 3-5. Plots of temperature from two sensors embedded in the CIR-foam layer against air temperature from weather

3.2 Moisture Content and Temperature of CIR-foam Layer

In order to develop a better analysis tool to monitor the CIR layer in preparation for a timely placement of the wearing surface, a moisture loss index concept was introduced. The main objective of the moisture loss index is to determine an optimal timing of an overlay based on the initial moisture and climate conditions without continually measuring moisture contents using a nuclear gauge. To develop moisture loss indices for CIR layer, the actual moisture content of CIR layer was measured by ECH2O moisture sensors and climate data were collected from the weather stations installed at CIR project sites.

To predict the moisture change in the CIR layer over time, using a multiple linear regression technique, the following moisture loss index formula was developed as a function of initial moisture condition, average CIR layer temperature, and average humidity.

$$\Delta MC/hr = a1 + a2\ IMC + a3\ Temp + a4\ Hum$$

Where, $\Delta MC/hr$ = Moisture change per hour during curing time
IMC = Initial moisture content of CIR layer right after construction
Temp = Average CIR layer temperature (°C) during curing time
Hum = Average humidity (%) during curing time
a1, a2, a3, a4 = multiple linear regression coefficients

3.3.1 Moisture Loss Index for CIR-CSS-1-emulsion Layer

Moisture contents and climatic data were collected from the CIR-CSS-1-emulsion layer in Scott County. A new set of moisture content data was created when the rainfall had occurred. After discarding the initial moisture contents above 12% (unusually high due to 200-year flood), three moisture content data sets from sensor A, six sets from sensor B, and fourteen sets from sensor C were obtained.

Figure 3-6 shows plots of moisture content change per hour against three independent variables. As can be seen from Figure 3-6, a positive correlation of moisture content change per hour against initial moisture content and CIR-CSS-1-emulsion layer

temperature indicates that the rate of moisture change in CIR layer increases as the initial moisture content and average CIR layer temperature increase. A negative correlation of moisture content change per hour against the average humidity indicates that the rate of moisture change in CIR layer decreases as the average humidity increases.

As shown in the regression equation below, Δmoisture content per hour in CIR-CSS-1-emulsion layer can be predicted as a function of the initial moisture content and the average CIR pavement temperature and the average humidity.

$$\Delta MC/hr = 0.123 + 0.015\ IMC + 0.005\ Temp - 0.002\ Hum$$

(R-square = 71.6%)

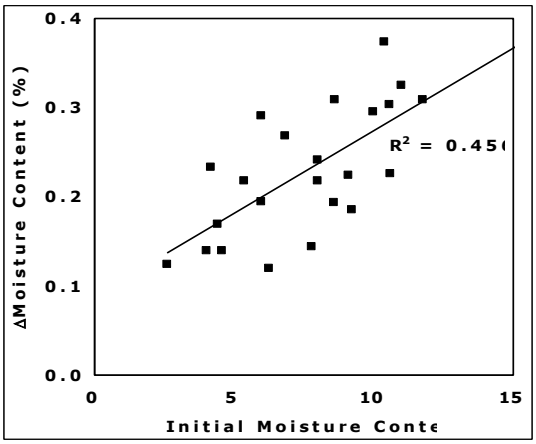

(a) ΔMC/h vs. IMC

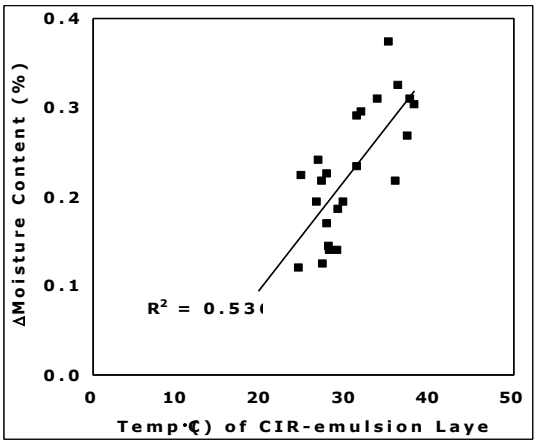

(b) ΔMC/hour vs. Temperature

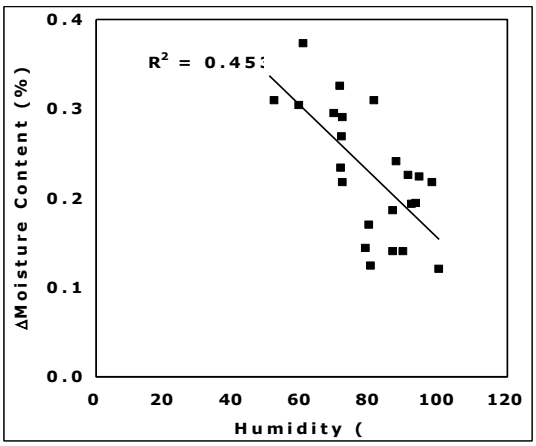

(c) ΔMC/h vs. Humidity

Figure 3-6. Plots of moisture change per hour against each of three independent variables at 3.5 inches of surface from for CIR-CSS-1-emulsion layer

3.3.2 Moisture Loss Index for CIR-foam Layer

Moisture contents and climatic data were collected from the CIR-foam layer in Grundy

County. After discarding the initial moisture contents above 12% (unusually high due to 200-year flood), thirty moisture content data sets from sensor A', twenty-three sets from sensor A, and sixteen sets from sensor B were obtained.

Figure 3-7 and Figure 3-8 show plots of moisture content change per hour against three independent variables for sensor A' at 2.0 inches from surface of CIR-foam layer and for sensor A and B at 3.5 inches from surface of CIR-foam layer, respectively. As can be seen from Figure 3-7 and Figure 3-8, a positive correlation of moisture content change per hour against initial moisture content and CIR-foam layer temperature indicates that the rate of moisture change in CIR layer increases as the initial moisture content and average CIR layer temperature increase. A negative correlation of moisture content change per hour against the average humidity indicates that the rate of moisture change in CIR layer decreases as the average humidity increases.

As shown in the regression equation below, Δmoisture content per hour in CIR-foam layer can be predicted as a function of the initial moisture content and the average CIR pavement temperature and the average humidity.

$$\text{A' (2.0 inches): } \Delta MC/hr = -0.005 + 0.033\ IMC + 0.003\ Temp - 0.001\ Hum$$
$$(\text{R-square} = 82.8\%)$$

$$\text{A\&B (3.5 inches): } \Delta MC/hr = -0.012 + 0.042\ IMC - 0.003\ Temp - 0.002\ Hum$$
$$(\text{R-square} = 62.7\%)$$

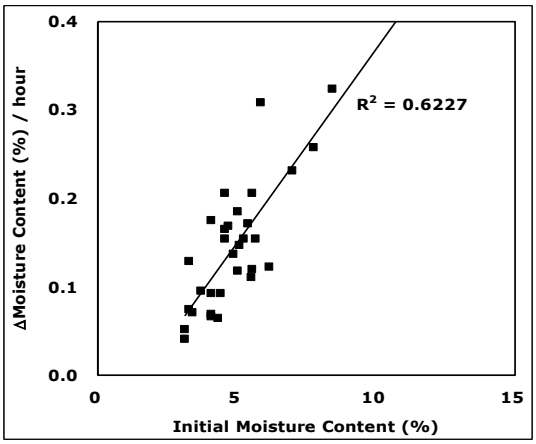

(a) ΔMC/h vs. IMC

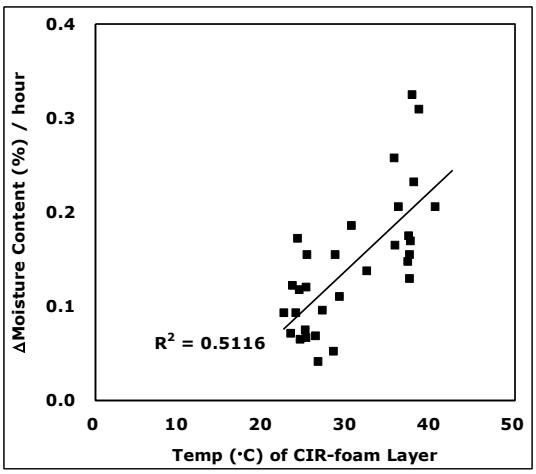

(b) ΔMC/h vs. Temperature

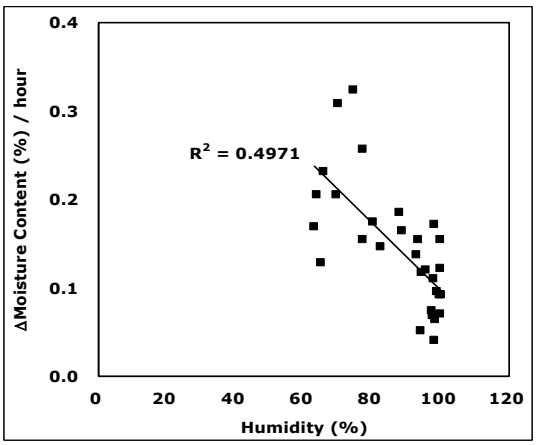

(c) ΔMC/h vs. Humidity

Figure 3-7. Plots of moisture change per hour against each of three independent variables at 2.0 inches of surface from CIR-foam layer

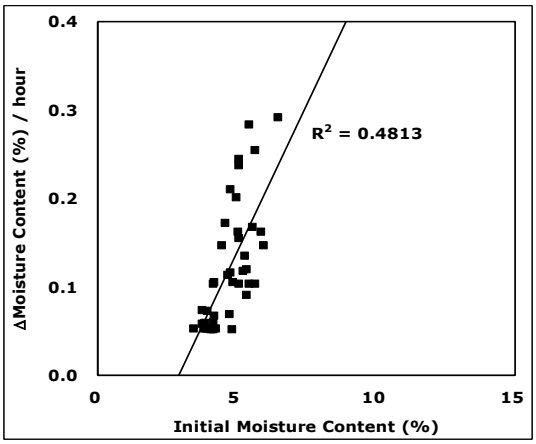

(a) ΔMC/h vs. IMC

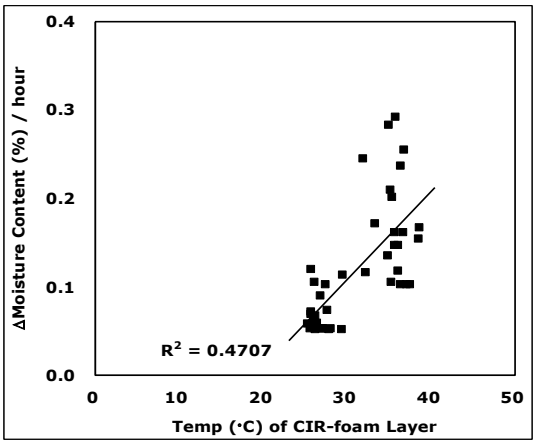

(b) ΔMC/h vs. Temperature

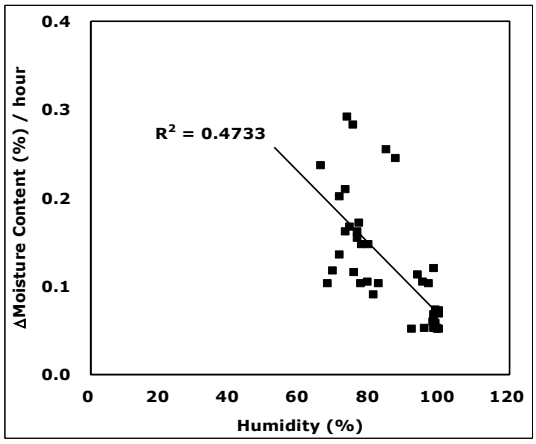

(c) ΔMC/h vs. Humidity

Figure 3-8. Plots of moisture change per hour against each of three independent variables at 3.5 inches of surface from CIR-foam layer

4. LABORATORY EVALUATION OF CAPACITANCE MOISTURE SENSOR

To verify the capacitance moisture sensor against the actual moisture content, three RAP specimens were prepared in the rectangular container. The RAP materials were mixed with water at 2.0%, 4.0%, and 6.0% of RAP weight of 2700g. As shown in Figure 4-1 (a), for each RAP specimens, two capacitance moisture sensors were buried at 2.0 inches from the surface (2.0% MC for sensor A and B, 4.0% MC for sensor C and D, and 6.0% MC for sensor E and F) and RAP specimens were then compacted using a manual Marshall hammer. As shown in Figure 4-1 (b), the RAP specimens were cured at 40°C for 50 days to achieve at 0% of the moisture content. As summarized shown in Figure 4-2, changes of moisture content from six sensors were monitored for 50 days and the actual moisture contents from real weight were computed.

Table 4-1 summarizes the moisture contents measured from six sensors buried at 2.0 inches from the surface at three different moisture levels and the moisture contents measured from by measuring the weight loss of three RAP specimens during the curing period. Figure 4-2 shows plots of the moisture contents from six sensors buried at 2.0 inches from the surface against the actual moisture content.

(a) Moisture sensors buried at 2.0 inches

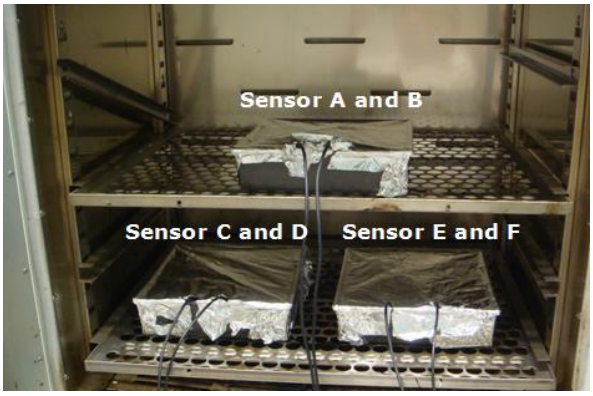

(b) Curing process at 40°C

Figure 4-1. Verification of capacitance moisture sensors in the laboratory

Table 4-1. Comparisons between moisture content from six sensors and moisture content from real weight

Curing day	Measured moisture content (%) from sensor						Measured moisture (%) content from actual weight		
	A	B	C	D	E	F	A, B	C, D	E, F
1 day	1.8	1.7	2.4	2.7	4.7	4.4	1.3	2.5	3.4
3 days	1.6	1.5	2.1	2.3	3.3	3.1	0.9	2.1	2.7
4 days	1.3	1.3	2.1	2.2	3.1	3.0	0.7	1.7	2.4
5 days	0.9	0.9	1.9	1.9	2.8	2.7	0.5	1.3	1.9
9 days	0.4	0.4	0.6	0.4	1.7	1.3	0.0	0.6	0.6
10 days	0.4	0.4	0.1	0.3	1.1	0.7	0.0	0.3	0.4
11 days	0.4	0.3	0.1	0.3	0.7	0.6	0.0	0.2	0.2
12 days	0.3	0.2	0.1	0.3	0.4	0.5	0.0	0.1	0.1
13 days	0.3	0.2	0.1	0.2	0.4	0.4	0.0	0.0	0.0
19 days	0.2	0.1	0.0	0.0	0.1	0.1	0.0	0.0	0.0
20 days	0.2	0.1	0.0	0.0	0.1	0.1	0.0	0.0	0.0
21 days	0.2	0.1	0.0	0.0	0.1	0.1	0.0	0.0	0.0
50 days	0.0	0.0	0.0	0.0	0.0	0.0	0.0	0.0	0.0

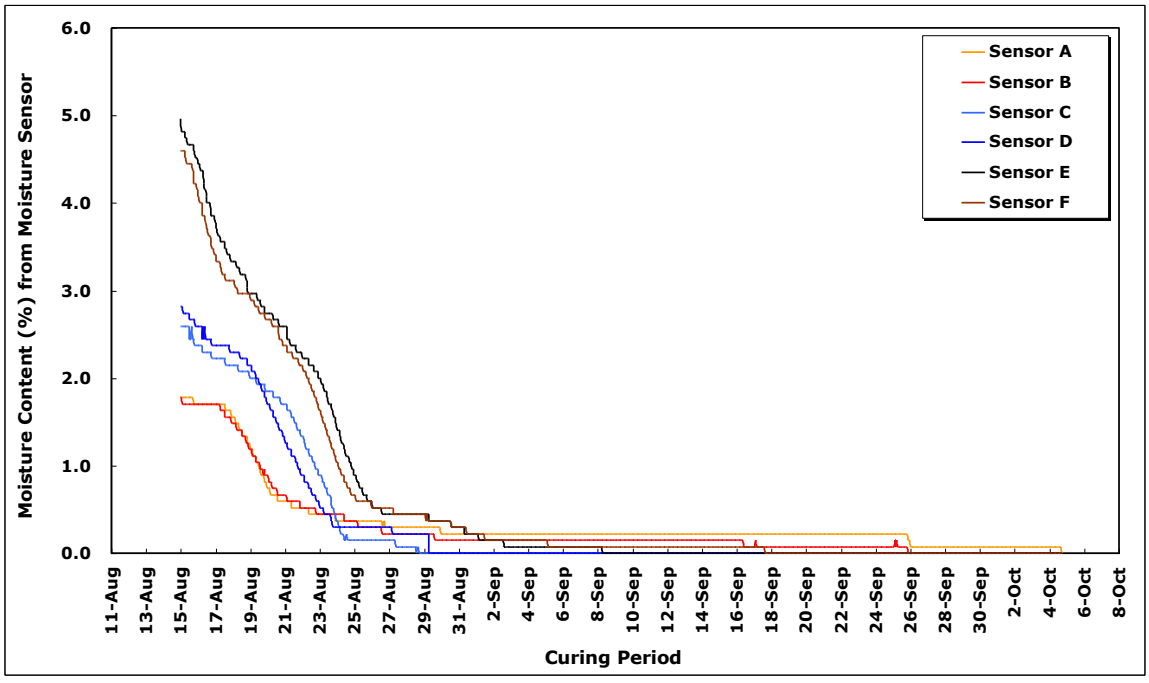

Figure 4-2. Plots of moisture content changes from six sensors buried at 2.0 inches

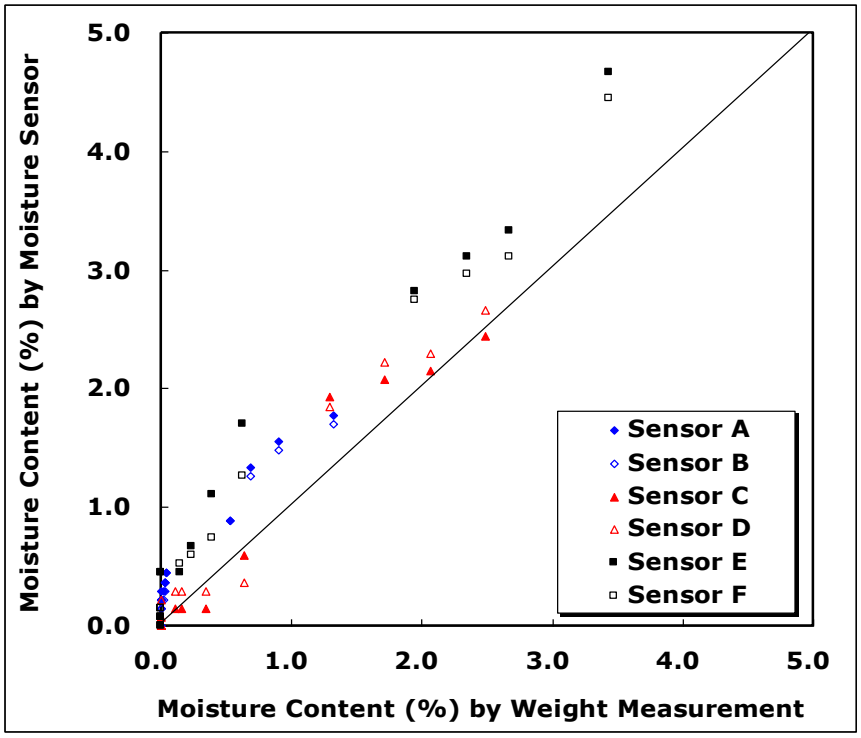

Figure 4-3. Plots of moisture content from six sensors buried at 2.0 inches from the surface against moisture content from real

5. MEASUREMENT OF MOISTURE CONTENT FROM CIR-EMULSION PROJECT IN CLINTON COUNTY

To measure the field moisture contents and temperature of CIR-emulsion layer, as shown in Figure 5-1, cold in-place recycling with high float medium setting-high viscosity with solvent emulsified asphalt (HFMS-2S-emulsion) project site in Clinton County was selected. HFMS-2S-emulsion project site is located from 11th street north in city of Dewitt to Iowa Highway 136, Iowa. The 11.2-mile section of County Road Y-70 and Z2E was rehabilitated from 11th street north in city of Dewitt to Iowa Highway 136, Iowa from August 18th to September 24th, 2009.

Figure 5-1. Locations of CIR-HFMS-2S-emulsion project sites in Clinton

5.1 Measurement of Field Moisture Content and Temperature

To monitor actual moisture contents of the CIR-HFMS-2S-emulsion layer in the field, as shown in Figure 5-2, three ECH2O moisture sensors and three temperature sensors were embedded at 2.0 inches from the surface of the CIR-HFMS-2S layer. A weather station was also installed to collect air temperature, humidity, rainfall and wind speed.

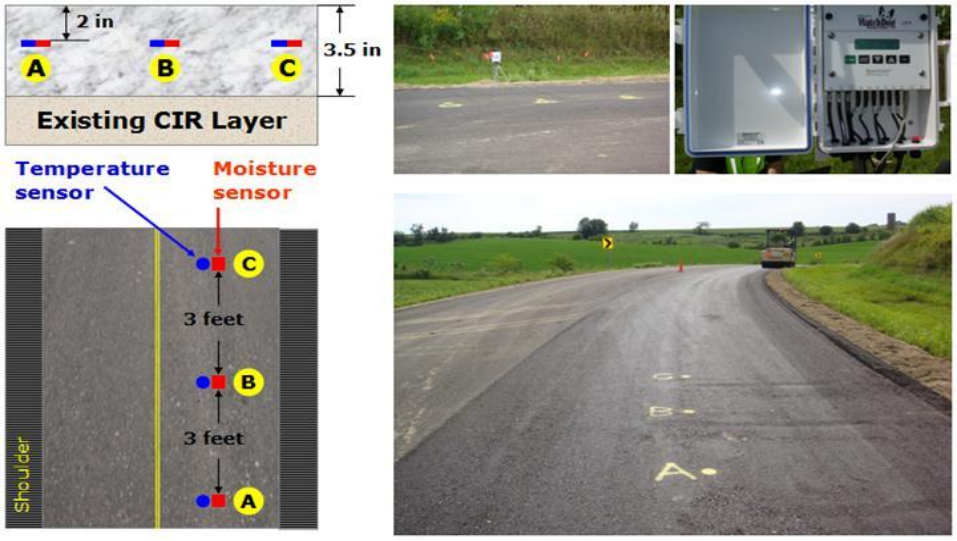

Figure 5-2. Embedded moisture and temperature sensors installed 2.0 inches from the surface of the CIR- HFMS-2S layer

Figure 5-3, Figure 5-4, Figure 5-5, and Figure 5-6 show plots of moisture content, rainfall, temperature, and humidity, respectively, measured during the curing duration of 36 days when ten rainfalls with a total amount of 6.18 inches have occurred. The moisture contents measured by three sensors are consistent with the time and amount of rainfall. The moisture contents at 2.0 inches from the surface of the CIR- HFMS-2S layer were measured as 3.6% from sensor A, 3.35% from sensor B, and 3.30% from sensor C. Despite the actual moisture content of CIR-HFMS-2S-emulsion layer being above 2.0%, the base HMA overlay was constructed after 37 days of curing. Figure 5-7 shows plots of temperature from three sensors embedded in the CIR-HFMS-2S-emulsion layer against air temperature from the weather station. As shown in Figure 5-7, as expected, temperature of CIR-HFMS-2S-emulsion layer was significantly higher than air temperature.

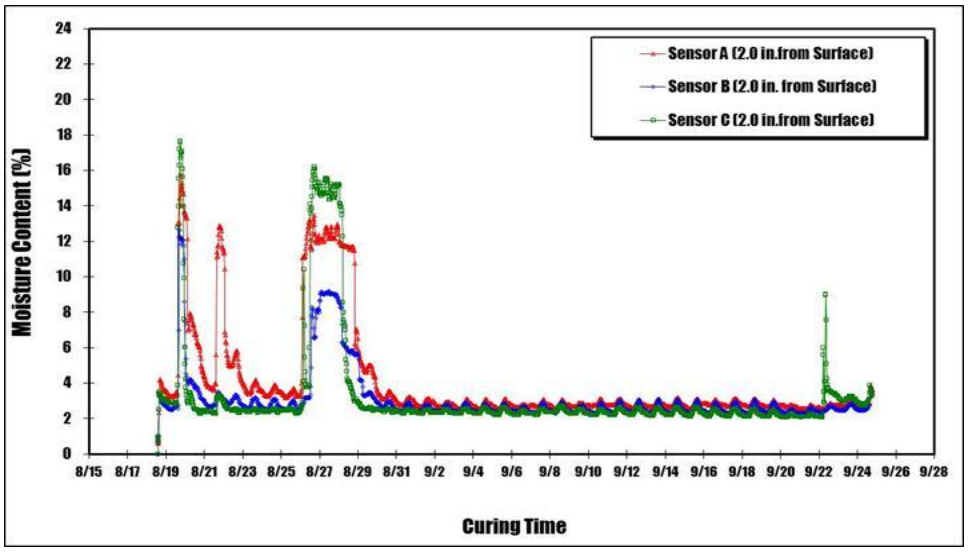

Figure 5-3. Plots of moisture contents against the curing period from three sensors embedded in the CIR-HMFS-2S layer

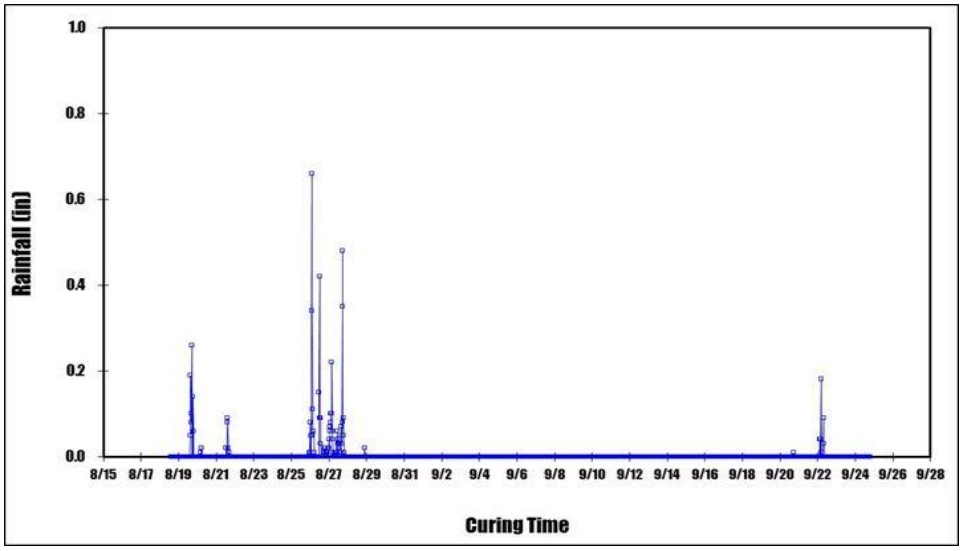

Figure 5-4. Plots of rainfalls against the curing period from weather station device

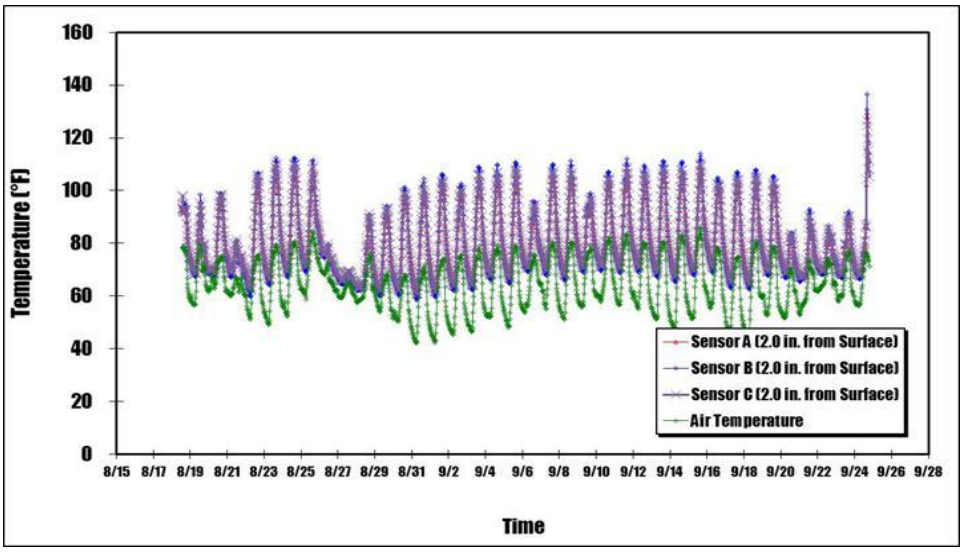

Figure 5-5. Plots of temperature against the curing period from three sensors embedded in the CIR-HFMS-2S-emulsion layer and air temperature from weather station device

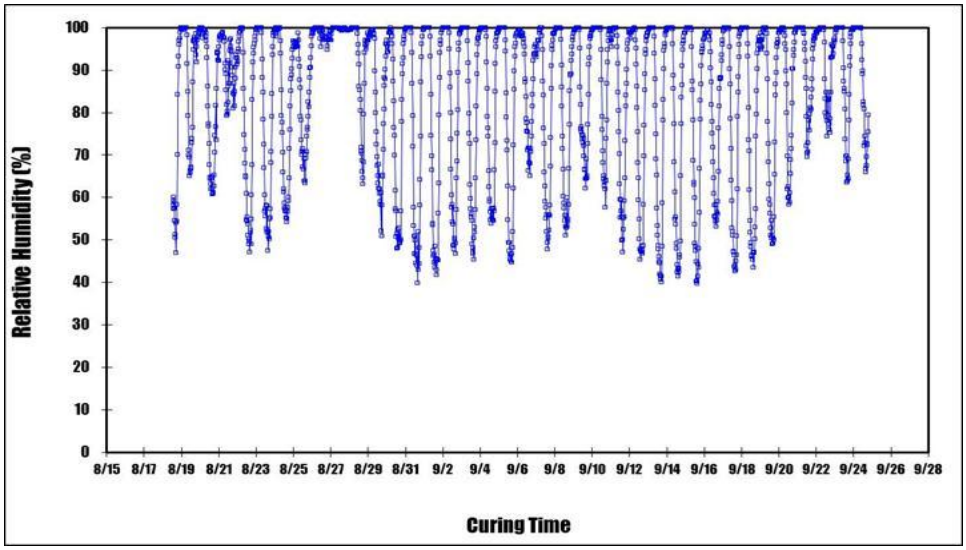

Figure 5-6. Plots of humidity against the curing period from weather station device

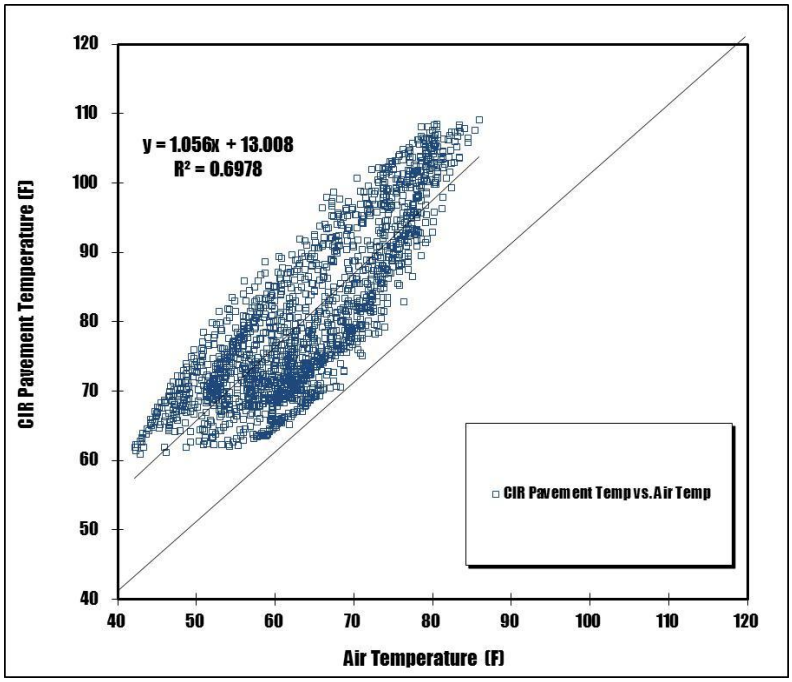

Figure 5-7. Plots of temperature from three sensors embedded in the CIR-HFMS-2S-emulsion layer against air temperature from weather station device

As shown in Figure 5-8 (a), using a portable TDR device, field moisture contents were measured from three different locations between 9:30 a.m. to 3:30 p.m. for 37 days between August 18th and September 24th, 2009. Three measurements by a portable TDR device were made from each of three locations and the average value was recorded for each day. Figure 5-9 shows plots of moisture contents measured between August 18th and September 24th, 2009.

As shown in Figure 5-8 (b), using nuclear gauge, field moisture contents were measured from three different locations between 9:00 a.m. to 9:30 a.m. for 6 days between August 19th and August 24th, 2009. A single measurement was made by nuclear gauge from each of three locations. Figure 5-10 shows plots of moisture contents measured between August 19th and August 24th, 2009.

(a) Portable TDR device

(b) Nuclear gauge

Figure 5-8. Moisture measurements for each of three locations using a portable TDR and nuclear gauge in CIR-HFMS-2S-emulsion project site

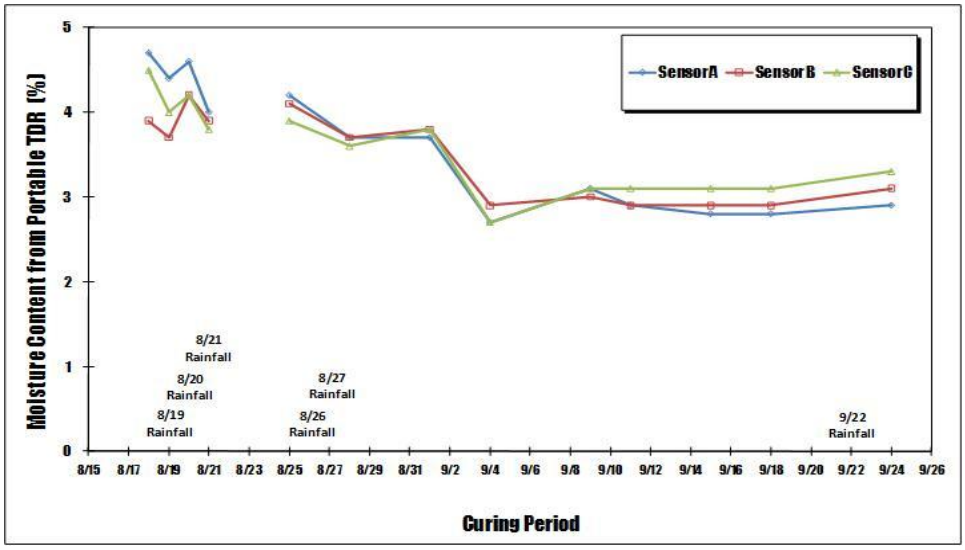

Figure 5-9. Plots of field moisture contents measured by a portable TDR in CIR-HFMS-2S-emulsion project site

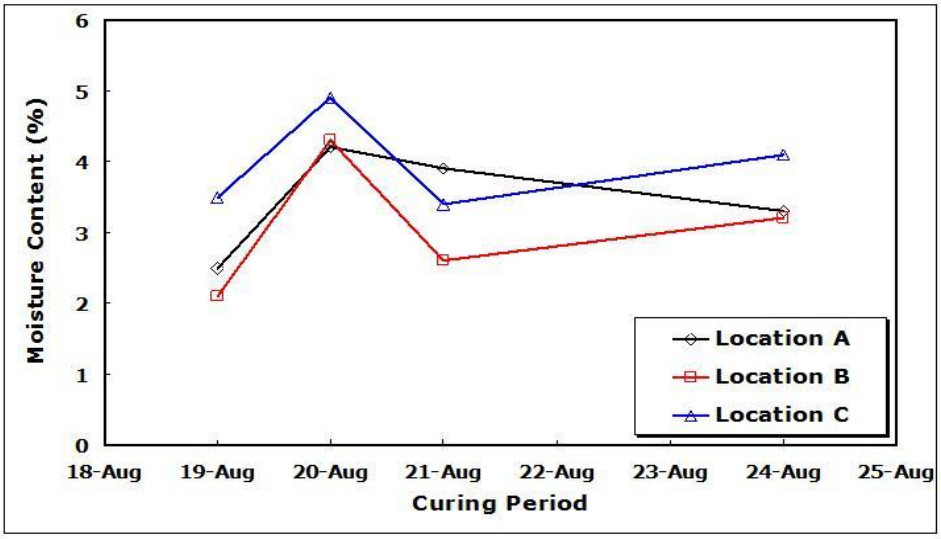

Figure 5-10. Plots of field moisture contents measured by nuclear gauge in CIR-HFMS-2S-emulsion project site

Figure 5-11 shows plots of field moisture content measured by a potable TDR device (or by moisture sensors) against field moisture content measured by a nuclear gauge. It should be noted that the moisture contents measured using a portable TDR, a nuclear gauge, and moisture sensors represent the moisture contents between the surface and 1.5 inches to 2.0 inches from the surface and they were above the minimum moisture content of 2.0% required before an HMA overlay. As shown in Figure 5-11, overall, the moisture content measured by a portable TDR device is higher than those measured by a nuclear gauge but the moisture content measured by moisture sensors is lower than those measured by a nuclear gauge.

Figure 5-12 shows plots of field moisture content measured by a potable TDR against field moisture content measured by moisture sensors. As shown in Figure 5-12, the moisture content measured by a portable TDR device is higher than ones measured by moisture sensors.

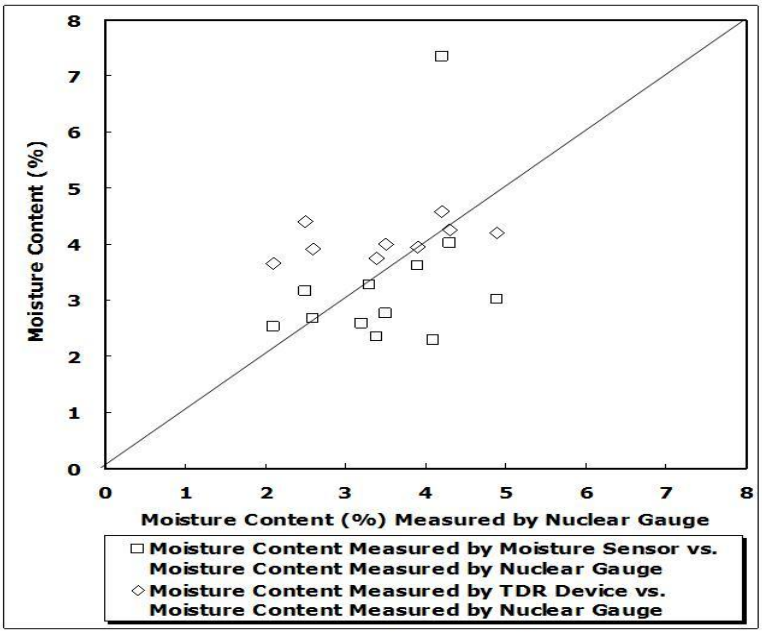

Figure 5-11. Plots of field moisture content measured by a potable TDR (or moisture sensors) against field moisture content measured by a nuclear gauge

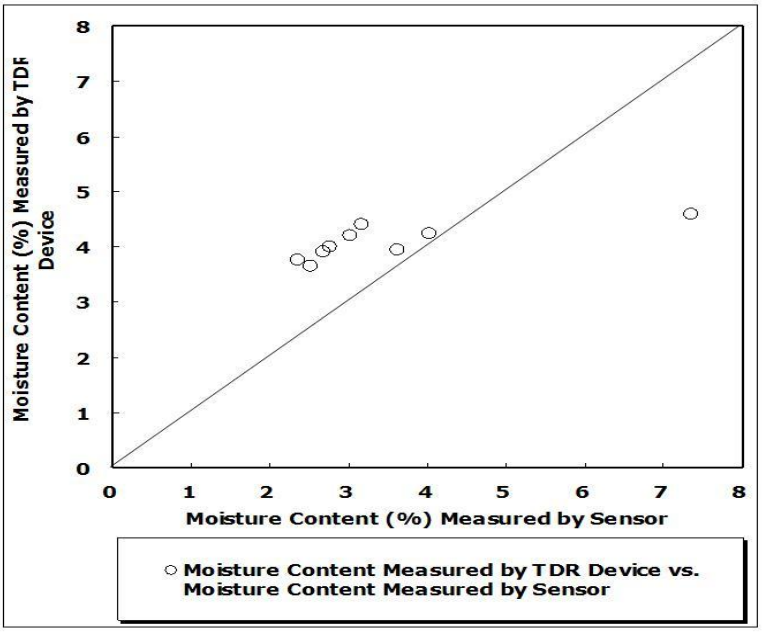

Figure 5-12. Plots of field moisture content measured by a potable TDR against field moisture content measured by moisture

5.2 Measurement of Density and Stiffness

The density and stiffness of the CIR-HFMS-2S-emulsion layer was measured using a nuclear gauge and geo-gauge, respectively, throughout the duration of curing. As shown in Figure 5-13, the density and stiffness were measured at three different locations: 1) A (Sensor A), 2) B (Sensor B) and 3) C (Sensor C).

Figure 5-13. Location of three spots for measuring density and stiffness

5.2.1 Density Measurements using Nuclear Gauge

A nuclear gauge was used to measure densities of CIR-HFMS-2S-emulsion layer. As shown in Figure 5-14, density values were measured four times between August 19th and August 24th, 2009 from three locations between 9:00 a.m. to 9:30 a.m. The density value of CIR-HFMS-2S layer slightly increased as the curing time increased at the early stage of curing and remained constant in the remaining curing period.

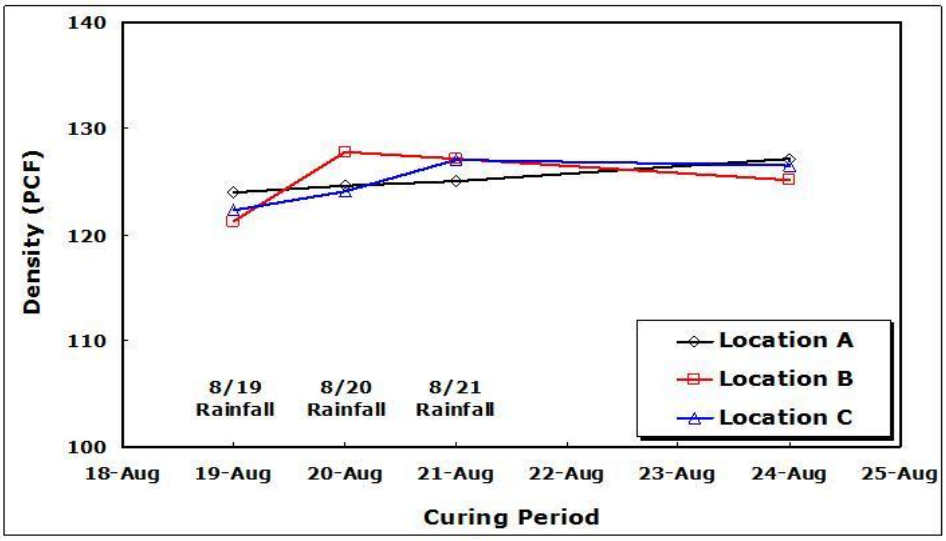

Figure 5-14. Plots of density against curing period from three locations in the CIR-HFMS-2S-emulsion layer

5.2.2 Stiffness Measurements using Geo-Gauge

The geo-gauge was used to measure the stiffness of CIR-HFMS-2S-emulsion layer. The geo-gauge is a portable device capable of measuring the in-situ stiffness of soil. As shown in Figure 5-15, stiffness was measured thirteen times between August 18th and September 24th, 2009 from three locations (all stiffness measurements were made between 9:30 a.m. to 3:30 p.m.). Right after the construction, the stiffness of CIR-HFMS-2S-emulsion layer increased in three days. However, after reaching the stiffness of approximately 30 MN/m, the stiffness remained constant for one month. Figure 5-16 shows plots of density measured by a nuclear gauge against stiffness measured by geo-gauge at three different locations between August 19th and August 21st, 2009. Figure 5-17 shows there too be little correlation between stiffness and moisture content measured by the embedded sensors. Moisture contents above 7% were considered outliers for Figure 5-17.

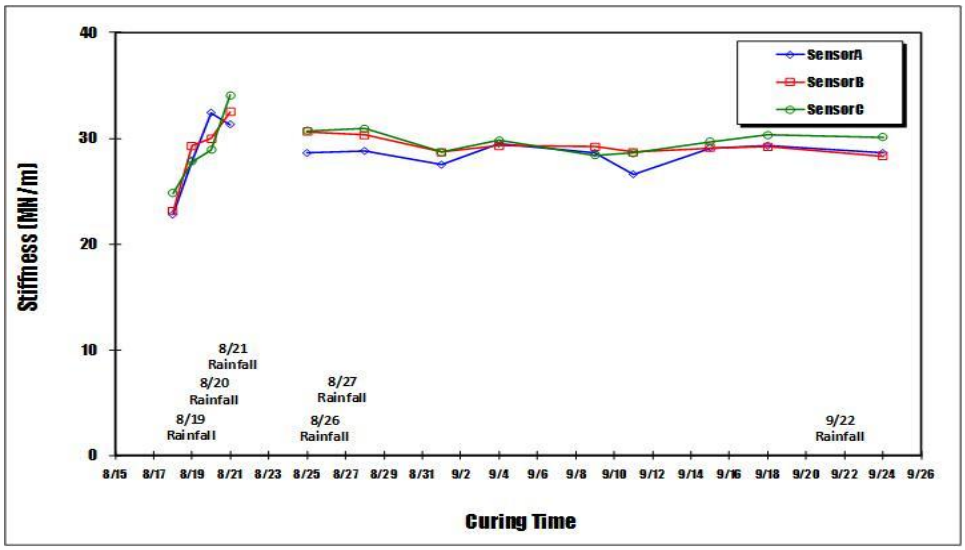

Figure 5-15. Plots of stiffness against the curing period from three locations in the CIR-HFMS-2S-emulsion layer

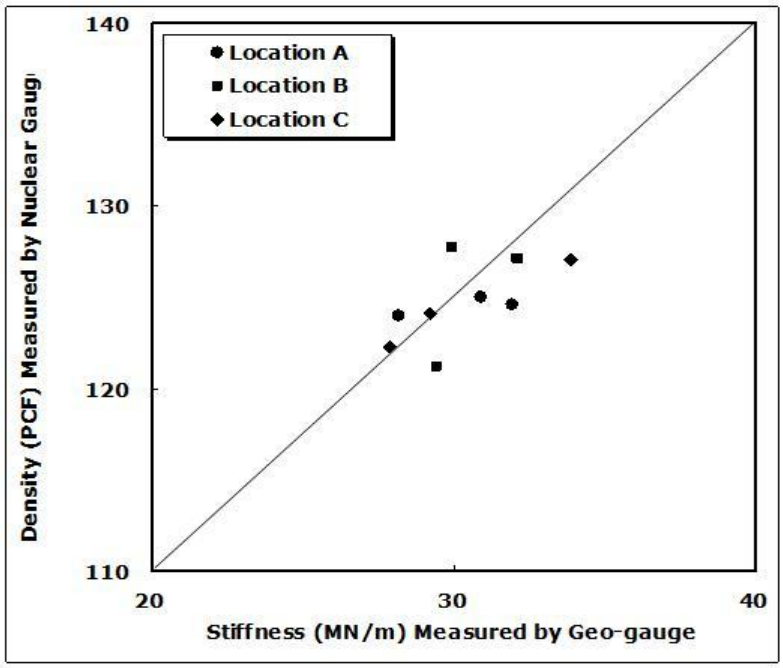

Figure 5-16. Plots of density measured by a nuclear gauge against stiffness measured by geo-gauge at three different locations

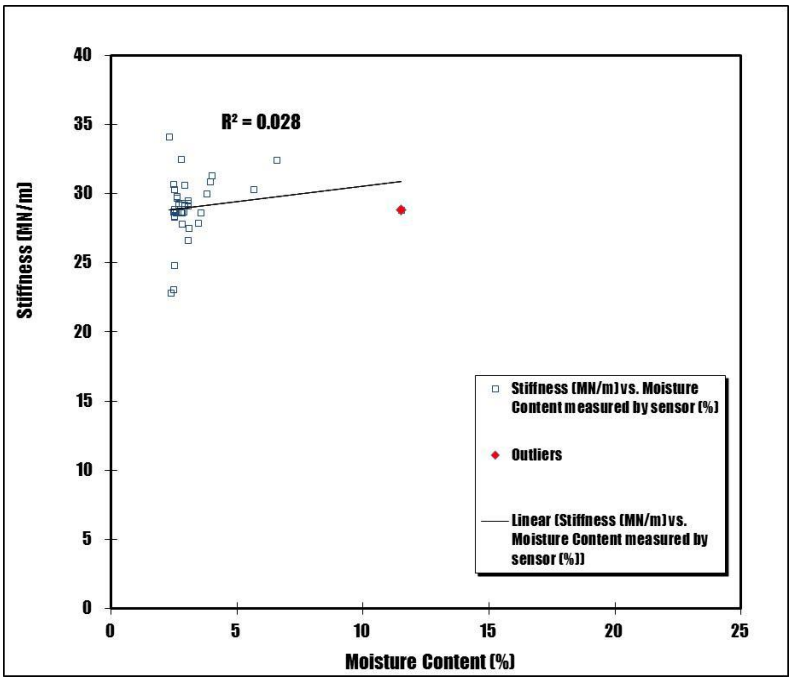

Figure 5-17. Plots of stiffness measured by a geo-gauge against moisture content measured by embedded sensors at three different locations

6. MEASUREMENT OF MOISTURE CONTENT FROM CIR-FOAM PROJECT IN IOWA COUNTY

To measure the field moisture contents and temperature of CIR-foam layer, as shown in Figure 6-1, cold in-place recycling with foamed asphalt (CIR-foam) project site in Iowa County was selected. The CIR-foam project site is located from West of North English on County Road F 67 to Keswick on County G 13, Iowa. 5.0-mile section of Country road F 67 and G 13 was rehabilitated from West of North English on County Road F 67 to Keswick on County G 13, Iowa between August 20th and September 16th, 2009.

Figure 6-1. Locations of CIR-foam project sites in Iowa

6.1 Measurement of Field Moisture Content and Temperature

To monitor actual moisture contents of the CIR-foam-emulsion layer in the field, as shown in Figure 6-2, three ECH2O moisture sensors and three temperature sensors were embedded at 2.0 inches from the surface of the CIR-foam layer. A weather station was also installed to collect air temperature, humidity, rainfall and wind speed.

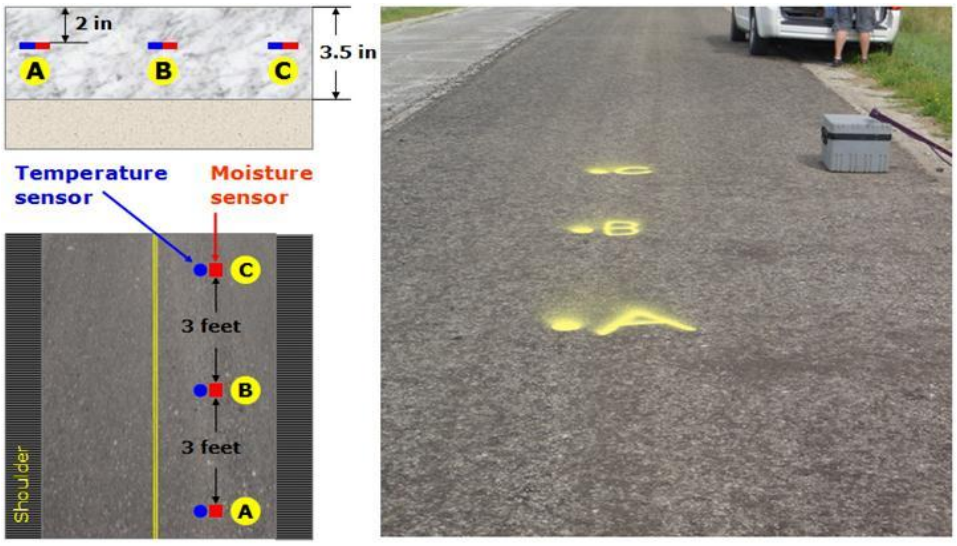

Figure 6-2. Embedded moisture and temperature sensors installed 2.0 inches from the surface of the CIR- foam layer

Figure 6-3, Figure 6-4, Figure 6-5, and Figure 6-6 show plots of moisture content, rainfall, temperature, and humidity, respectively, measured during the curing time of 27 days when four rainfalls with a total amount of 4.65 inches have occurred. The moisture contents measured by three sensors peaked when there was a heavy rainfall on August 27. This supports that the moisture sensors are accurate. The moisture contents at 2.0 inches from the surface of the CIR-foam layer were measured as 2.74% from sensor A, 3.22% from sensor B, and 2.85% from sensor C. Despite the actual moisture content of CIR-foam layer being above 2.0%, the base HMA overlay was constructed after 36 days of curing. Figure 6-7 shows plots of temperature from three sensors embedded in the CIR-foam layer against air temperature from weather station device. As shown in Figure 6-7, as expected, temperature of CIR-foam layer is higher than air temperature.

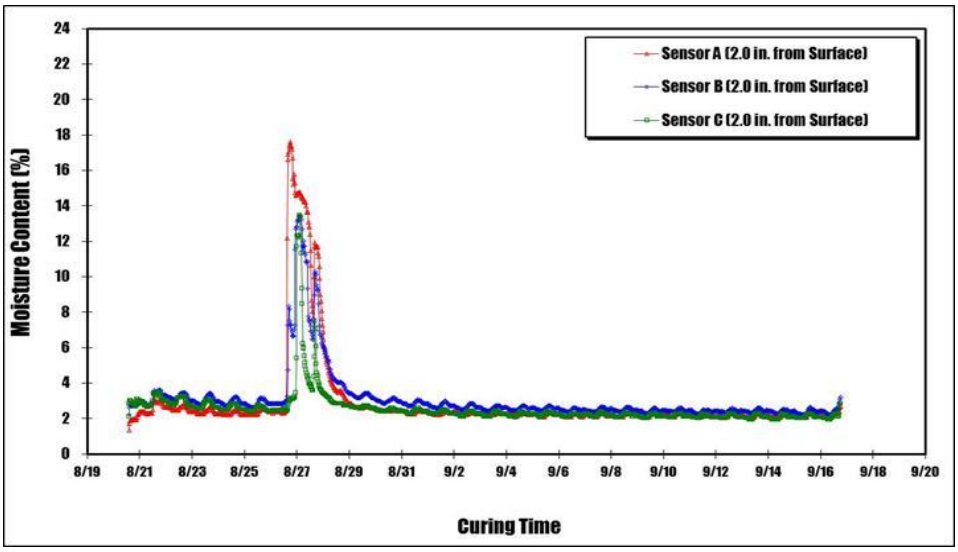

Figure 6-3. Plots of moisture contents against the curing period from three sensors embedded in the CIR-foam layer

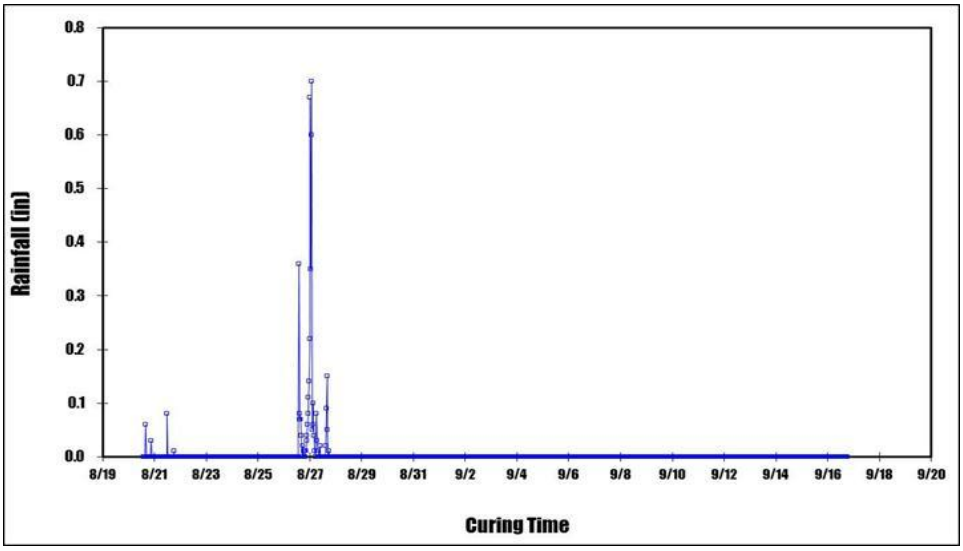

Figure 6-4. Plots of rainfalls against the curing period from weather station device

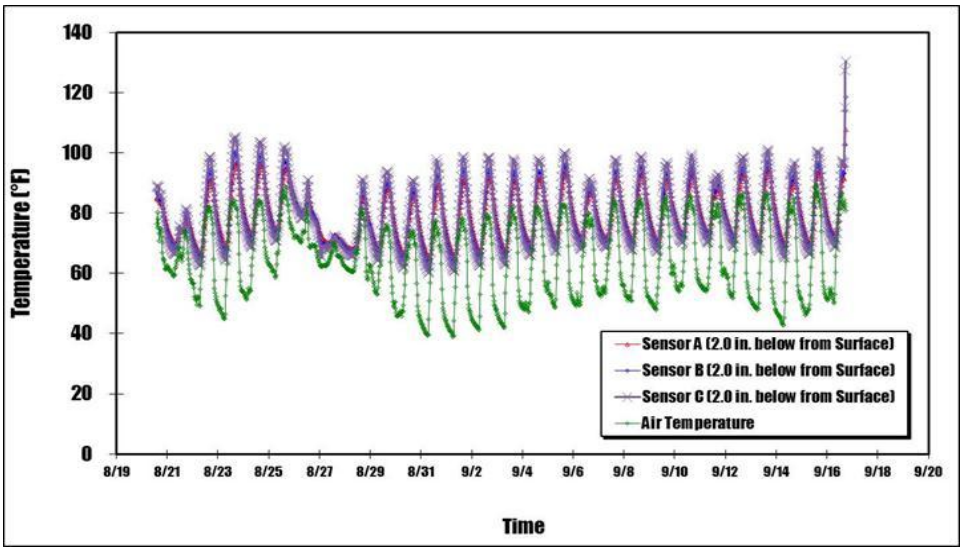

Figure 6-5. Plots of temperature against the curing period from three sensors embedded in the CIR-foam layer and air temperature from weather station device

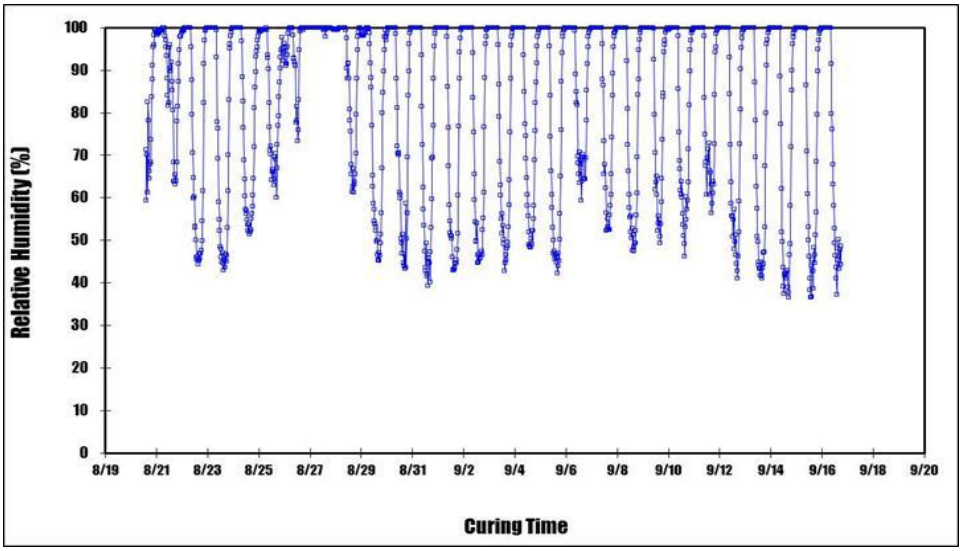

Figure 6-6. Plots of humidity against the curing period from weather station device

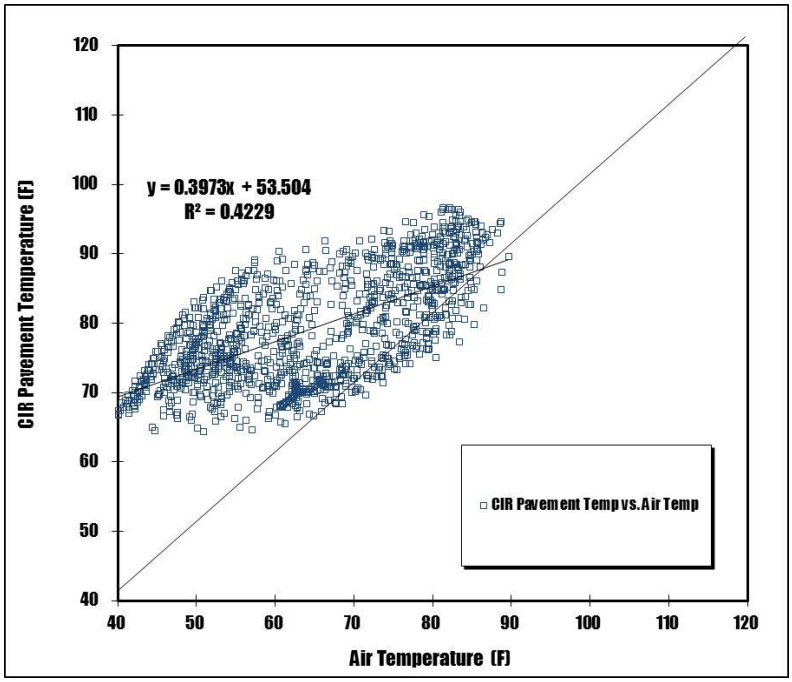

Figure 6-7. Plots of temperature from three sensors embedded in the CIR-foam layer against air temperature from weather station device

Using a portable TDR device, field moisture contents were measured from three different locations between 9:30 a.m. to 3:30 p.m. for 36 days between August 20th and September 14th, 2009. Two measurements by a potable TDR device were made from each of three locations and the average value was recorded. Figure 6-8 shows plots of moisture contents measured between August 20th and September 16th, 2009. As can be seen from Figure 6-8, the moisture content as measured by the TDR device continuously decreased despite the heavy rainfall on August 26 and 27. It indicates that the TDR device may not be accurate in measuring the moisture content of the CIR-foam layer.

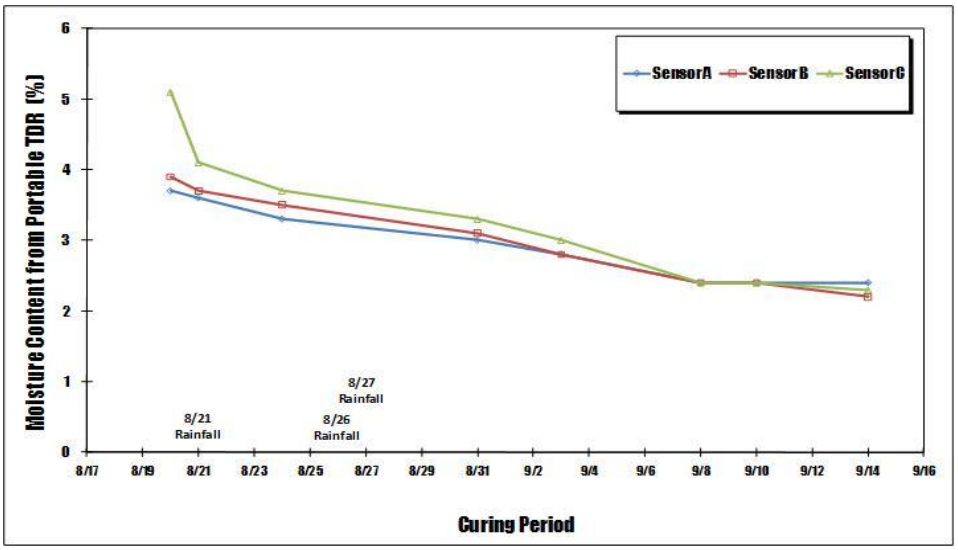

Figure 6-8. Plots of field moisture contents measured by a portable TDR in CIR-foam project site

Figure 6-9 shows plots of field moisture content measured by a potable TDR against field moisture content measured by moisture sensors. It should be noted that the moisture contents measured using a portable TDR and moisture sensors represent the moisture contents between the surface and 1.5 inches to 2.0 inches from the surface and they were above the minimum moisture content of 2.0% required before an HMA overlay. As shown in Figure 6-9, the moisture content measured by a portable TDR device is higher than ones measured by moisture sensors.

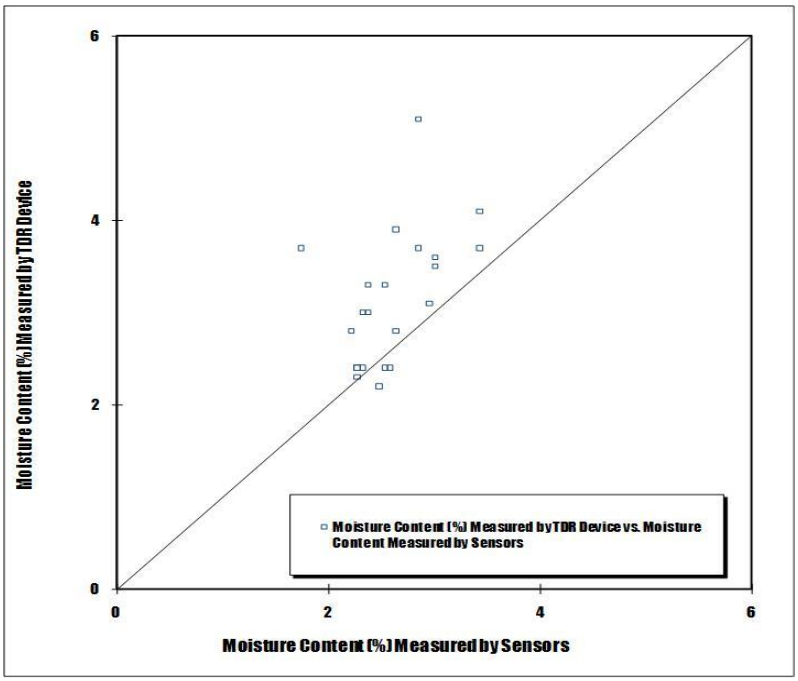

Figure 6-9. Plots of field moisture content measured by a potable TDR against field moisture content measured by moisture sensors

6.2 Stiffness Measurements using Geo-Gauge

The stiffness of the CIR-foam layer was measured using a geo-gauge throughout the duration of curing. The stiffness was measured at three different locations that were spaced at approximately 3 feet: 1) A (Sensor A), 2) B (Sensor B) and 3) C (Sensor C). As shown in Figure 6-10, stiffness was measured thirteen times between August 20th and September 16th, 2009 from three locations (all stiffness measurements were made between 9:30 a.m. to 3:30 p.m.). Despite a heavy rainfall on August 27, the stiffness of CIR-foam layer steadily increased and stabilizing at between 25 and 30 MN/m as curing time increased. Figure 6-11 shows that stiffness and moisture content had little correlation.

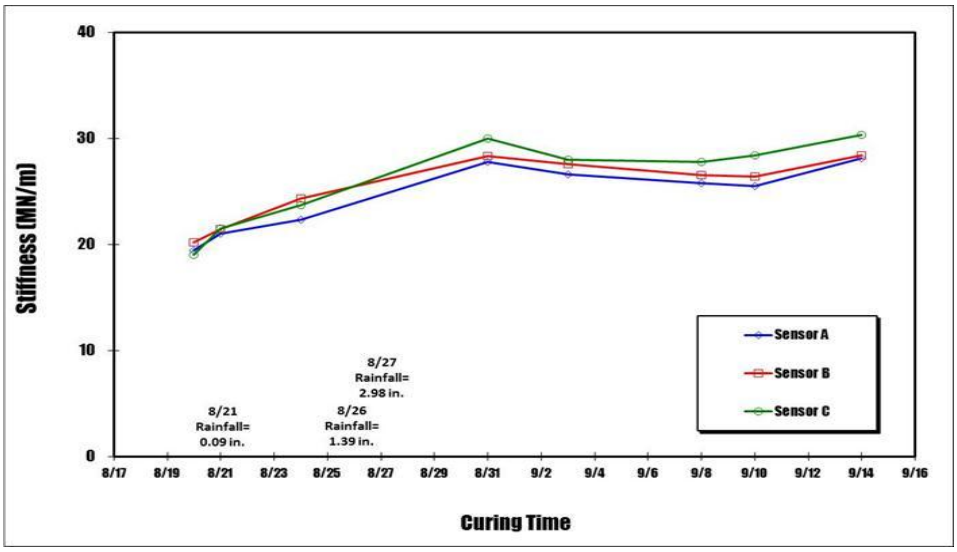

Figure 6-10. Plots of stiffness against the curing period from three locations in the CIR-foam layer

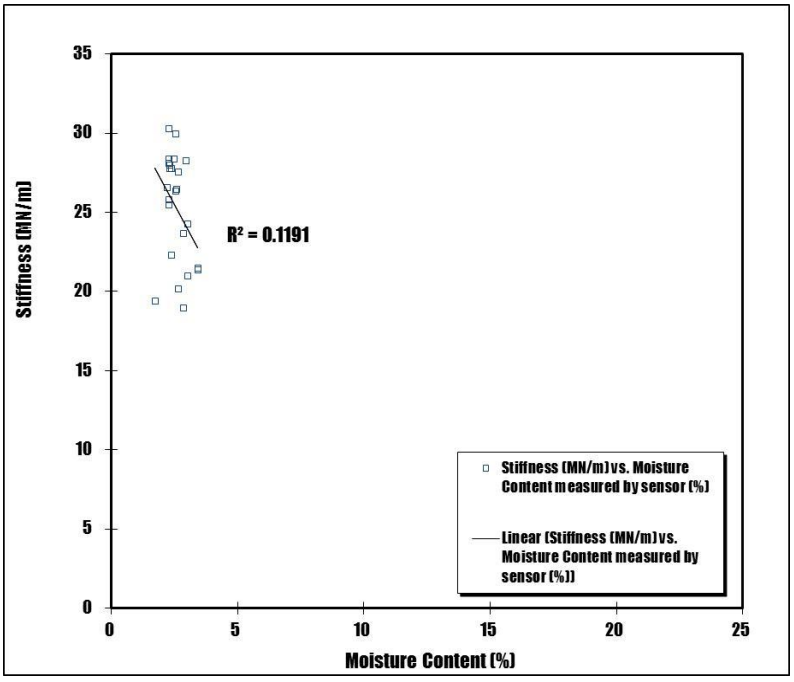

Figure 6-11. Plots of stiffness measured by a geo-gauge against moisture content measured by embedded sensors at three different locations

7. MEASUREMENT OF MOISTURE CONTENT FROM CIR-FOAM PROJECT IN BENTON COUNTY

To measure the field moisture contents and temperature of CIR-foam layer, as shown in Figure 7-1, CIR-foam project site in Benton County was selected. The CIR-foam project site is located on highway 30 and was rehabilitated between June 3rd and June 30th 2010.

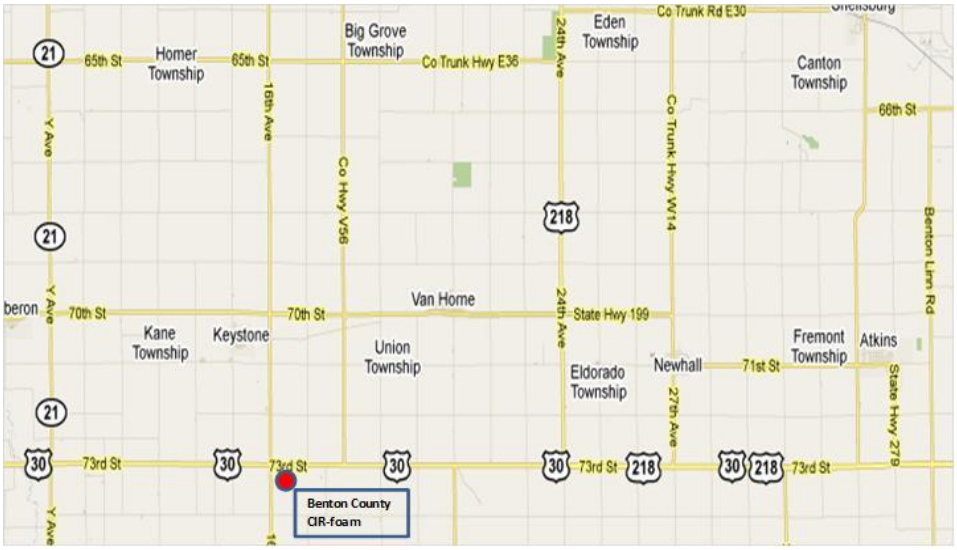

Figure 7-1. Locations of CIR-foam project site in Benton

7.1 Measurement of Field Moisture Content and Temperature

To monitor actual moisture contents of the CIR-foam layer in the field, as shown in Figure 7-2, three ECH2O moisture sensors and three temperature sensors were embedded at 2.0 inches from the surface of the CIR-foam layer. A weather station was also installed to collect air temperature, humidity, rainfall and wind speed.

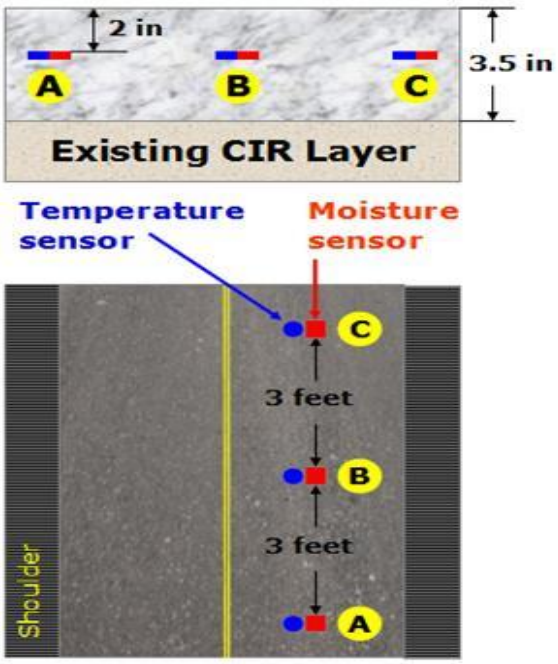

Figure 7-2. Embedded moisture and temperature sensors installed 2.0 inches from the surface of the CIR- foam layer

Figure 7-3, Figure 7-4, Figure 7-5, and Figure 7-6 show plots of moisture content, rainfall, temperature, and humidity, respectively, measured during the curing duration of 28 days when eighteen rainfalls with a total amount of 7.81 inches have occurred. Due to the heavy rainfall throughout the curing period, the moisture contents remained high from 4% to 24%. The moisture contents before the intermediate HMA overlay were measured at 8.9% from sensor A, 3.6% from sensor B, and 4.45% from sensor C. Despite the actual moisture contents of CIR-foam layer remaining above 2.0%, the intermediate HMA overlay was constructed after 28 days of curing. Figure 7-7 shows plots of temperature from three sensors embedded in the CIR-foam layer against air temperature from the weather station. As shown in Figure 7-7, as expected, temperature of CIR-foam layer was significantly higher than air temperature.

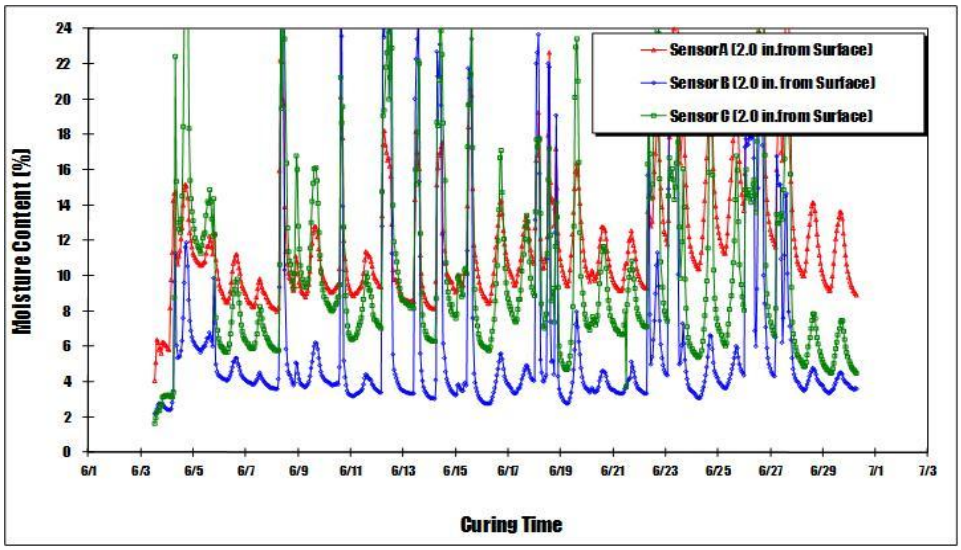

Figure 7-3. Plots of moisture contents against the curing period from three sensors embedded in the CIR-foam layer

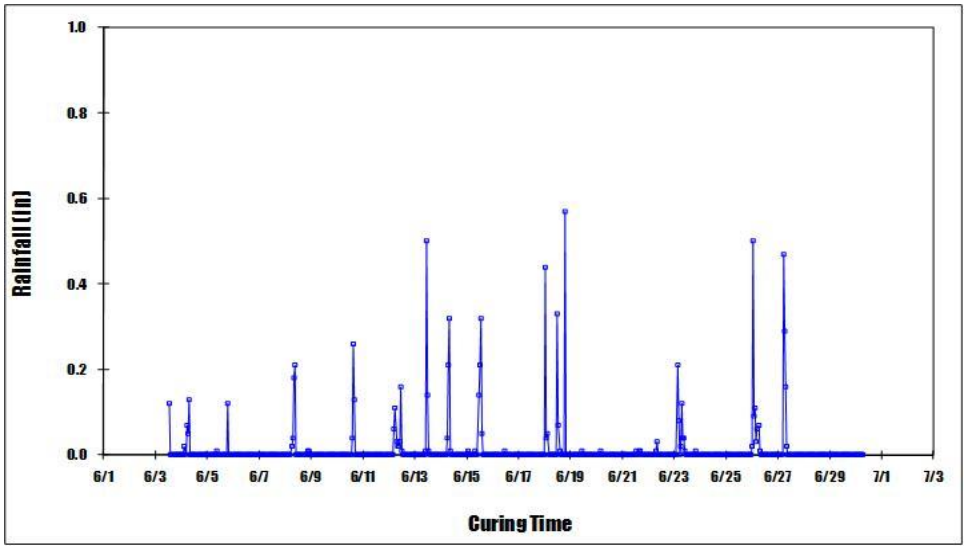

Figure 7-4. Plots of rainfalls against the curing period from weather station device

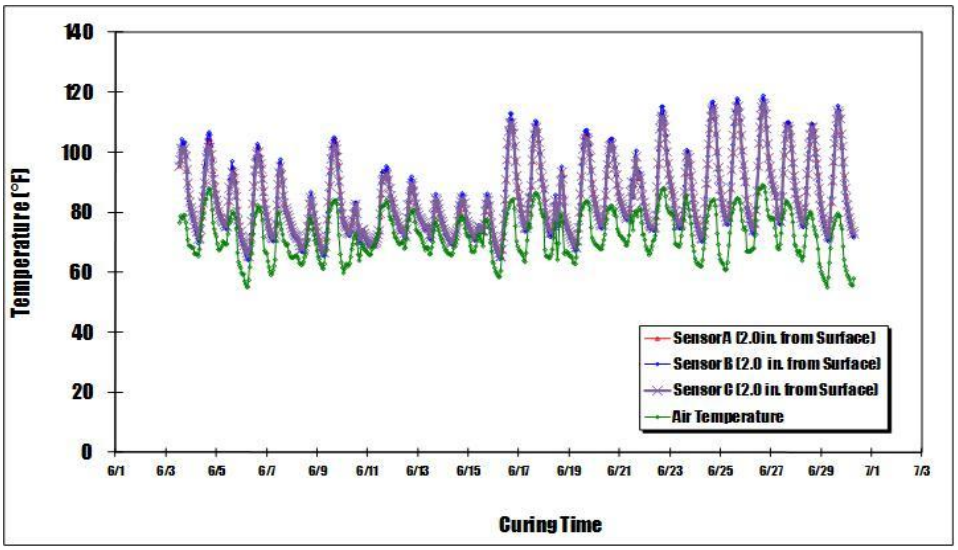

Figure 7-5. Plots of temperature against the curing period from three sensors embedded in the CIR-foam layer and air temperature from weather station device

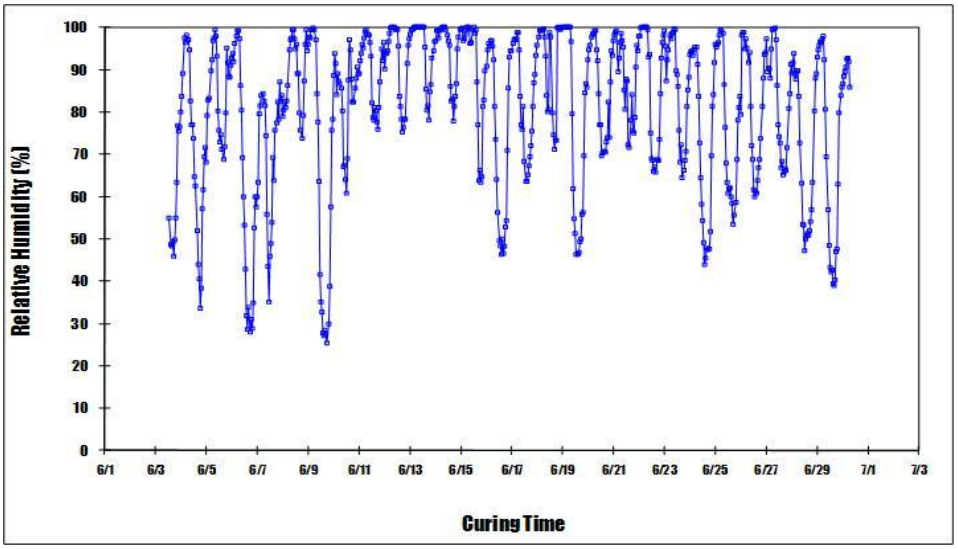

Figure 7-6. Plots of humidity against the curing period from weather station device

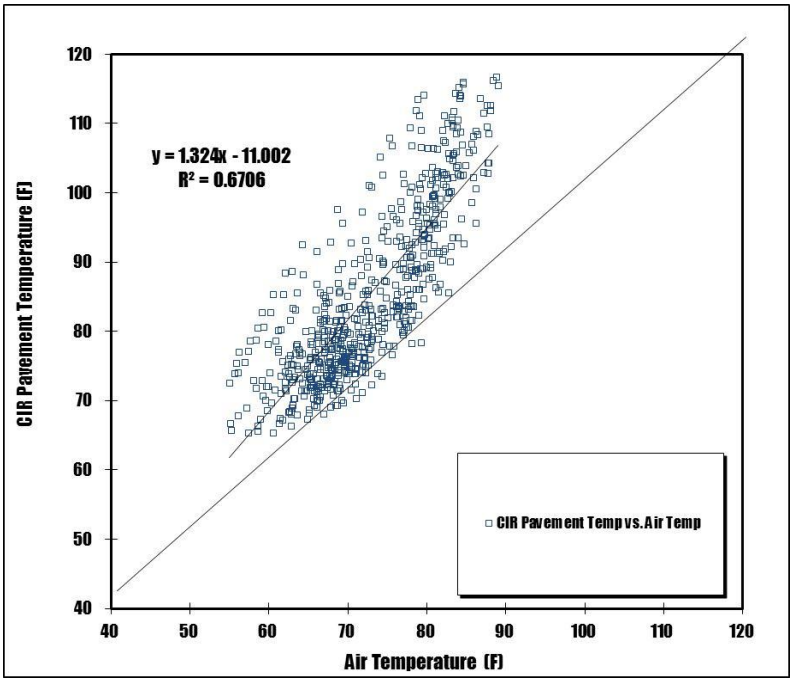

Figure 7-7. Plots of temperature from three sensors embedded in the CIR-foam layer against air temperature from weather station device

Using a portable TDR device, field moisture contents were measured from three different locations between 9:30 a.m. to 3:30 p.m. for 18 days between June 3rd and June 21st, 2010. Three measurements by a portable TDR device were made from each of three locations and the average value was recorded. Figure 7-8 shows plots of moisture contents measured between June 3rd and June 21st, 2010. As can be seen from Figure 7-8, the moisture content remained high between 14 to 28% and it stabilized at around 14% as the curing time increased.

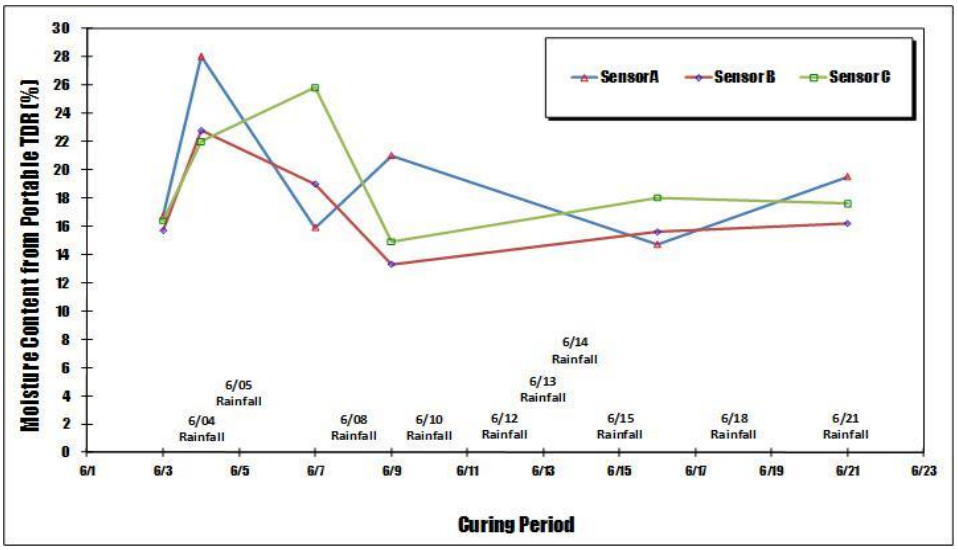

Figure 7-8. Plots of field moisture contents measured by a portable TDR in CIR-foam project site

Figure 7-9 shows plots of field moisture content measured by a potable TDR against field moisture content measured by moisture sensors. As shown in Figure 7-9, the moisture content measured by a portable TDR device were significantly higher than ones measured by moisture sensors. It should be noted that the moisture contents measured were above the minimum moisture content of 2.0% required before an HMA overlay.

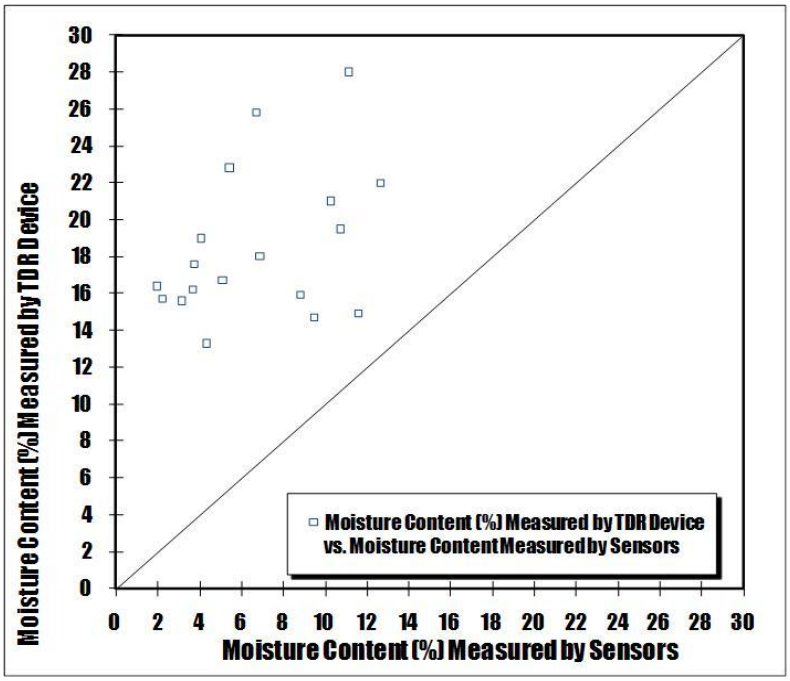

Figure 7-9. Plots of field moisture content measured by a potable TDR against field moisture content measured by moisture sensors

7.2 Stiffness Measurements using Geo-Gauge

The stiffness of the CIR-foam layer was measured using a geo-gauge throughout the duration of curing. The stiffness was measured at three different locations: 1) A (Sensor A), 2) B (Sensor B) and 3) C (Sensor C).

The geo-gauge was used to measure the stiffness of the CIR-foam layer. As shown in Figure 7-10, stiffness was measured six times between June 3rd and June 21st, 2010 from three locations (all stiffness measurements were made between 9:30 a.m. to 3:30 p.m.). Right after the construction, the stiffness of the CIR-foam layer increased up to 20 MN/m in three days. When there was continuous rainfall between June 8th and 15th, however, the stiffness decreased. Despite continuous rainfall, however, the stiffness remained above the initial stiffness right after the construction. Figure 7-11 shows there was little correlation between stiffness and moisture content. Moisture contents above 7% were considered high and outliers for Figure 7-11.

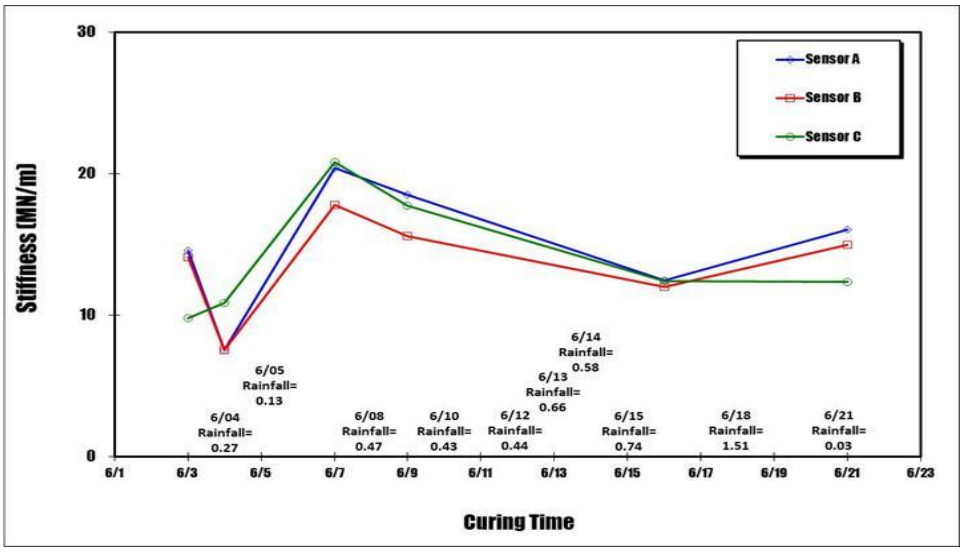

Figure 7-10. Plots of stiffness against the curing period from three locations in the CIR-foam layer

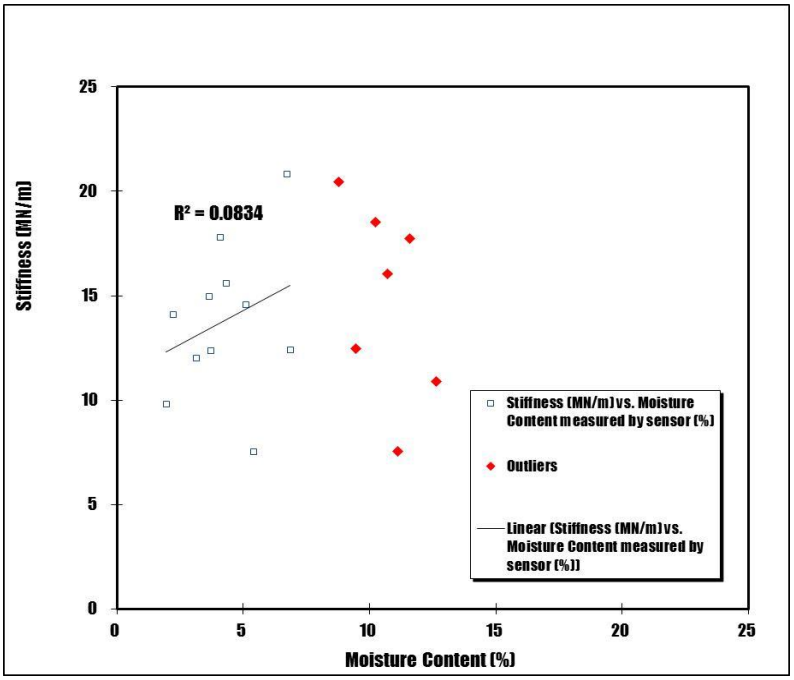

Figure 7-11. Plots of stiffness measured by a geo-gauge against moisture content measured by embedded sensors at three different locations

8. MEASUREMENT OF MOISTURE CONTENT FROM CIR-FOAM PROJECT IN MARSHALL COUNTY

To measure the field moisture contents and temperature of CIR-foam layer, as shown in Figure 8-1, CIR-foam project site in Marshall County was selected. The CIR-foam project site is located on 330th Street west of Highway 14. The road was rehabilitated between August 23rd and September 20th, 2010.

Figure 8-1. Location of CIR-foam project site in Marshall County

8.1 Measurement of Field Moisture Content and Temperature

To monitor actual moisture contents of the CIR-foam layer in the field, as shown in Figure 8-2, three ECH2O moisture sensors and three temperature sensors were embedded at 2.0 inches from the surface of the CIR-foam layer. The temperature sensor at location B was damaged during the installation process. A weather station was also installed to collect air temperature, humidity, rainfall and wind speed.

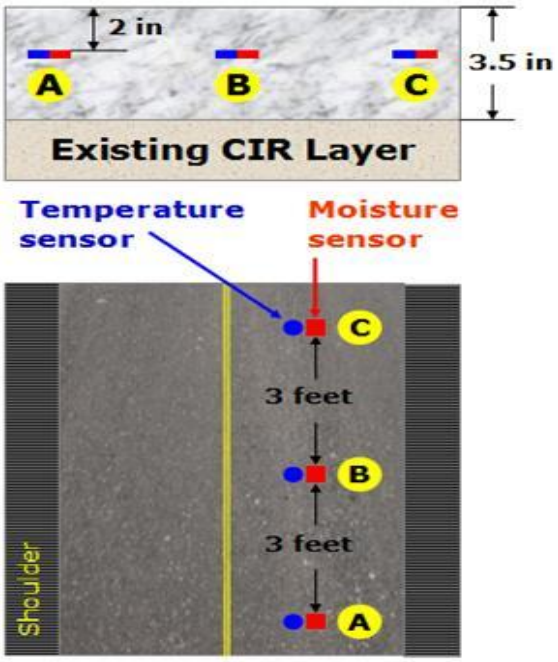

Figure 8-2. Embedded moisture and temperature sensors installed 2.0 inches from the surface of the CIR- foam layer

Figure 8-3, Figure 8-4, Figure 8-5, and Figure 8-6 show plots of moisture content, rainfall, temperature, and humidity, respectively, measured during the curing duration of 28 days when four rainfalls with a total amount of 4.22 inches have occurred. Throughout the curing period, the moisture contents measured by three sensors were consistent with rainfalls. The moisture contents before the intermediate HMA overlay were measured at 2.68% from sensor A, 4.07% from sensor B, and 4.51% from sensor C. Despite the actual moisture contents of CIR-foam layer remaining above 2.0%, the intermediate HMA overlay was constructed after 28 days of curing. Figure 8-7 shows plots of temperature from two sensors embedded in the CIR-foam layer against air temperature from the weather station. As shown in Figure 8-7, as expected, temperature of the CIR-foam layer was significantly higher than air temperature.

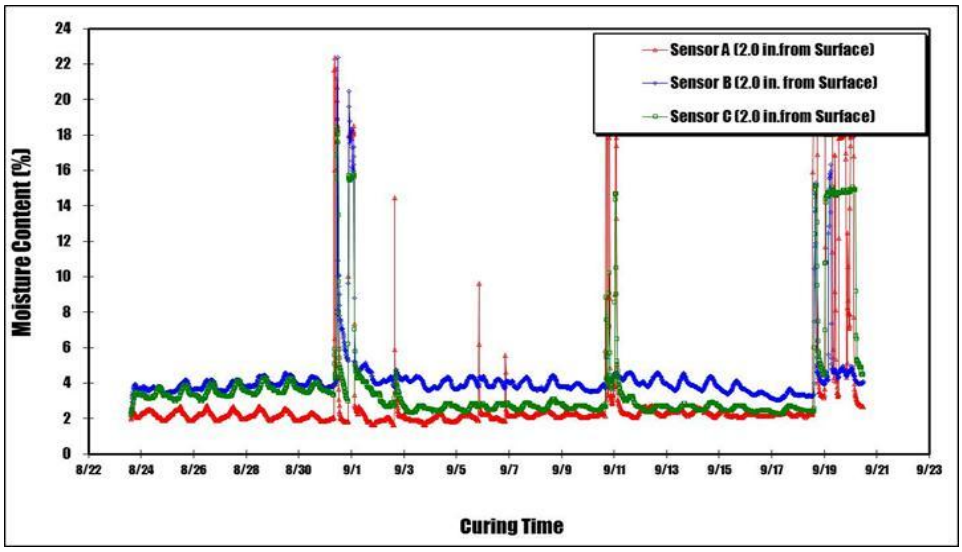

Figure 8-3. Plots of moisture contents against the curing period from three sensors embedded in the CIR-foam layer

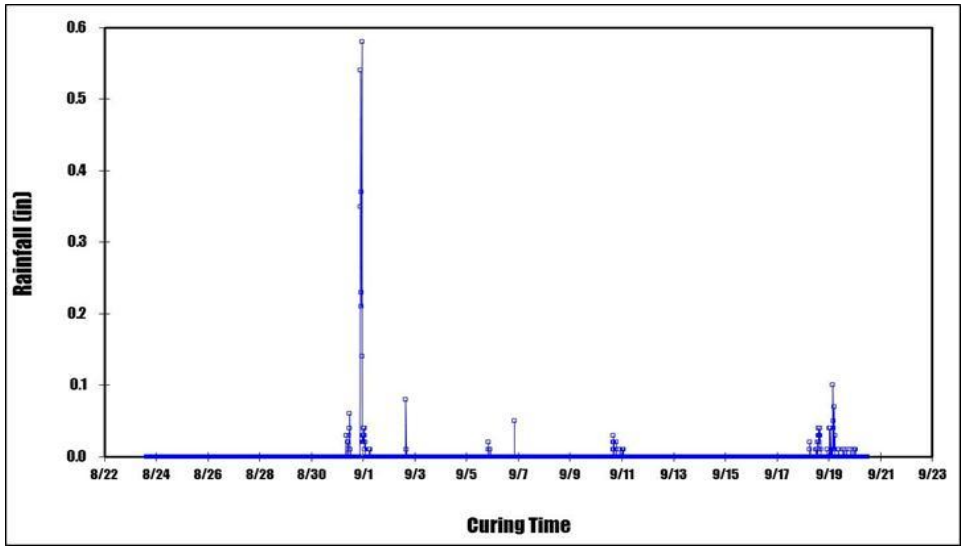

Figure 8-4. Plots of rainfalls against the curing period from weather station device

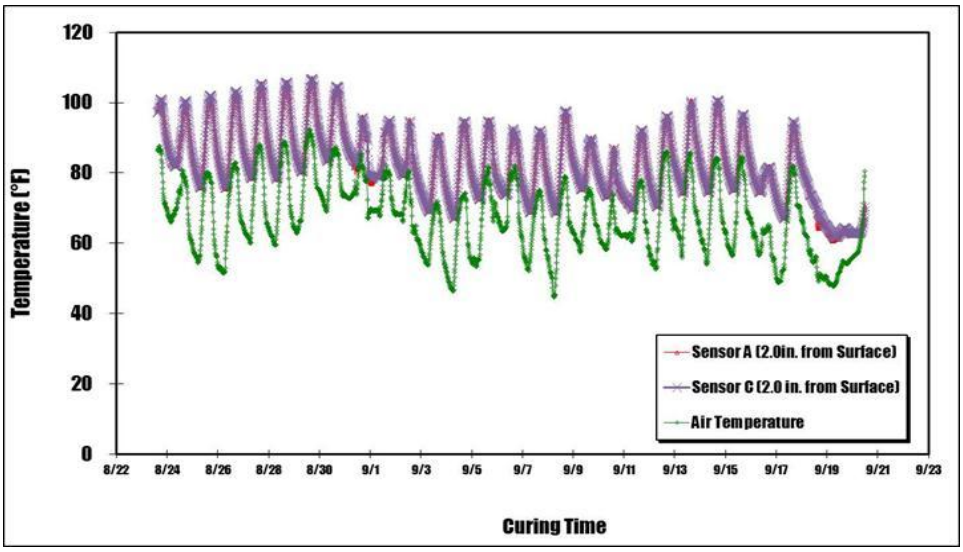

Figure 8-5. Plots of temperature against the curing period from two sensors embedded in the CIR-foam layer and air temperature from weather station device

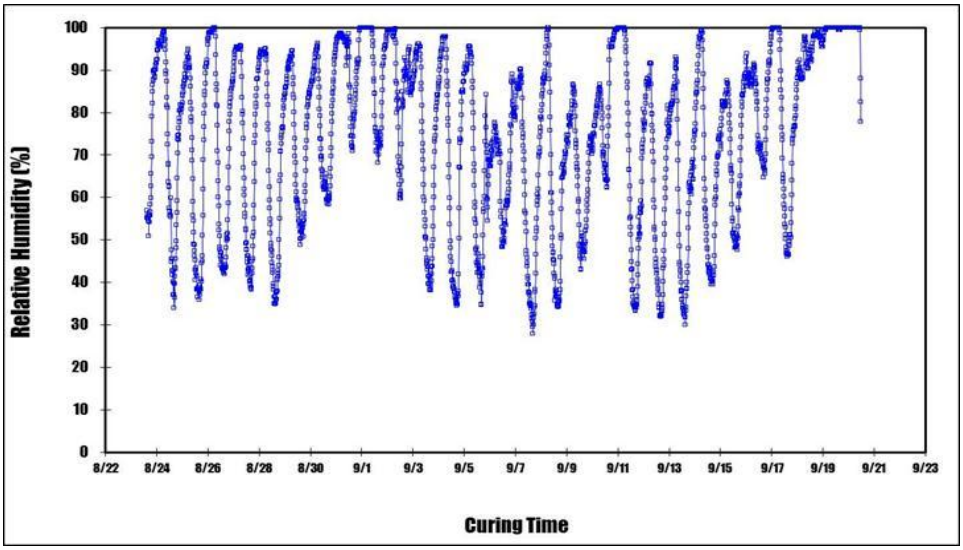

Figure 8-6. Plots of humidity against the curing period from weather station device

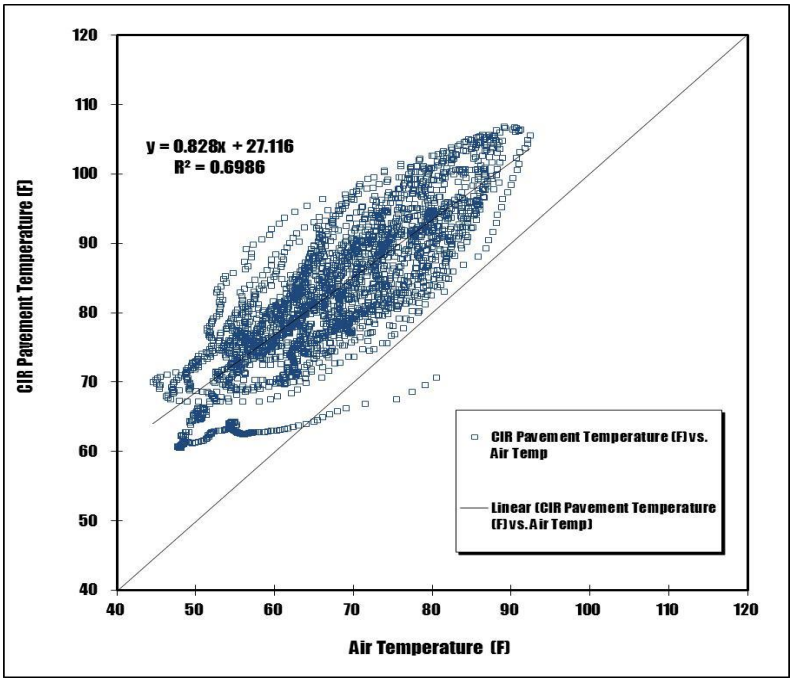

Figure 8-7. Plots of temperature from three sensors embedded in the CIR-foam layer against air temperature from weather station device

As shown in Figure 8-8, using a portable TDR device, field moisture contents were measured from three different locations between 9:30 a.m. to 3:30 p.m. for 14 days between August 25th and September 8th, 2010. Three measurements by a portable TDR device were made from each of three locations and the average value was recorded. Figure 8-8 shows plots of moisture contents measured between August 25th and September 8th, 2010. Although there was no major rainfall until September 1, the moisture content measured by TDR device peaked at 28% on August 27 and decreased to 4% on September 2 right after the heavy rainfall. It support that the TDR device is not consistent with rainfalls.

As shown in Figure 8-9, using nuclear gauge, field moisture contents were measured from one location between 9:00 a.m. to 9:30 a.m. for 5 days between August 23rd and August 28th, 2010. As can be seen from Figure 8-9, the moisture content remained relatively constant between 2.5% and 4.0%. It is interesting to note that the moisture content increased on August 27 although there was no rainfall since construction.

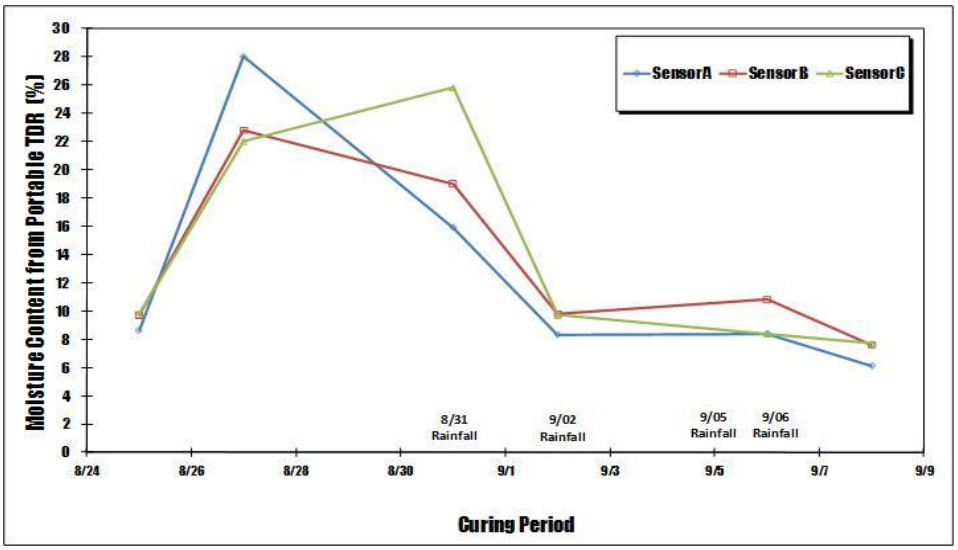

Figure 8-8. Plots of field moisture contents measured by a portable TDR in CIR-foam project site

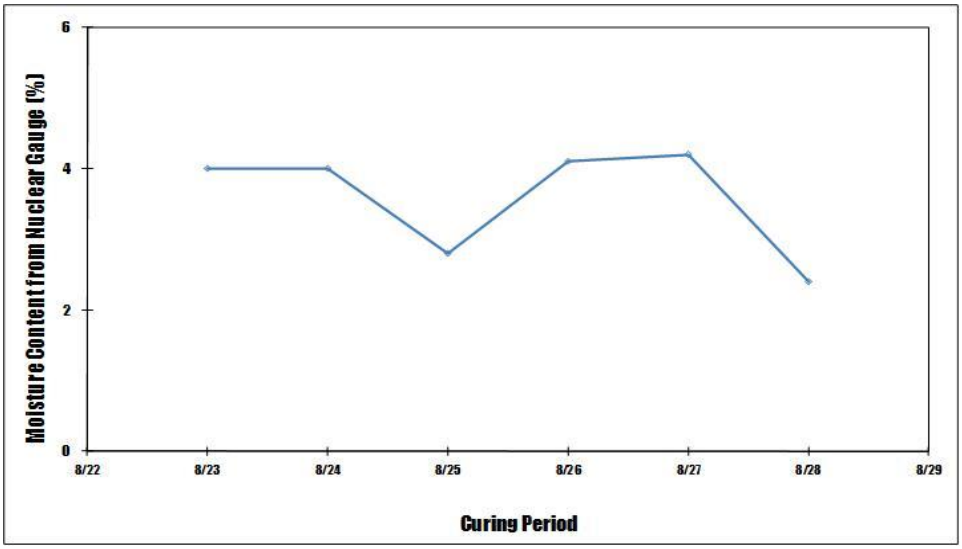

Figure 8-9. Plots of field moisture contents measured by nuclear gauge in CIR-foam project site

Figure 8-10 shows plots of field moisture content measured by moisture sensors against field moisture content measured by a nuclear gauge. It should be noted that the moisture contents measured using a portable TDR, a nuclear gauge, and moisture sensors represent the moisture contents between the surface and 1.5 inches to 2.0 inches from the surface and they were above the minimum moisture content of 2.0% required before an HMA overlay. As shown in Figure 8-10, overall, the moisture contents measured by a portable

TDR device or the moisture sensors were higher than those measured by a nuclear gauge.

Figure 8-11 shows plots of field moisture content measured by a potable TDR against field moisture content measured by moisture sensors. As shown in Figure 8-11, the moisture content measured by a portable TDR device is significantly higher than ones measured by moisture sensors.

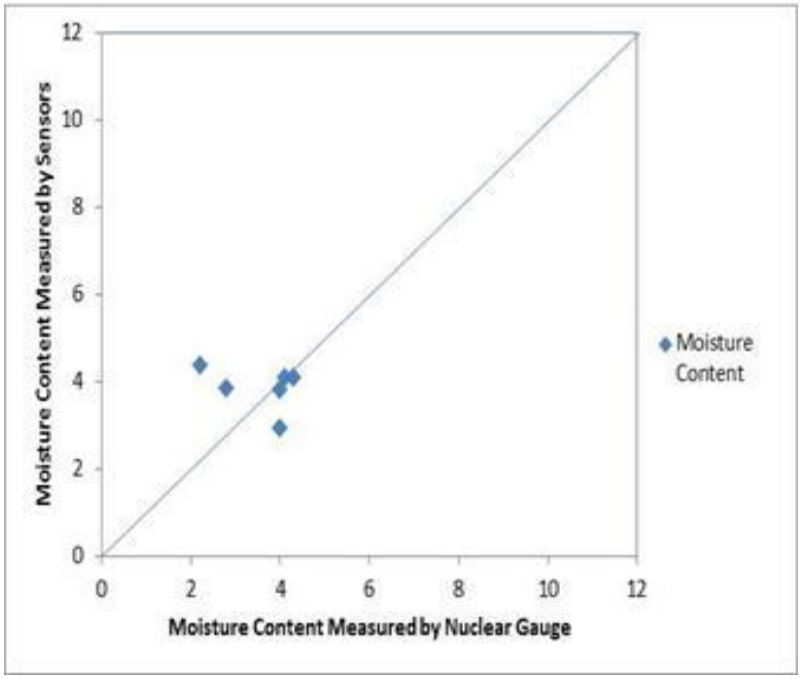

Figure 8-10. Plots of field moisture content measured by moisture sensors against moisture content measured by nuclear gauge

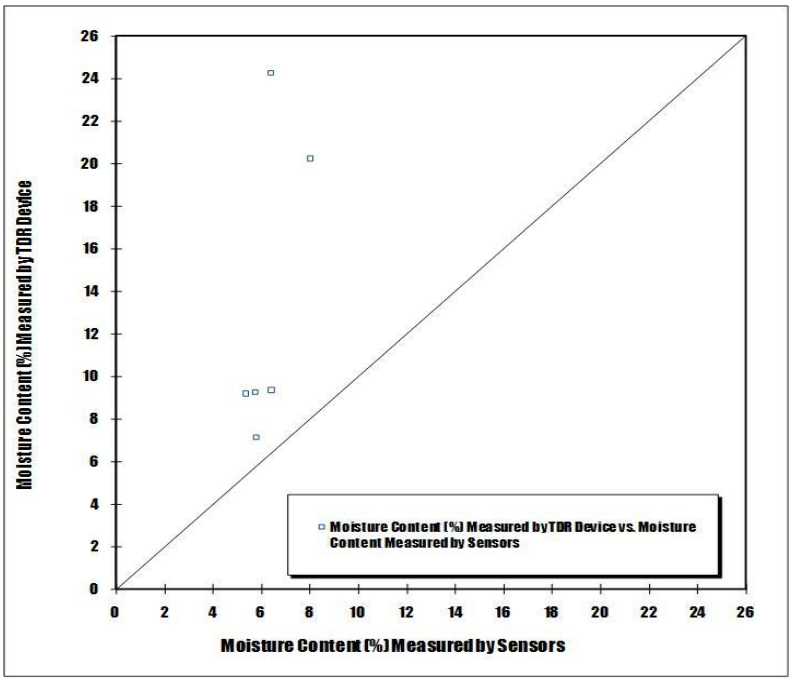

Figure 8-11. Plots of field moisture content measured by a potable TDR against field moisture content measured by moisture sensors

8.2 Measurement of Density and Stiffness

The density and stiffness of the CIR-foam layer were measured using a nuclear gauge and geo-gauge, respectively, throughout the duration of curing. The stiffness was measured at three locations, while the density was measured at only one location.

8.2.1 Density Measurements using Nuclear Gauge

A nuclear gauge was used to measure densities of the CIR-foam layer. As shown in Figure 8-12, density values were measured six times between August 23rd and August 28th, 2010. The density value of CIR-foam layer slightly decreased as the curing time increased but increased at the last day of measurement.

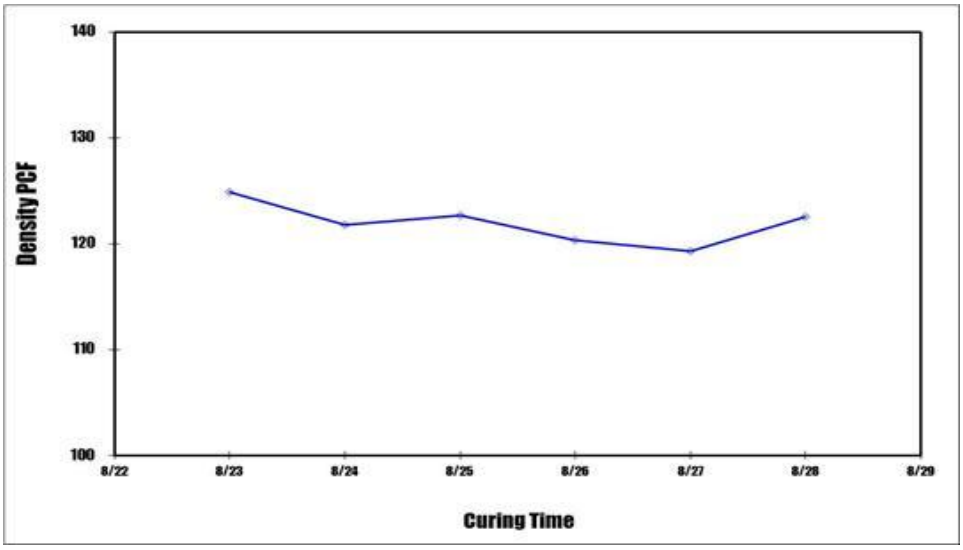

Figure 8-12. Plots of density against curing period from three locations in the CIR-foam layer

8.2.2 Stiffness Measurements using Geo-Gauge

The geo-gauge was used to measure the stiffness of the CIR-foam layer. As shown in Figure 8-13, stiffness was measured six times between August 25th and September 13th, 2010 from three locations (all stiffness measurements were made between 9:30 a.m. to 3:30 p.m.). The stiffness of the CIR-foam layer remained constant during the early stage of curing from August 25 to September 9 but increased significantly above 20 MN/m when the stiffness was measured on September 13. Figure 8-14 shows plots of density measured by a nuclear gauge against stiffness measured by geo-gauge for August 25th, 2010 but there was no correlation between them likely due to a lack of data points. Figure 8-15 showed little correlation between stiffness and moisture content.

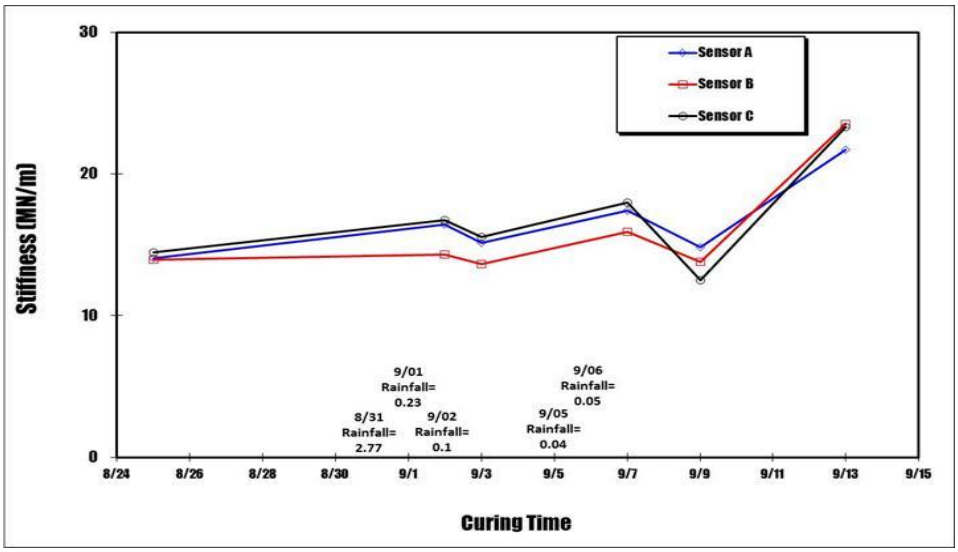

Figure 8-13. Plots of stiffness against the curing period from three locations in the CIR-foam layer

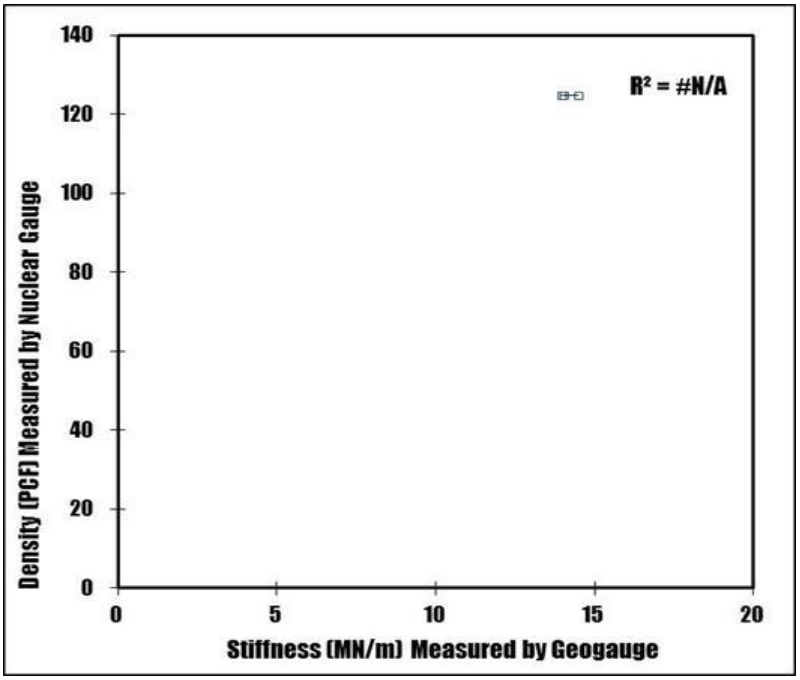

Figure 8-14. Plot of density measured by a nuclear gauge against stiffness measured by geo-gauge

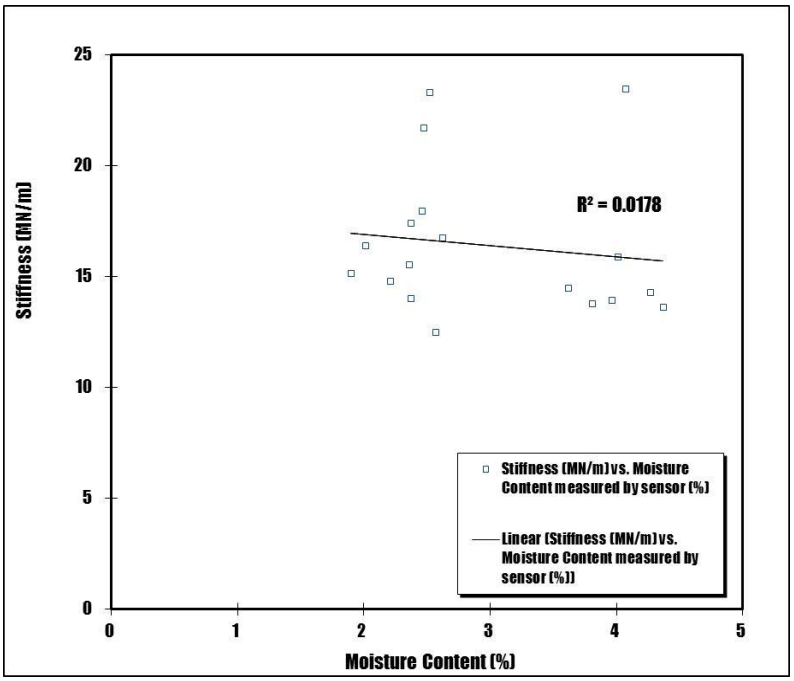

Figure 8-15. Plots of stiffness measured by a geo-gauge against moisture content measured by embedded sensors at three different locations

9. MEASUREMENT OF MOISTURE CONTENT FROM CIR-FOAM PROJECT IN DELAWARE COUNTY

To measure the field moisture contents and temperature of CIR-foam layer, as shown in Figure 9-1, CIR-foam project site in Delaware County was selected. The CIR-foam project site is located on Floyd Rd. north of Highway 136 and was rehabilitated between September 14th and October 25th, 2010.

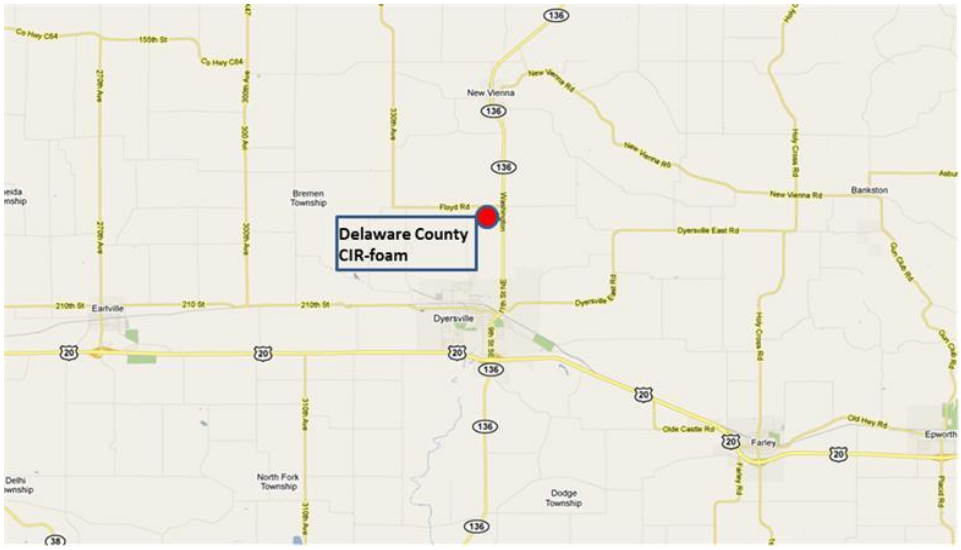

Figure 9-1. Locations of CIR-foam project site in Delaware County

9.1 Measurement of Field Moisture Content and Temperature

To monitor actual moisture contents of the CIR-HFMS-2S-emulsion layer in the field, as shown in Figure 9-2, three ECH2O moisture sensors and three temperature sensors were embedded at 2.0 inches from the surface of the CIR-foam layer. A weather station was also installed to collect air temperature, humidity, rainfall and wind speed.

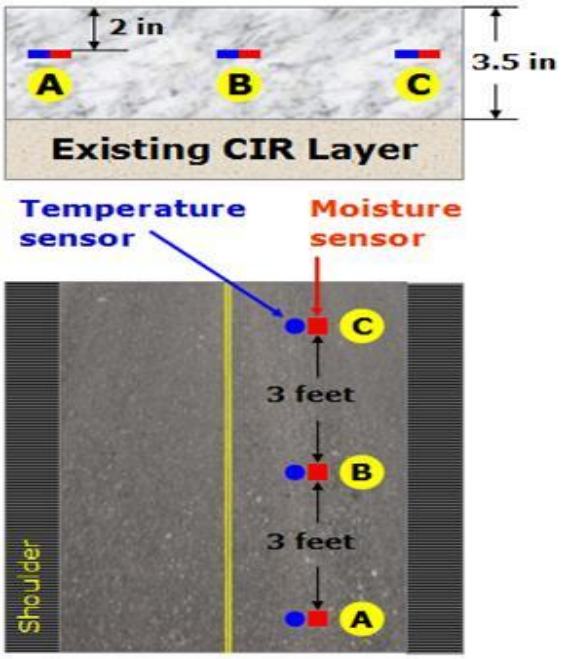

Figure 9-2. Embedded moisture and temperature sensors installed 2.0 inches from the surface of the CIR- foam layer

Figure 9-3, Figure 9-4, Figure 9-5, and Figure 9-6 show plots of moisture content, rainfall, temperature, and humidity, respectively, measured during the curing duration of 41 days when nine rainfalls with a total amount of 2.00 inches occurred. Due to a relatively small amount of rainfall, the moisture content measured by the moisture sensors A and C remained slightly above 2.0%. The moisture content measured by sensor B was consistently significantly higher and its values should be considered inaccurate. The moisture contents before the intermediate HMA overlay were measured at 2.5% from sensor A, 7.7% from sensor B, and 2.0% from sensor C. Despite the actual moisture contents of CIR-foam layer remaining above 2.0%, the intermediate HMA overlay was constructed after 35 days of curing. Figure 9-7 shows plots of temperature from three sensors embedded in the CIR-foam layer against air temperature from the weather station. As shown in Figure 9-7, temperature of CIR-foam layer was slightly higher than air temperature because the weather was cooler in September. The TDR device was damaged and not used at this project site. Due to its inconsistencies in measurement the TDR device was not used for any project sites after this.

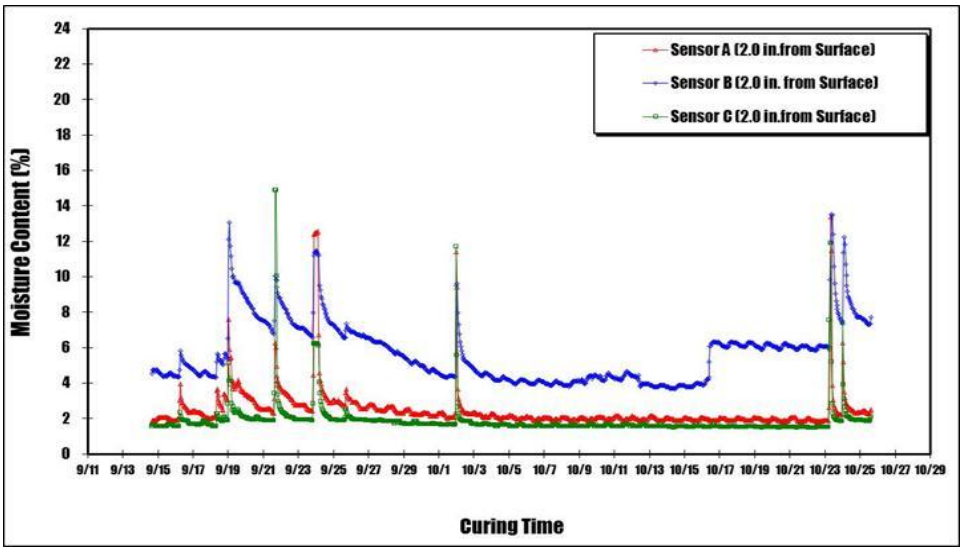

Figure 9-3. Plots of moisture contents against the curing period from three sensors embedded in the CIR-foam layer

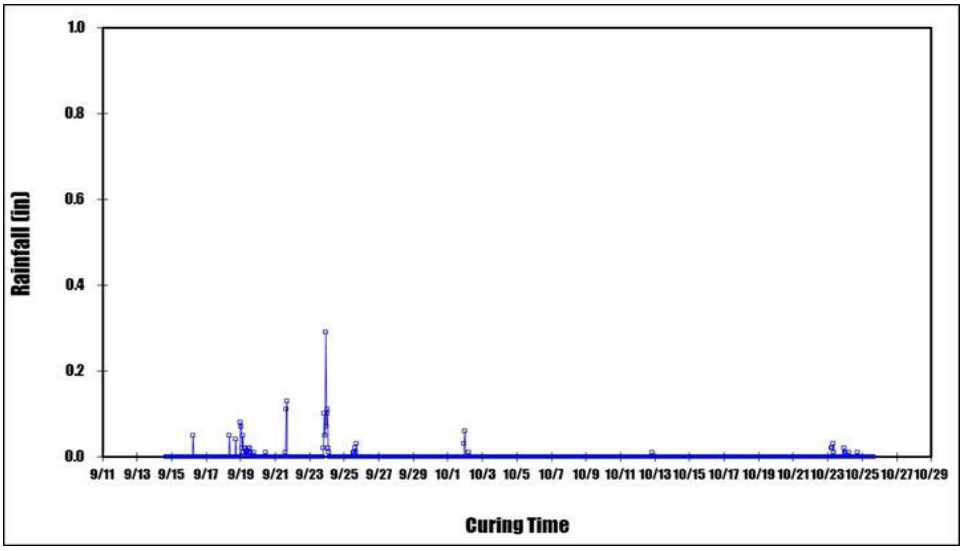

Figure 9-4. Plots of rainfalls against the curing period from weather station device

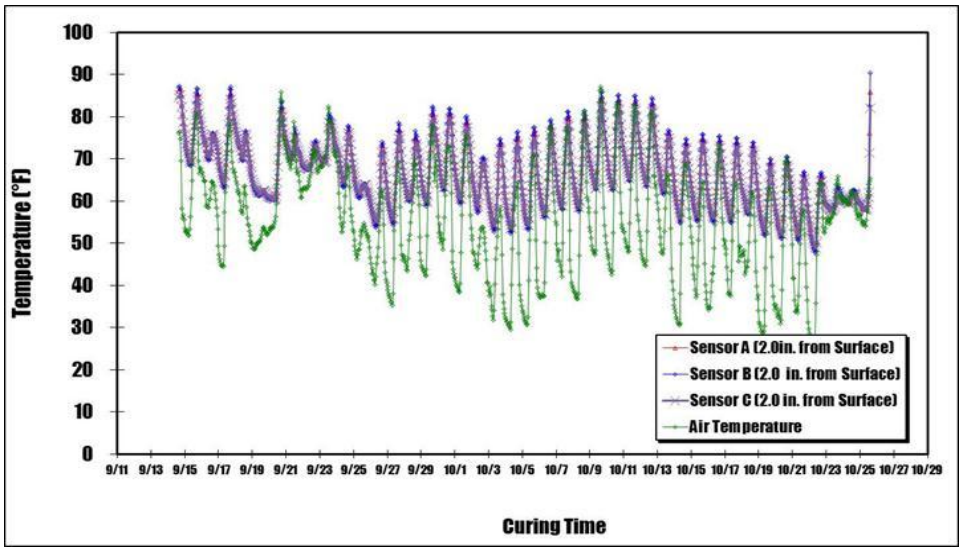

Figure 9-5. Plots of temperature against the curing period from three sensors embedded in the CIR-foam layer and air temperature from weather station device

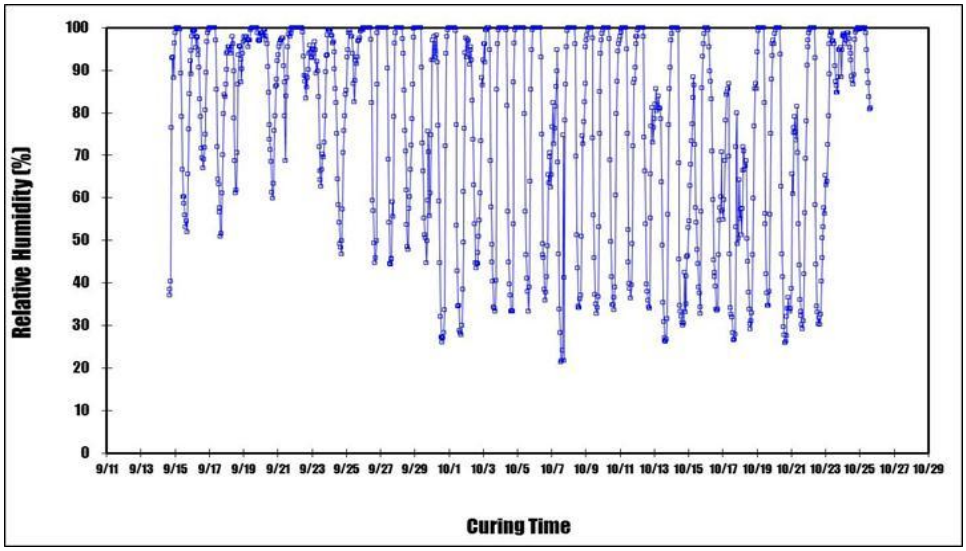

Figure 9-6. Plots of humidity against the curing period from weather station device

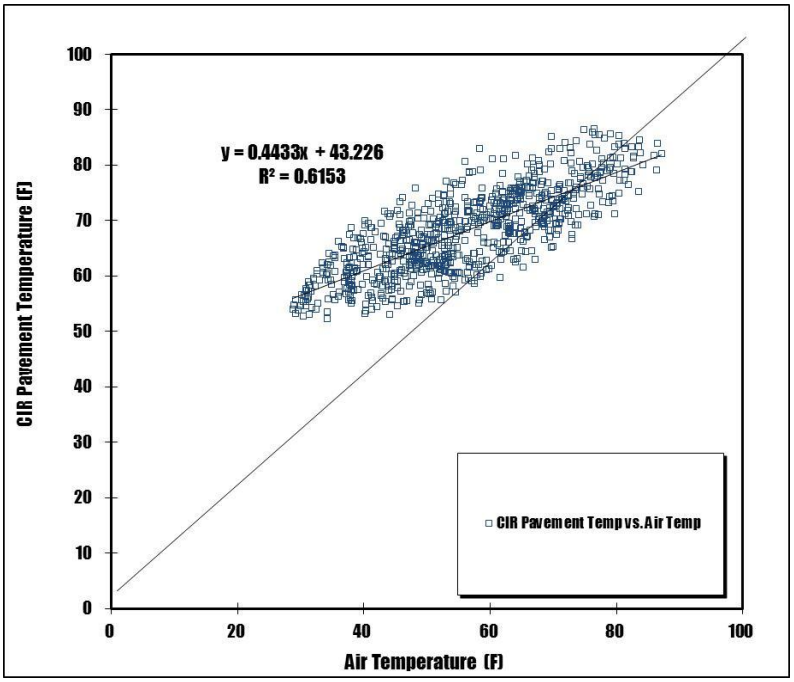

Figure 9-7. Plots of temperature from three sensors embedded in the CIR-foam layer against air temperature from weather station device

9.2 Stiffness Measurements using Geo-Gauge

The stiffness of the CIR-foam layer was measured using a geo-gauge throughout the curing period. The stiffness was measured at three different locations: 1) A (Sensor A), 2) B (Sensor B) and 3) C (Sensor C).

The geo-gauge was used to measure the stiffness of the CIR-foam layer. As shown in Figure 9-8, stiffness was measured six times between September 15th and September 27th, 2010 from three locations (all stiffness measurements were made between 9:30 a.m. to 3:30 p.m.). The stiffness right after the construction was relatively high at around 25 MN/m and the CIR layer did not gain stiffness throughout the curing period. It should be noted that there was no rain and the project was constructed in a late season when the pavement temperature was relatively low. Figure 9-9 shows that there was little correlation between stiffness and moisture content. Moisture contents above 7% were considered outliers for Figure 9-9.

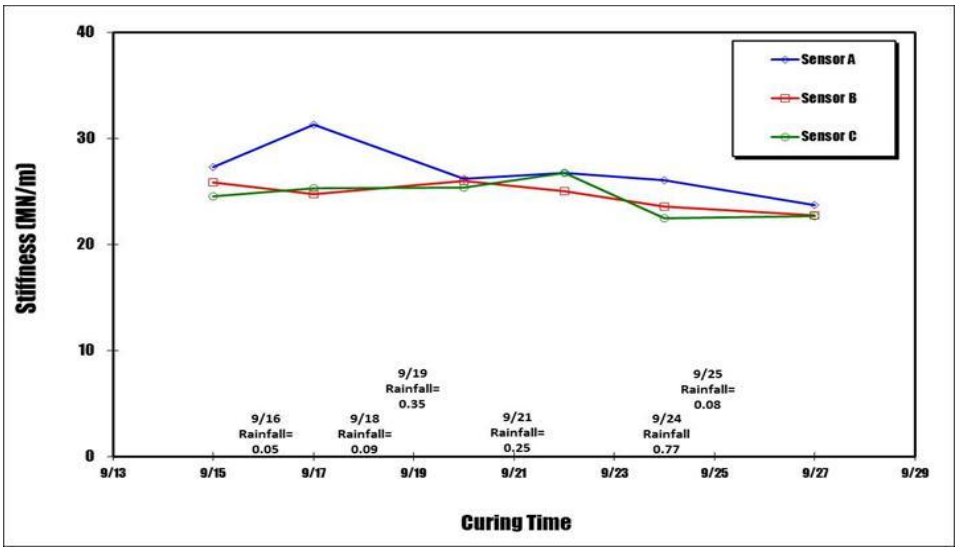

Figure 9-8. Plots of stiffness against the curing period from three locations in the CIR-foam layer

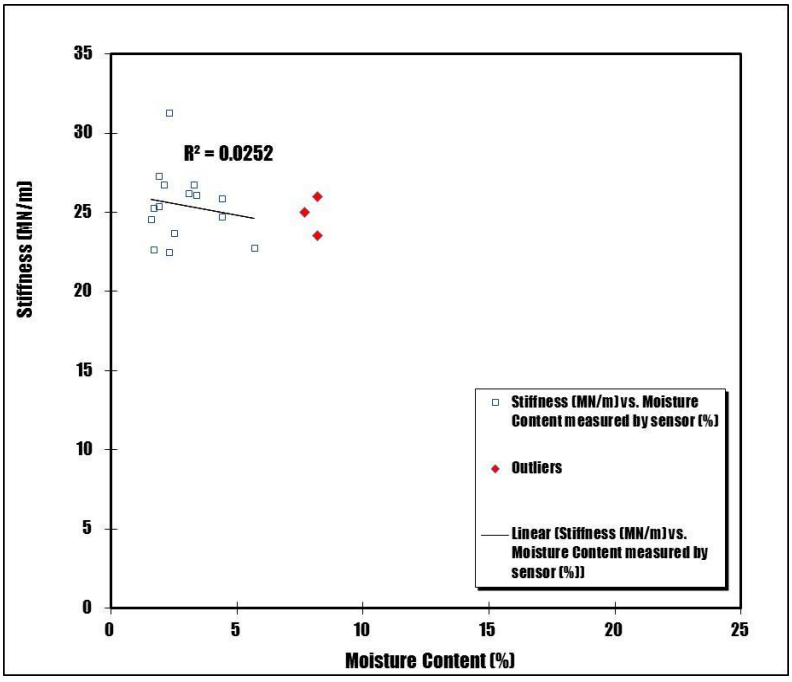

Figure 9-9. Plots of stiffness measured by a geo-gauge against moisture content measured by embedded sensors at three different locations

10. MEASUREMENT OF MOISTURE CONTENT FROM CIR-FOAM PROJECT IN DELAWARE COUNTY 2011

To measure the field moisture contents and temperature of CIR-foam layer, as shown in Figure 10-1, CIR-foam project site in Delaware County was selected. The CIR-foam project site is located on the corner of Canfield and Wellman Rd. The road was rehabilitated between July 11th and August 3rd, 2011.

Figure 10-1. Location of CIR-foam project site in Delaware

10.1 Measurement of Field Moisture Content and Temperature

To monitor actual moisture contents of the CIR-foam layer in the field, as shown in Figure 10-2, three ECH2O moisture sensors and three temperature sensors were embedded at 2.0 inches from the surface of the CIR-foam layer. The moisture sensor at location A became disconnected after 4 days of curing. A weather station was also installed to collect air temperature, humidity, rainfall and wind speed.

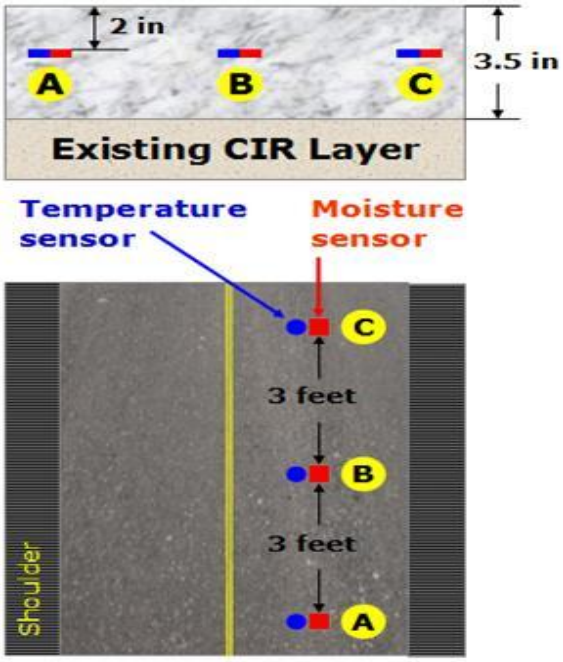

Figure 10-2. Embedded moisture and temperature sensors installed 2.0 inches from the surface of the CIR- foam layer

Figure 10-3, Figure 10-4, Figure 10-5, and Figure 10-6 show plots of moisture content, rainfall, temperature, and humidity, respectively, measured during the curing duration of 24 days when seven rainfalls with a total amount of 8.05 inches have occurred. Throughout the curing period, the moisture contents measured by three sensors were consistent with rainfalls. The moisture contents before the intermediate HMA overlay were measured at 9.26% from sensor B and 9.42% from sensor C. Despite the actual moisture contents of CIR-foam layer remaining above 2.0%, the intermediate HMA overlay was constructed after 24 days of curing. Figure 10-7 shows plots of temperature from the three sensors embedded in the CIR-foam layer against air temperature from the weather station. As shown in Figure 10-7, as expected, temperature of CIR-foam layer was significantly higher than air temperature.

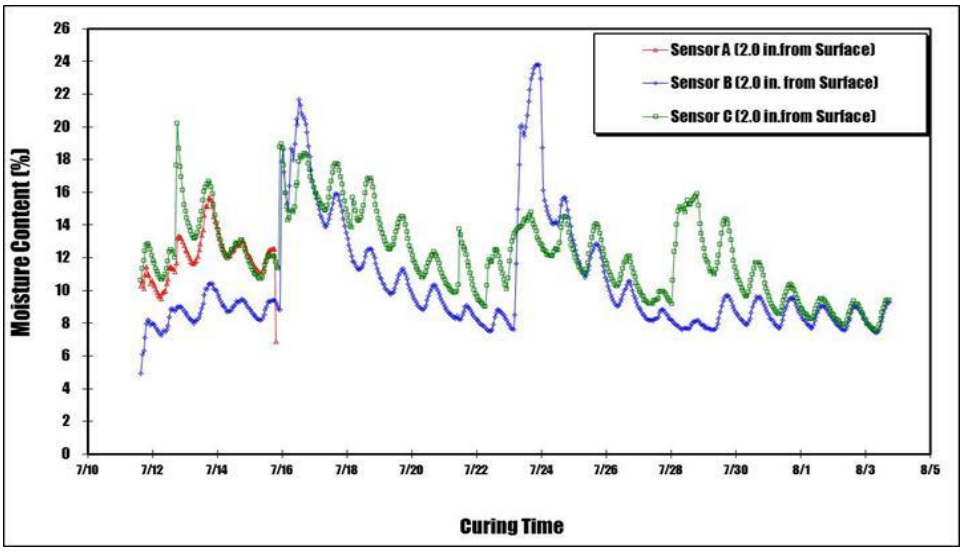

Figure 10-3. Plots of moisture contents against the curing period from three sensors embedded in the CIR-foam layer

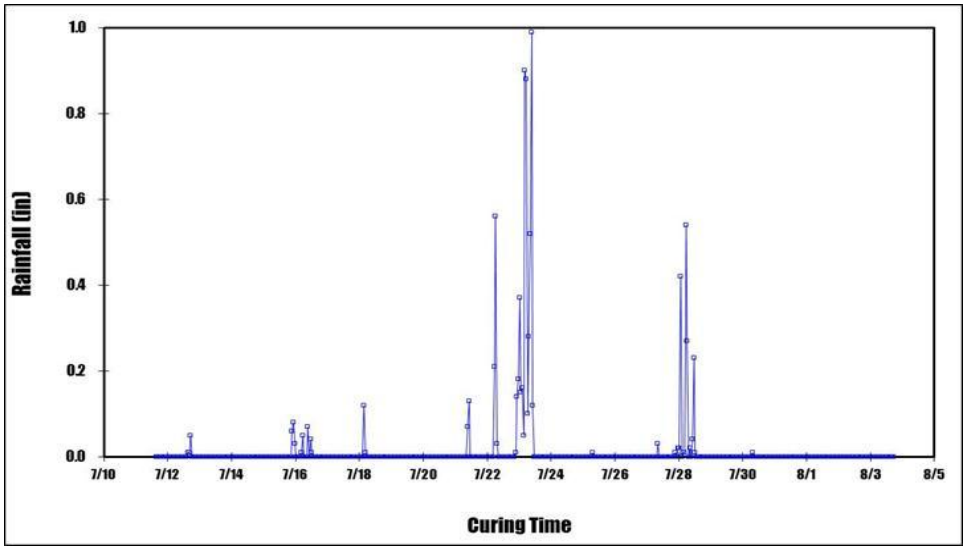

Figure 10-4. Plots of rainfalls against the curing period from weather station device

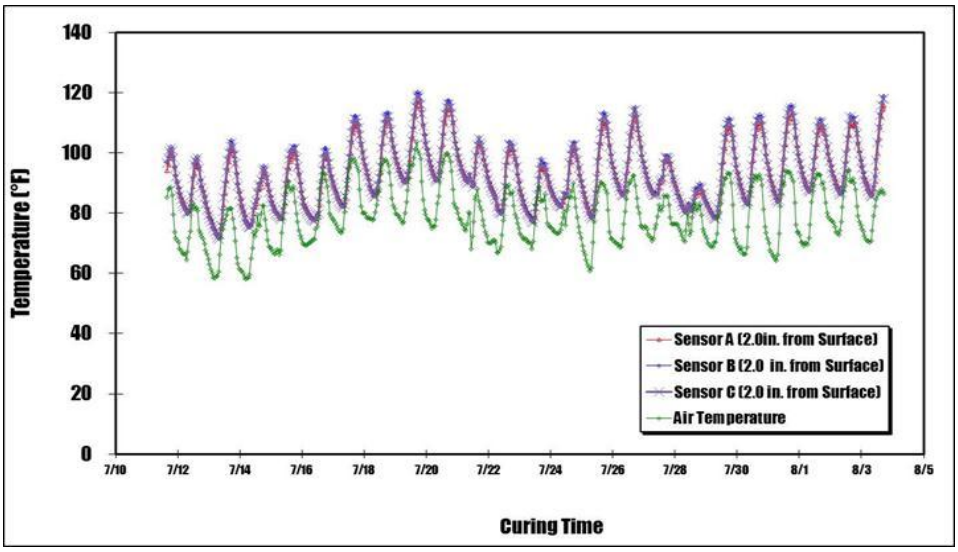

Figure 10-5. Plots of temperature against the curing period from three sensors embedded in the CIR-foam layer and air temperature from weather station device

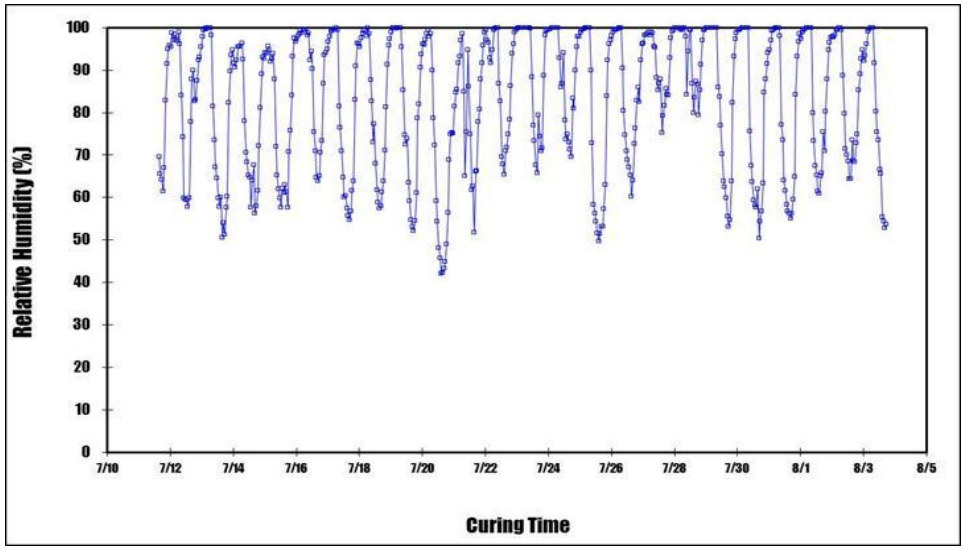

Figure 10-6. Plots of humidity against the curing period from weather station device

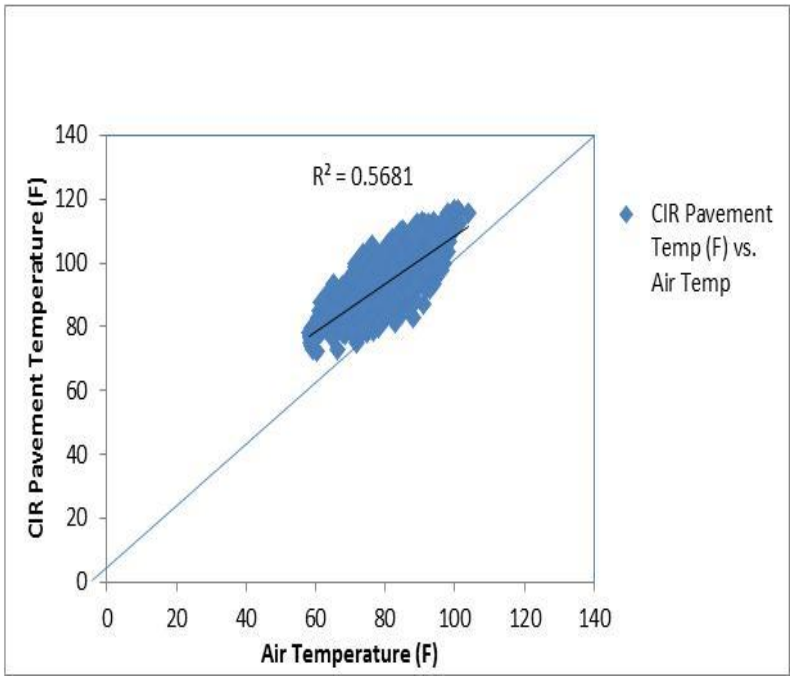

Figure 10-7. Plots of temperature from three sensors embedded in the CIR-foam layer against air temperature from weather station device

Based off of portable TDR moisture data from the previous sites it was decided that the portable TDR device was unreliable for measuring moisture content of asphalt pavement. Furthermore, the TDR device was not used to measure moisture content on the 2 projects monitored in the summer of 2011.

As shown in Figure 10-8, using a nuclear gauge, field moisture contents were measured from one location between 9:00 a.m. to 9:30 a.m. for 5 days between July 11th and July 15th, 2011. As can be seen from Figure 10-8, the moisture content decreased slightly from 10.8% to 9.8%. It should be noted that these moisture contents are fairly high.

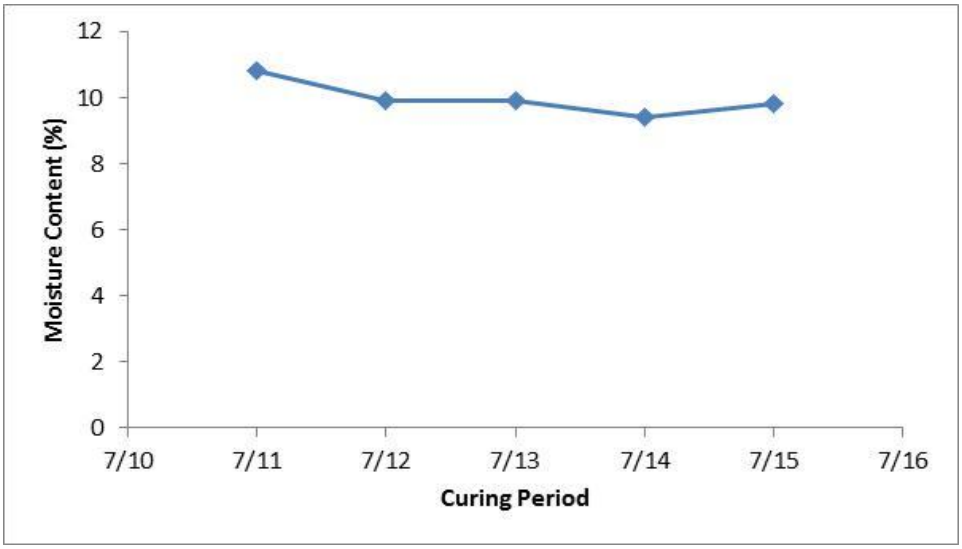

Figure 10-8. Plots of field moisture contents measured by nuclear gauge in CIR-foam project site

Figure 10-9 shows plots of field moisture content measured by the nuclear gauge against moisture contents measured by the embedded moisture sensors. It should be noted that the moisture contents measured using a nuclear gauge and moisture sensors represent the moisture contents between the surface and 1.5 inches to 2.0 inches from the surface and they were above the minimum moisture content of 2.0% required before an HMA overlay. As shown in Figure 10-9, overall, the moisture contents measured by the embedded sensors were higher than those measured by the nuclear gauge.

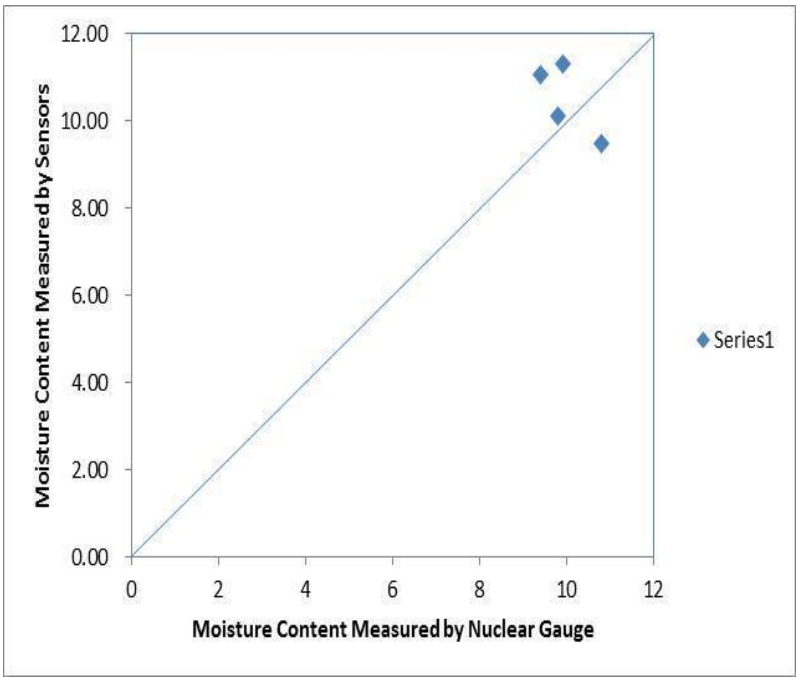

Figure 10-9. Plots of field moisture content measured by a nuclear gauge against field moisture content measured by the embedded moisture sensors

10.2 Measurement of Density and Stiffness

The density and stiffness of the CIR-foam layer were measured using a nuclear gauge and geo-gauge, respectively, throughout the duration of curing. The stiffness was measured at three locations, while the density was measured at only one location.

10.2.1 Density Measurements using Nuclear Gauge

A nuclear gauge was used to measure densities of the CIR-foam layer. As shown in Figure 10-10, density values were measured five times between July 11th and July 15th, 2011. The density value of CIR-foam layer increased at first then had a decrease on 7/13. The density then increased during the rest of the measurement period.

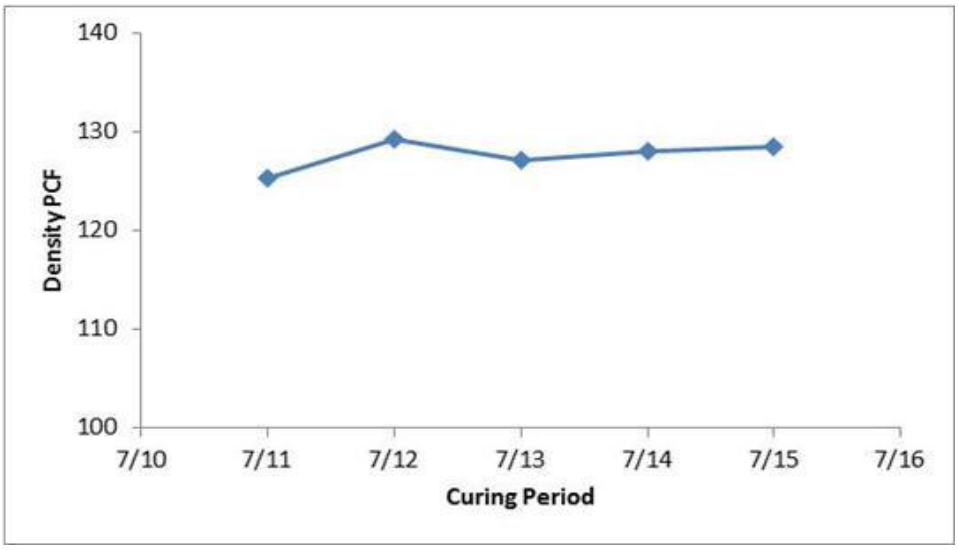

Figure 10-10. Plots of density against curing period from three locations in the CIR-foam layer

10.2.2 Stiffness Measurements using Geo-Gauge

The geo-gauge was used to measure the stiffness of the CIR-foam layer. In previous projects the stiffness was measured every 2-3 days during the curing period. For all projects during the summer of 2011 it was decided to measure stiffness every day in order to see a more detailed trend. As shown in Figure 10-11, stiffness was measured between July 11th and August 1st, 2011 from three locations (all stiffness measurements were made between 9:30 a.m. to 12:00 p.m.). The stiffness of the CIR-foam layer began by increasing after construction. There were some noticeable decreases in stiffness after rainfalls throughout the curing period with the most notable occurring a little after 7/14, in which a rainfall of 0.07 in. occurred. There was another dip beginning on 7/22 after an extremely large rainfall of 4.85 in. and again on 7/28 after a rainfall of 1.6 in. The stiffness tended to decrease after significant rain and then began to start increasing again each time. Overall, the stiffness fluctuated but was overlay occurred at roughly the same stiffness that the project bean at. Figure 10-12 shows plots of density measured by a nuclear gauge against stiffness measured by geo-gauge for July 11th, July 13th, July 14th and July 15th but there was little correlation between them. Figure 10-13 shows that there is little correlation between stiffness and moisture content. Moisture contents above 7.0% were considered outliers for the correlation and as seen every data point was an outlier.

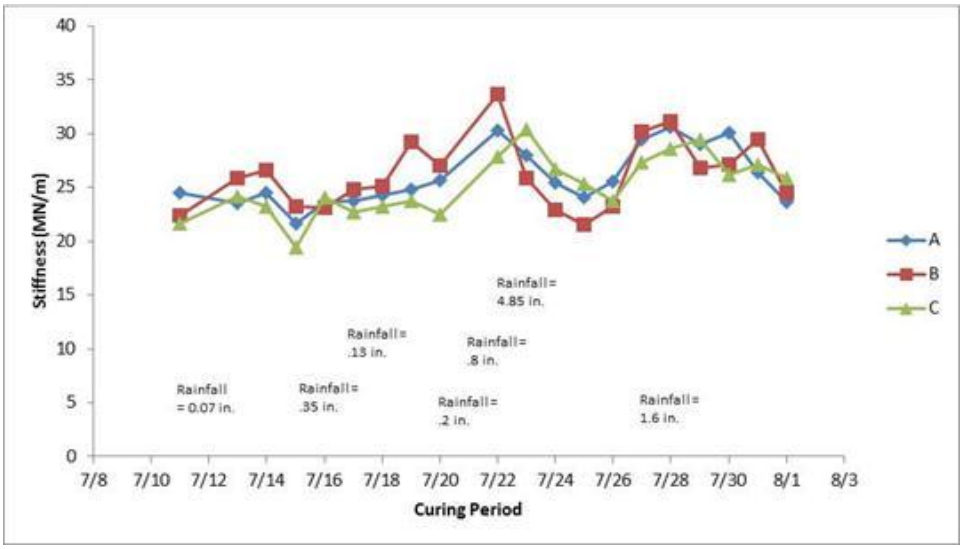

Figure 10-11. Plots of stiffness against the curing period from three locations in the CIR-foam layer

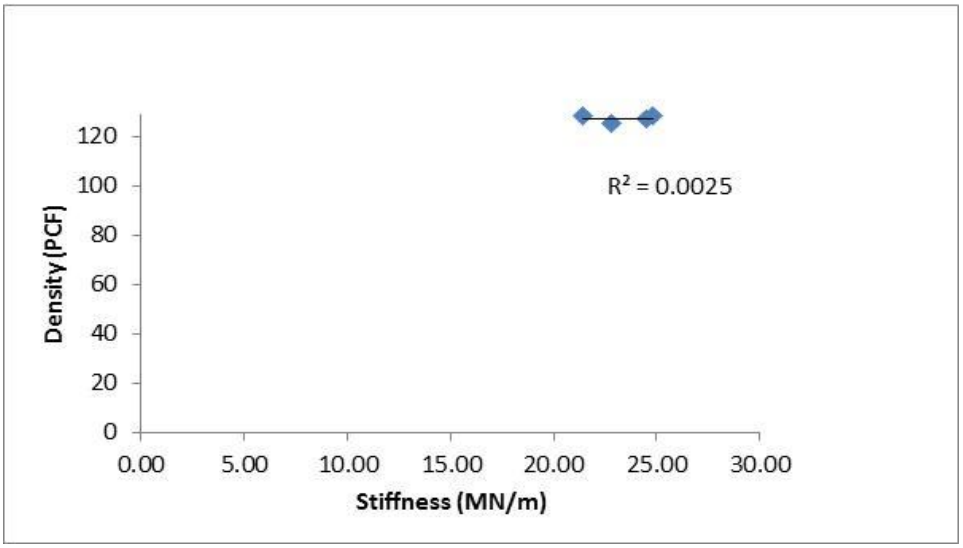

Figure 10-12. Plot of density measured by a nuclear gauge against stiffness measured by geo-gauge

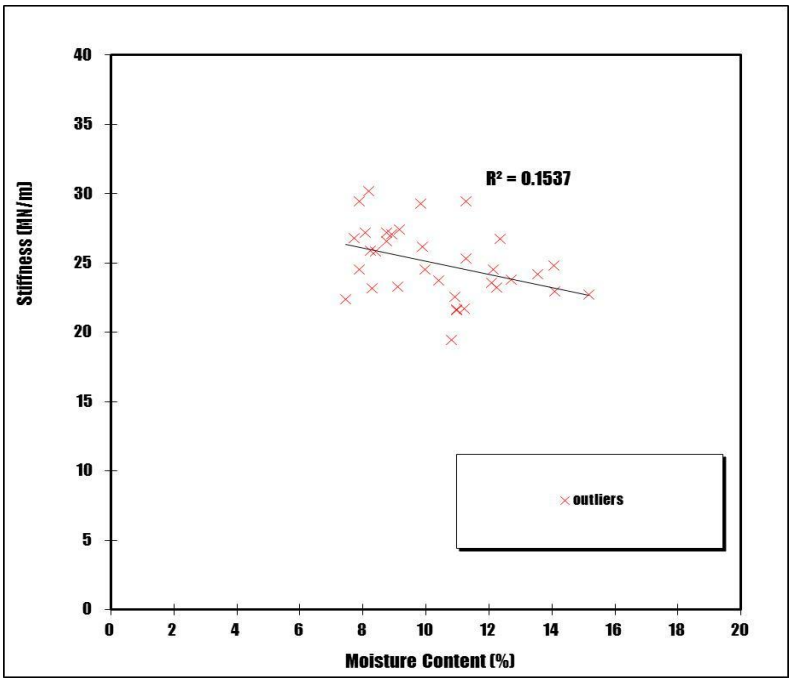

Figure 10-13. Plots of stiffness measured by a geo-gauge against moisture content measured by embedded sensors at three different locations

11. MEASUREMENT OF MOISTURE CONTENT FROM CIR-FOAM PROJECT IN BLACK HAWK COUNTY

To measure the field moisture contents and temperature of CIR-foam layer, as shown in Figure 11-1, CIR-foam project site in Black Hawk County was selected. The CIR-foam project site is located on County Highway D13 in Manchester, Iowa. The road was rehabilitated between July 21st and August 11th, 2011.

Figure 11-1. Location of CIR-foam project site in Black Hawk

11.1 Measurement of Field Moisture Content and Temperature

To monitor actual moisture contents of the CIR-foam layer in the field, as shown in Figure 11-2, three ECH2O moisture sensors and three temperature sensors were embedded at 2.0 inches from the surface of the CIR-foam layer. A weather station was also installed to collect air temperature, humidity, rainfall and wind speed.

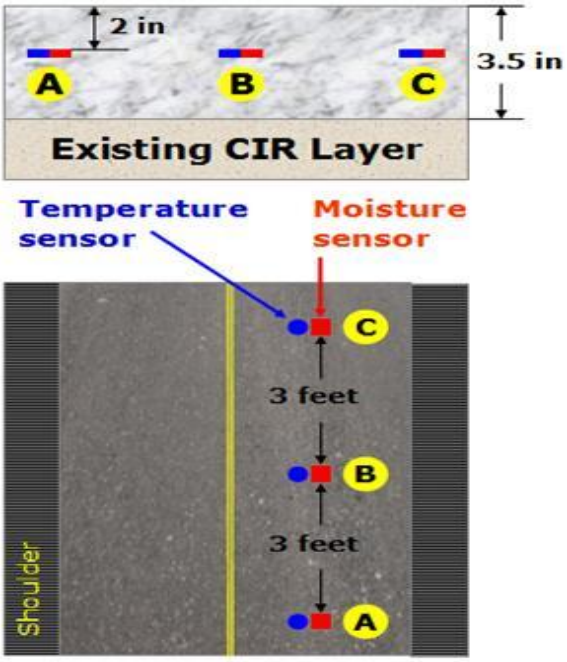

Figure 11-2. Embedded moisture and temperature sensors installed 2.0 inches from the surface of the CIR- foam layer

Figure 11-3, Figure 11-4, Figure 11-5, and Figure 11-6 show plots of moisture content, rainfall, temperature, and humidity, respectively, measured during the curing duration of 21 days when four rainfalls with a total amount of 3.91 inches have occurred. Throughout the curing period, the moisture contents measured by three sensors were consistent with rainfalls. The moisture contents before the intermediate HMA overlay were measured at 6.48% from sensor A, 6.90% from sensor B and 4.63% from sensor C. Despite the actual moisture contents of CIR-foam layer remaining above 2.0%, the intermediate HMA overlay was constructed after 21 days of curing. Figure 11-7 shows plots of temperature from the three sensors embedded in the CIR-foam layer against air temperature from the weather station. As shown in Figure 11-7, as expected, temperature of CIR-foam layer was significantly higher than air temperature.

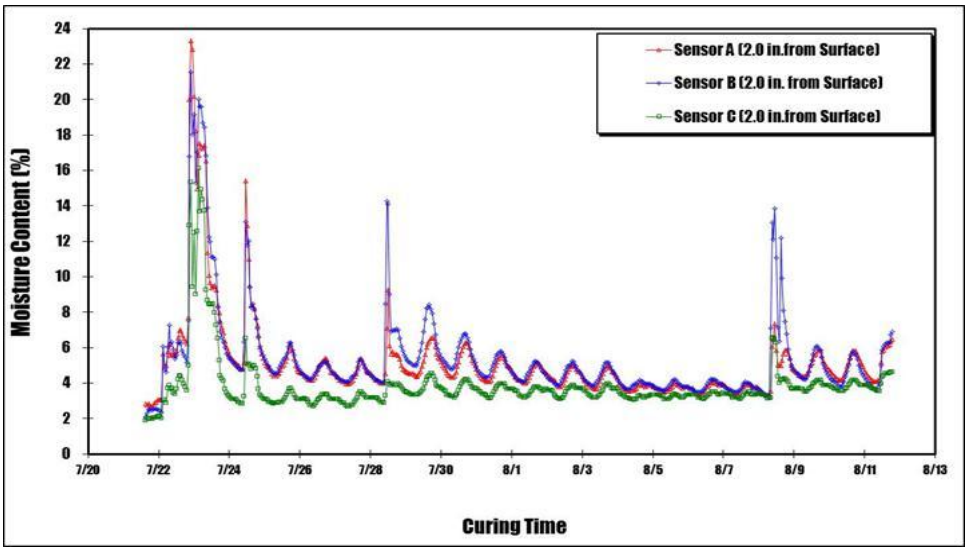

Figure 11-3. Plots of moisture contents against the curing period from three sensors embedded in the CIR-foam layer

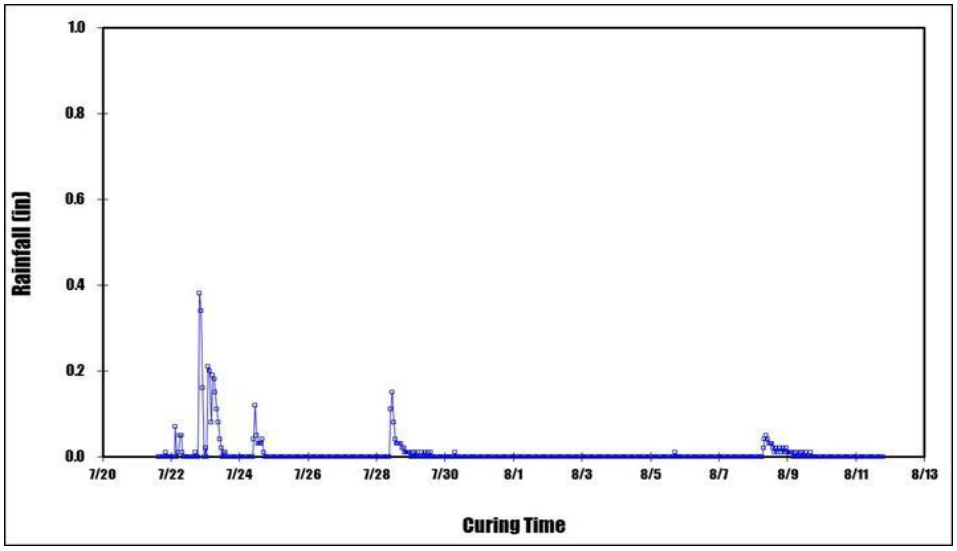

Figure 11-4. Plots of rainfalls against the curing period from weather station device

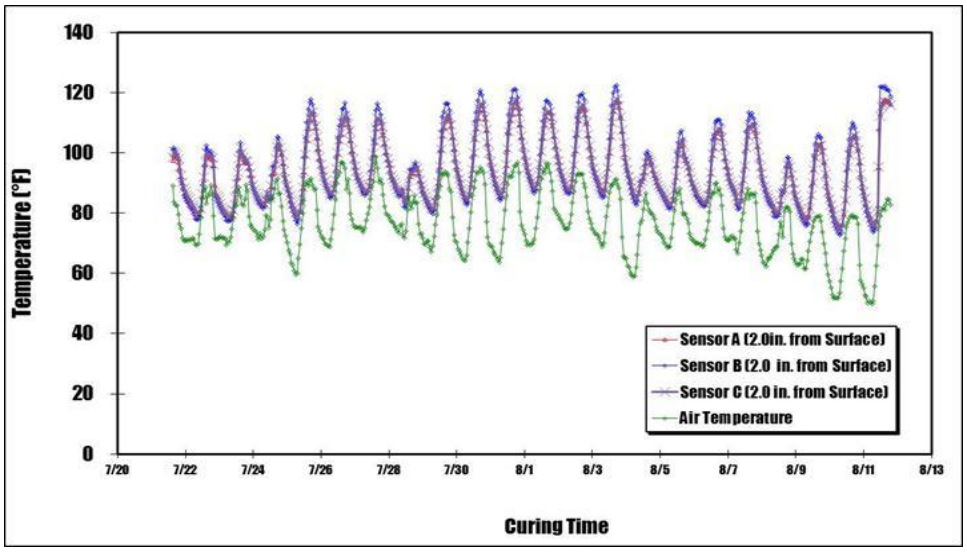

Figure 11-5. Plots of temperature against the curing period from three sensors embedded in the CIR-foam layer and air temperature from weather station device

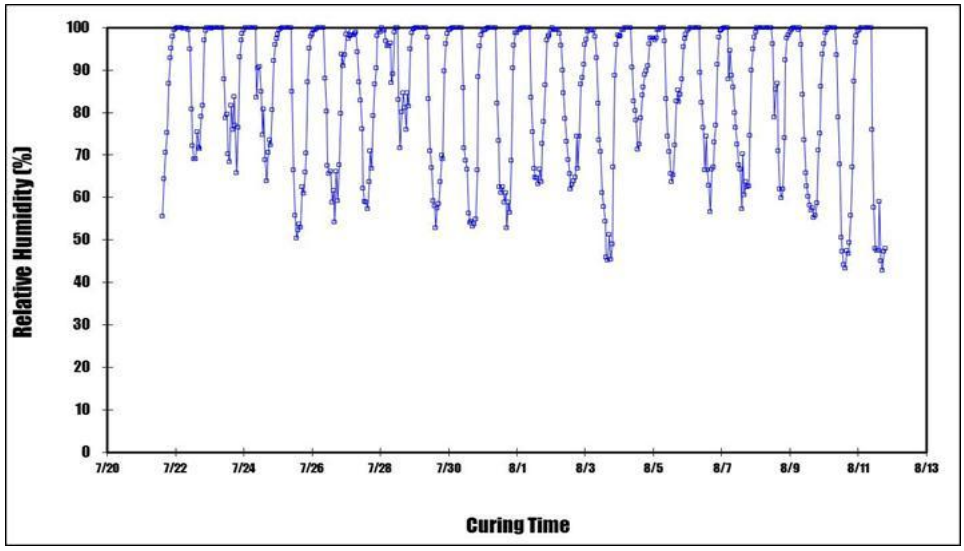

Figure 11-6. Plots of humidity against the curing period from weather station device

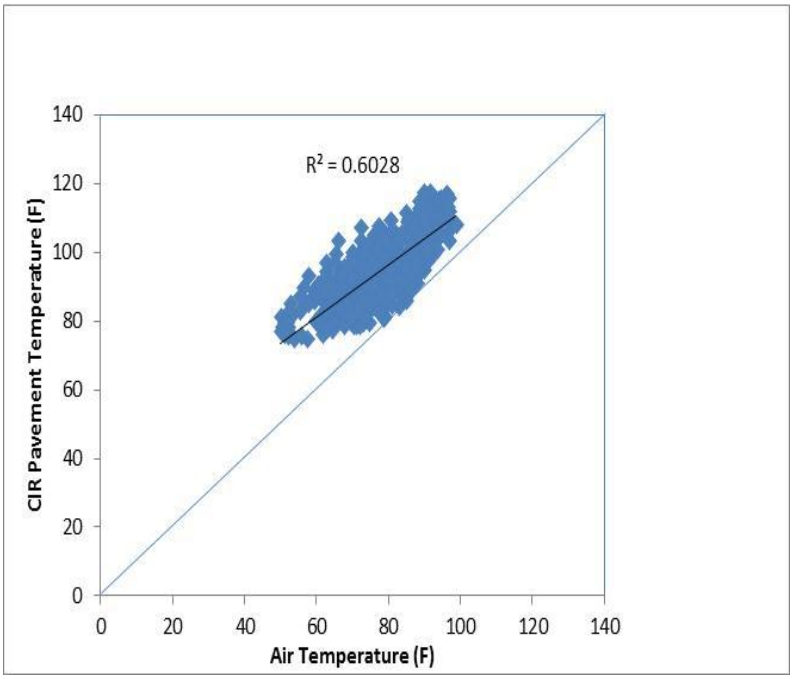

Figure 11-7. Plots of temperature from three sensors embedded in the CIR-foam layer against air temperature from weather station device

As stated earlier, the TDR device was not used to measure moisture content on the 2 projects monitored in the summer of 2011.

As shown in Figure 11-8, using a nuclear gauge, field moisture contents were measured from one location between 9:00 a.m. to 9:30 a.m. on 3 days between July 22nd and July 26th, 2011. As can be seen from Figure 11-8, the moisture content decreased slightly from 12.0% to 11.0%.

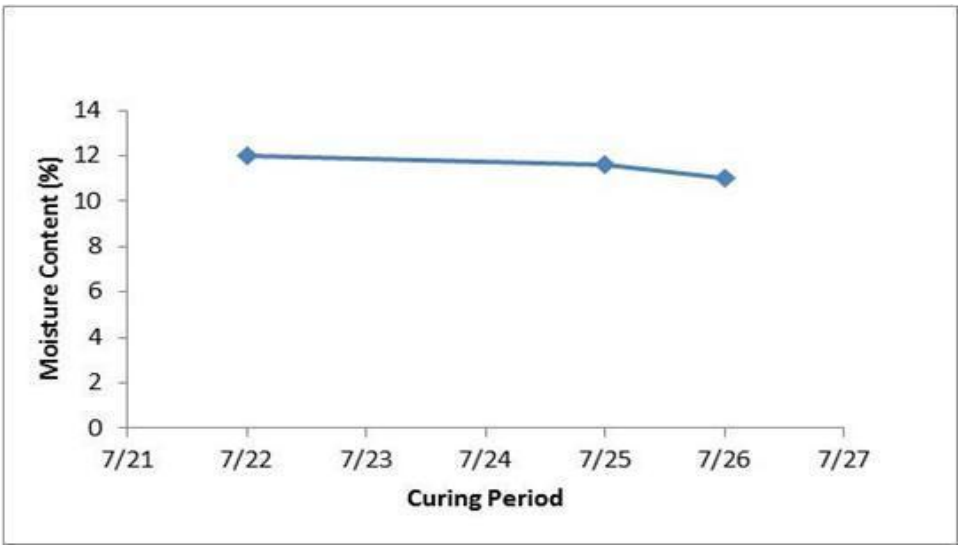

Figure 11-8. Plots of field moisture contents measured by nuclear gauge in CIR-foam project site

Figure 11-9 shows plots of field moisture content measured by the nuclear gauge against moisture contents measured by the embedded moisture sensors. It should be noted that the moisture contents measured using a nuclear gauge and moisture sensors represent the moisture contents between the surface and 1.5 inches to 2.0 inches from the surface and they were above the minimum moisture content of 2.0% required before an HMA overlay. As shown in Figure 11-9, overall, the moisture contents measured by the embedded sensors were higher than those measured by the nuclear gauge.

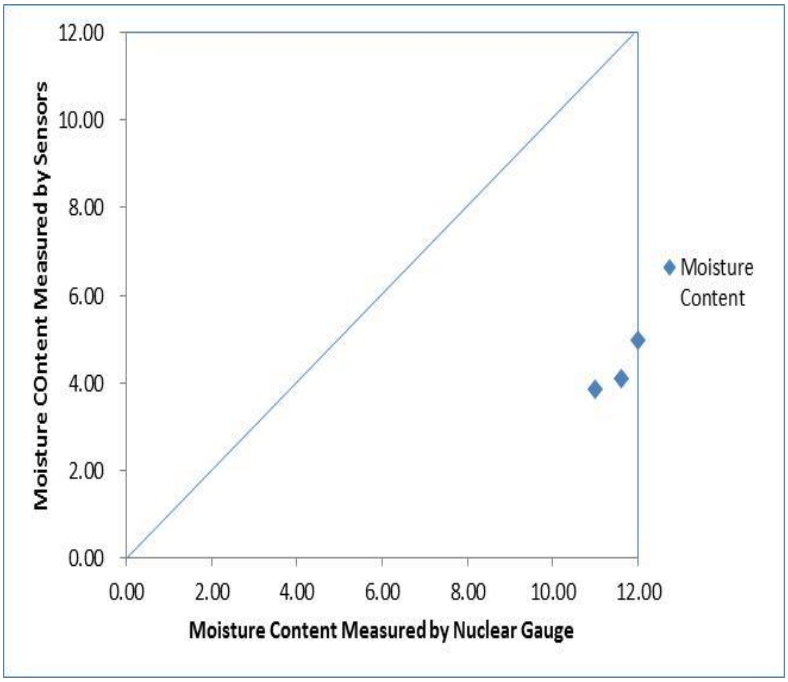

Figure 11-9. Plots of field moisture content measured by a nuclear gauge against field moisture content measured by the embedded moisture sensors

11.2 Measurement of Density and Stiffness

The density and stiffness of the CIR-foam layer were measured using a nuclear gauge and geo-gauge, respectively, throughout the duration of curing. The stiffness was measured at three locations, while the density was measured at only one location.

11.2.1 Density Measurements using Nuclear Gauge

A nuclear gauge was used to measure densities of the CIR-foam layer. As shown in Figure 11-10, density values were measured three times between July 22nd and July 26th, 2011. The density value of CIR-foam layer increased in a liner fashion during the measurement period.

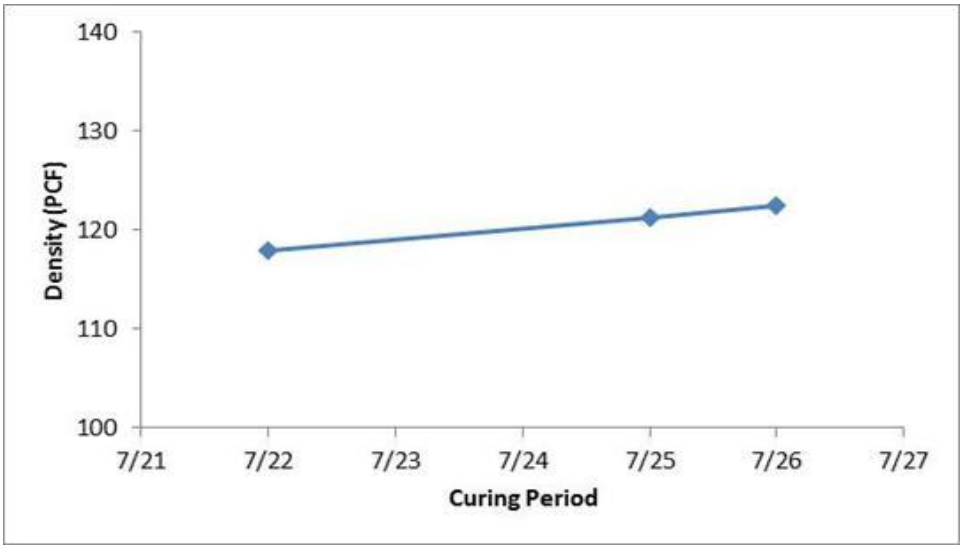

Figure 11-10. Plots of density against curing period from three locations in the CIR-foam layer

11.2.2 Stiffness Measurements using Geo-Gauge

The geo-gauge was used to measure the stiffness of the CIR-foam layer. In previous projects the stiffness was measured every 2-3 days during the curing period. For all projects during the summer of 2011 it was decided to measure stiffness every day in order to see a more detailed trend. As shown in Figure 11-11, stiffness was measured between July 22nd and August 10th, 2011 from three locations (all stiffness measurements were made between 9:30 a.m. to 12:00 p.m.). The stiffness of the CIR-foam layer began by increasing after construction. There were some noticeable decreases in stiffness after rainfalls throughout the curing period with the most notable occurring a little after 7/23, in which an extremely large rainfall of 2.19 in. occurred. There was another dip beginning on 7/29 after a 0.65 in. rainfall and 8/8 after a 0.50 in. rainfall. The stiffness tended to decrease after significant rain and then began to start increasing again each time. Overall, the stiffness increased from around the 25 MN/m range to the low 30 MN/m range. Figure 11-12 shows plots of density measured by a nuclear gauge against stiffness measured by geo-gauge for July 22nd, July 25th, and July 26th but there was little correlation between them. Figure 11-13 shows little correlation between stiffness and moisture content. Moisture contents above 7% were considered outliers for Figure 11-13.

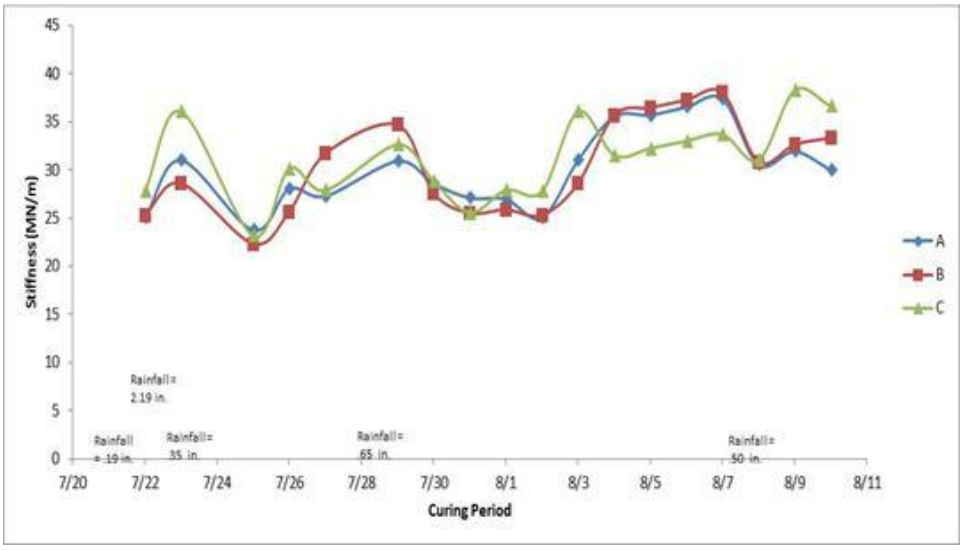

Figure 11-11. Plots of stiffness against the curing period from three locations in the CIR-foam layer

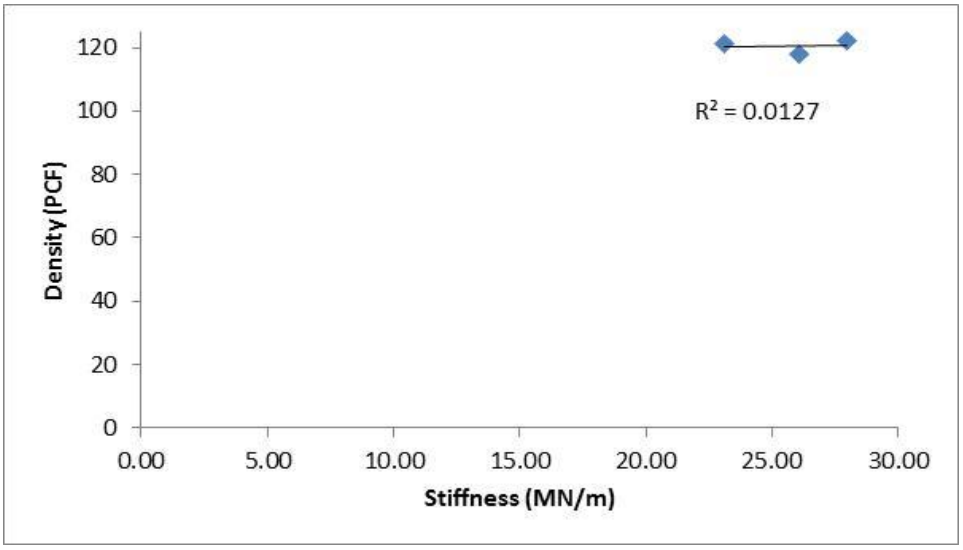

Figure 11-12. Plot of density measured by a nuclear gauge against stiffness measured by geo-gauge

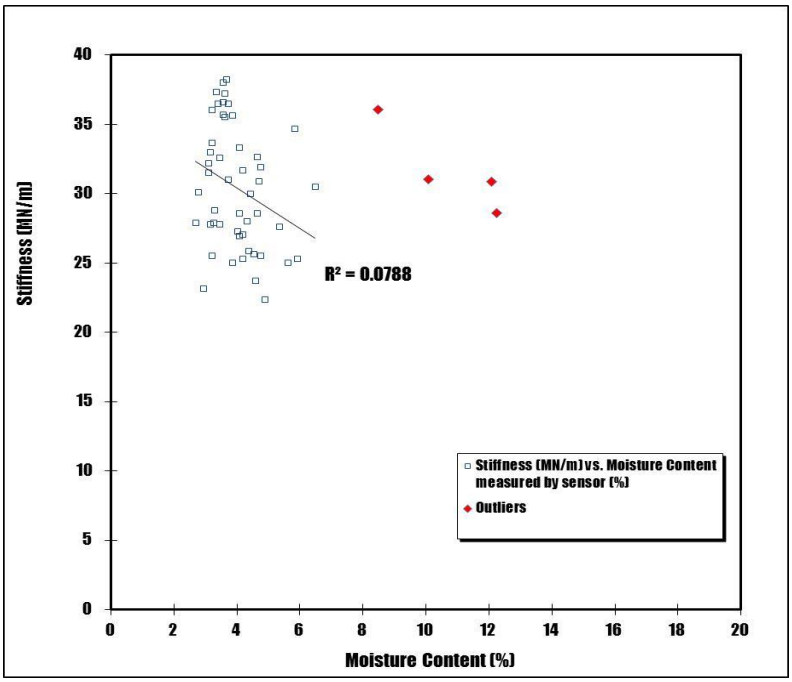

Figure 11-13. Plots of stiffness measured by a geo-gauge against moisture content measured by embedded sensors at three different locations

12. Development of Moisture Loss Index for CIR Layer

To develop moisture loss indices for CIR layer, the actual moisture content of CIR layer was measured by ECH2O moisture sensors and climate data were collected from the weather stations installed at CIR project sites.

To predict the moisture change in the CIR layer over time, using a multiple linear regression technique, the following moisture loss index formula was developed as a function of initial moisture condition, average CIR layer temperature, and average humidity and average wind speed.

$$\Delta MC/hr = a1 + a2\ IMC + a3\ Temp + a4\ Hum + a5\ Wind$$

where,

$\Delta MC/hr$ = Moisture change per hour during curing time

IMC = Initial moisture content of CIR layer right after construction

Temp = Average CIR layer temperature (°F) during curing time

Hum = Average humidity (%) during curing time

Wind= Average wind speed (mph) during curing time

a1, a2, a3, a4, a5 = multiple linear regression coefficients

12.1 CIR-HFMS-2S-emulsion Project Site in Clinton County

Moisture contents and climatic data were collected from the CIR-HFMS-2S-emulsion layer in Clinton County. A new set of moisture content data was created when the rainfall had occurred. After discarding the initial moisture contents above 12% (unusually high), thirty-two moisture content data sets from sensor A, thirty-four sets from sensor B, and thirty nine sets from sensor C were obtained.

Figure 12-1, Figure 12-2 and Figure 12-3 show plots of moisture content change per hour against three independent variables for sensor A, B and C. As can be seen from Figures 12-1, 12-2, 12-3 initial moisture content had the largest R-square value.

As shown in the regression equations below, Δmoisture content per hour in CIR-HFMS-2S-emulsion layer can be predicted as a function of the initial moisture content, the average CIR pavement temperature, the average humidity and the average wind speed.

$\Delta MC/hr = 0.17262 + 0.03017\ IMC - 0.00074\ Temp$ (R-square = 74.4%)

Overall, the R-square value for this project was reasonable, which suggests this equation can be used for predicting moisture level in a typical CIR-HFMS-2S emulsion project. The individual sensors offered higher R-square values than the overall equation because of a significant variation among moisture contents measured by three different sensors.

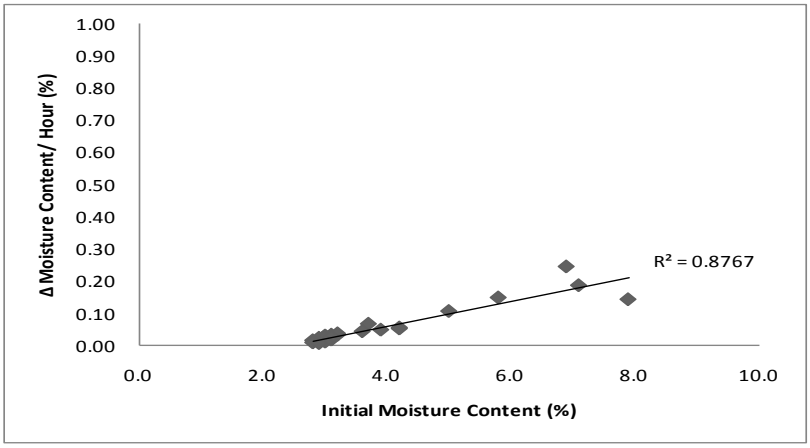

(a) ΔMC/h vs. IMC

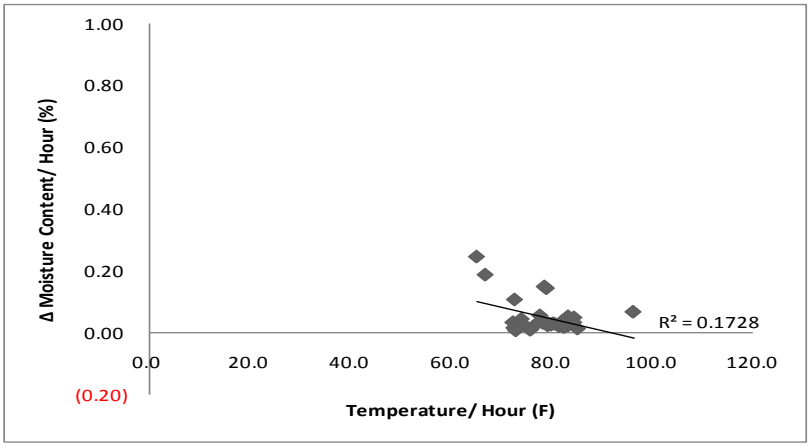

(b) ΔMC/hour vs. Temperature

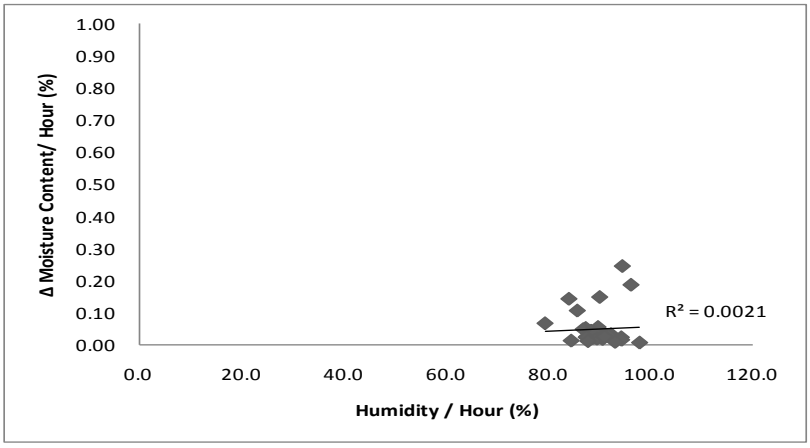

(c) ΔMC/h vs. Humidity

Figure 12-1. Plots of moisture change per hour against each of three independent variables at sensor A

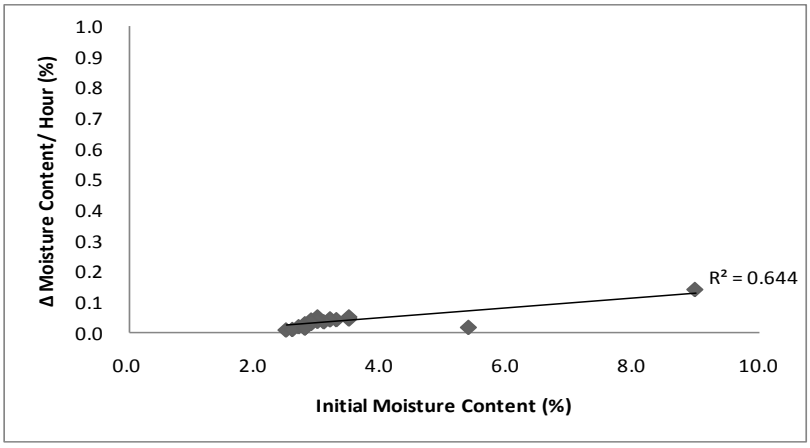

(a) ΔMC/h vs. IMC

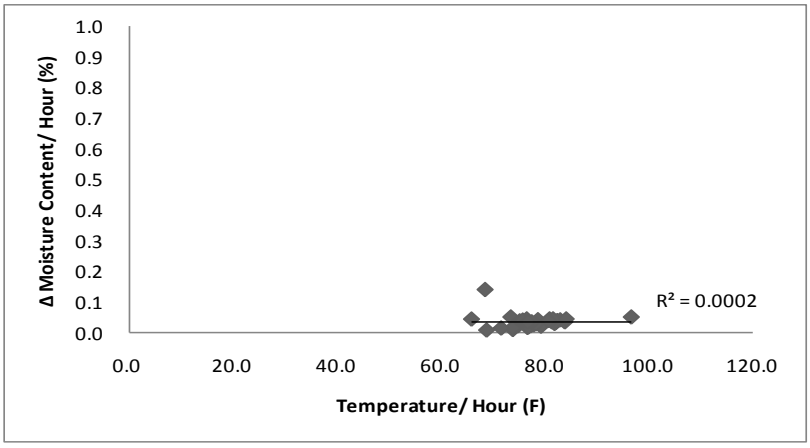

(b) ΔMC/hour vs. Temperature

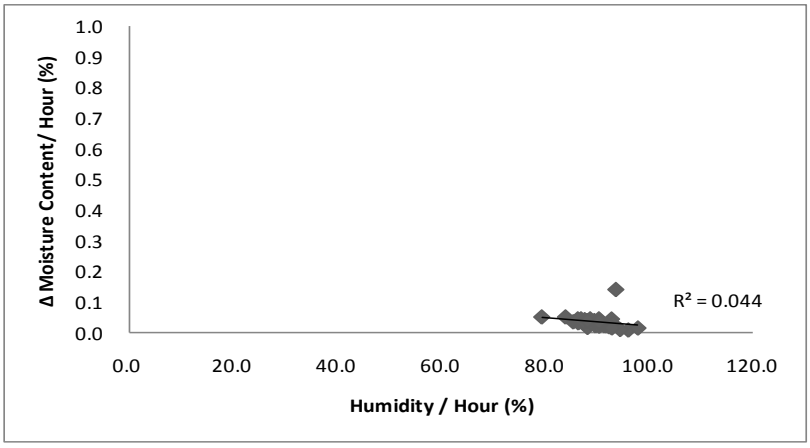

(c) ΔMC/h vs. Humidity

Figure 12-2. Plots of moisture change per hour against each of three independent variables at sensor B

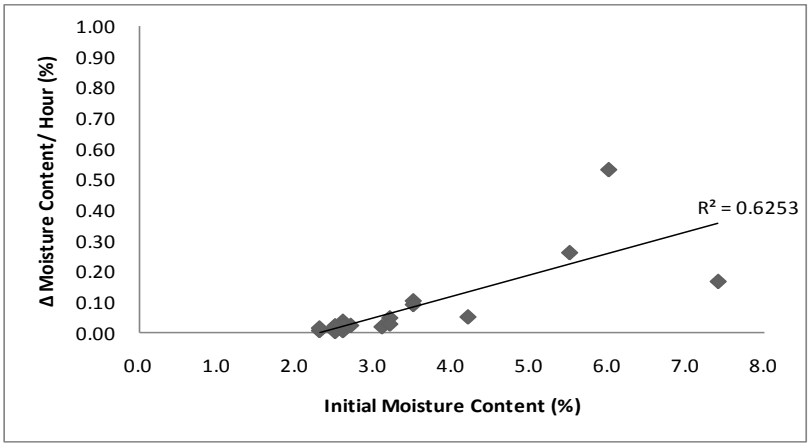

(a) ΔMC/h vs. IMC

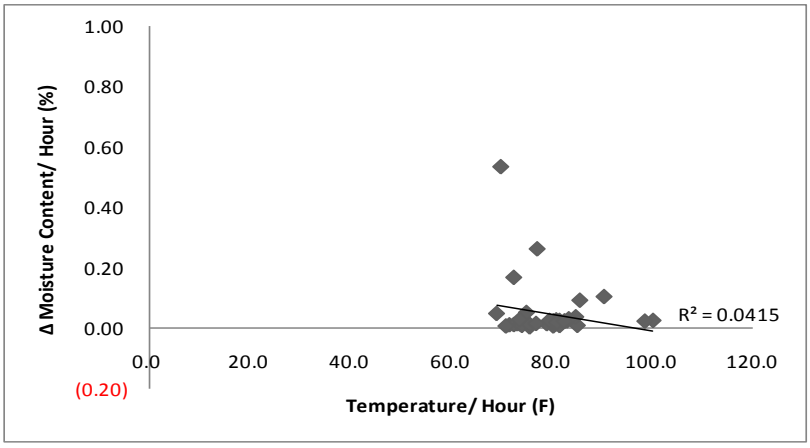

(b) ΔMC/hour vs. Temperature

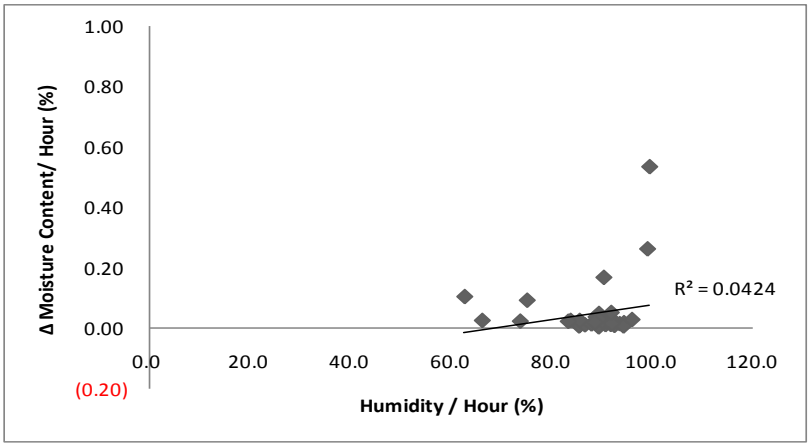

(c) ΔMC/h vs. Humidity

Figure 12-3. Plots of moisture change per hour against each of three independent variables at sensor C

12.2 CIR-foam Project Site in Iowa County

Moisture contents and climatic data were collected from the CIR-foam layer in Iowa County. After discarding the initial moisture contents above 12% (unusually high), twenty-three moisture content data sets from sensor A, twenty-three sets from sensor B, and twenty-four sets from sensor C were obtained.

Figure 12-4, Figure 12-5 and Figure 12-6 show plots of moisture content change per hour against three independent variables for sensor A, B and C. As can be seen from Figures 12-4, 12-5, 12-6 initial moisture content had the largest R-square value.

As shown in the regression equations below, Δmoisture content per hour in CIR-foam layer can be predicted as a function of the initial moisture content, the average CIR pavement temperature, the average humidity and the average wind speed.

$$\Delta MC/hr = -0.01659 + 0.021151\ IMC + 0.000268\ Temp \quad (R\text{-square} = 82.3\%)$$

Overall, the R-square value for this project was relatively high, which suggests this equation is more reliable for predicting moisture level in a typical CIR-foam project than the one developed for CIR-HFMS-2S-emulsion. Overall R-square value was close to ones developed for individual sensors, which indicates that the data from three sensors are consistent among them.

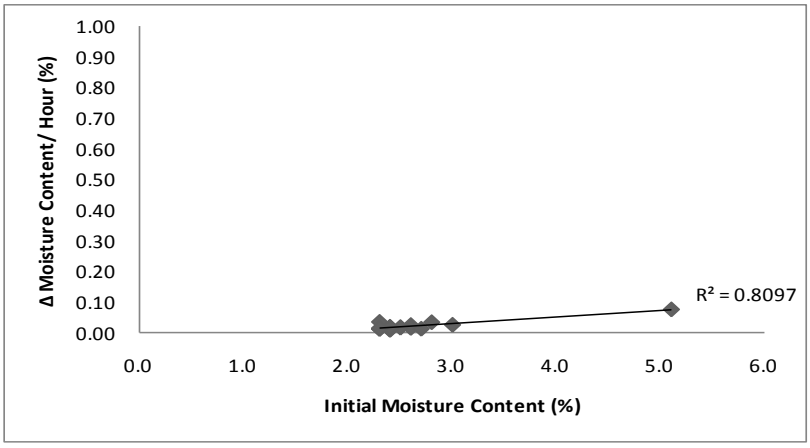

(a) ΔMC/h vs. IMC

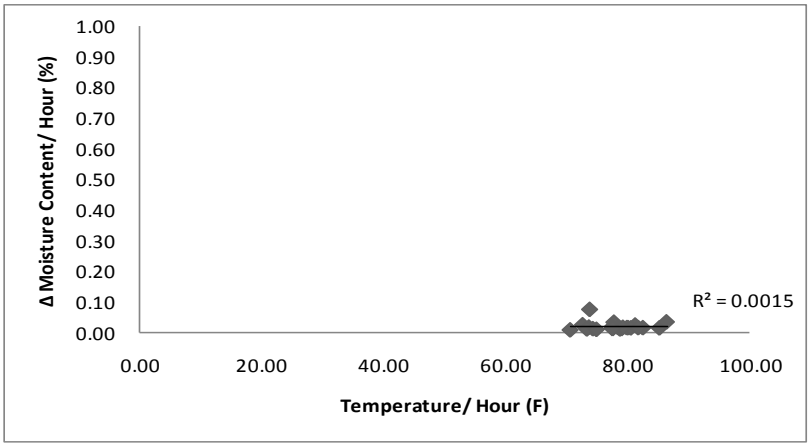

(b) ΔMC/hour vs. Temperature

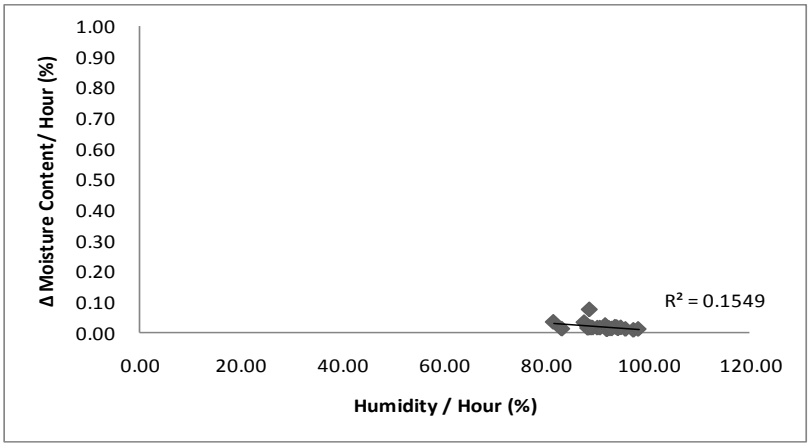

(c) ΔMC/h vs. Humidity

Figure 12-4. Plots of moisture change per hour against each of three independent variables at sensor A

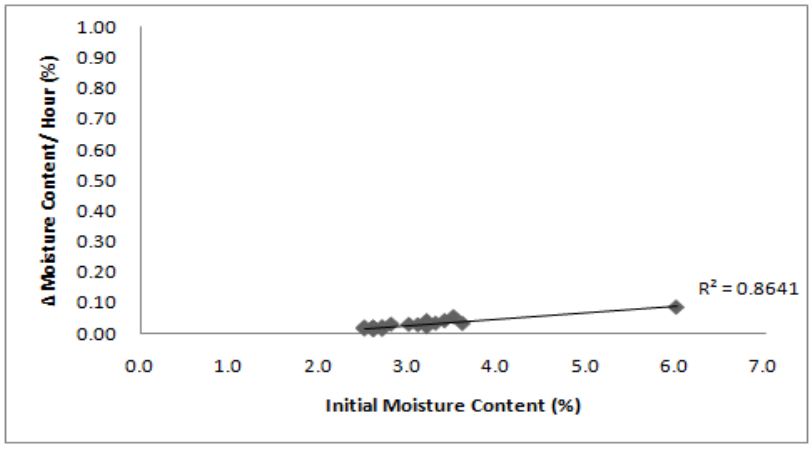

(a) ΔMC/h vs. IMC

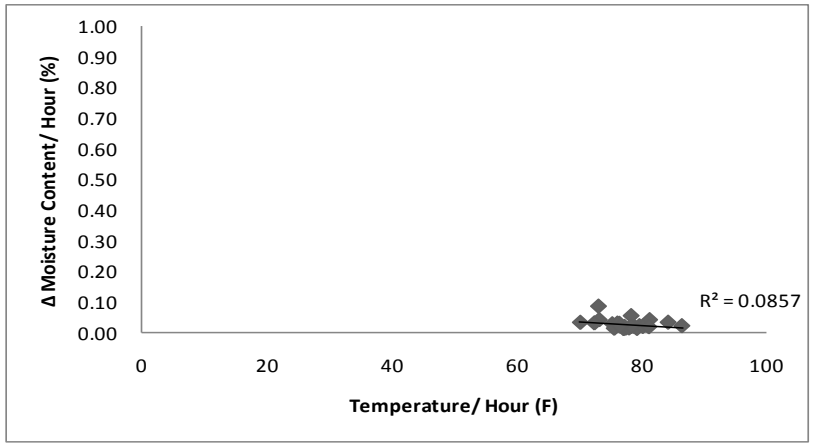

(b) ΔMC/hour vs. Temperature

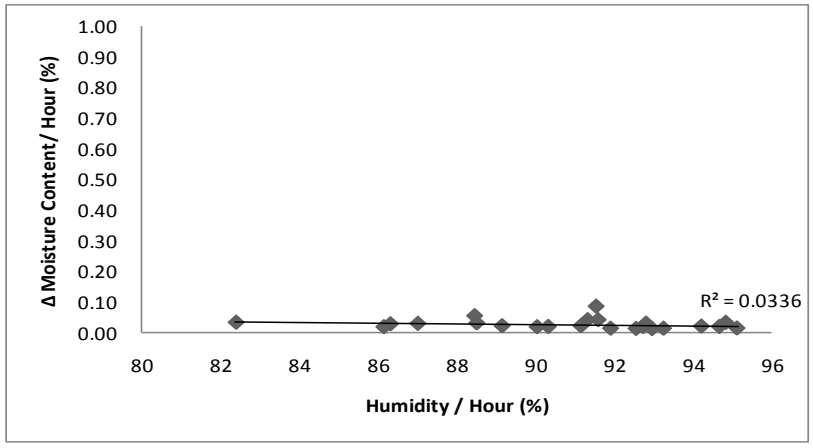

(c) ΔMC/h vs. Humidity

Figure 12-5. Plots of moisture change per hour against each of three independent variables at sensor B

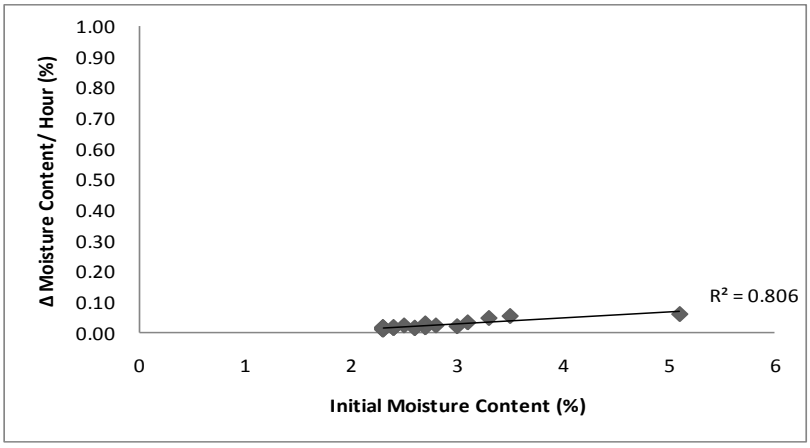

(a) ΔMC/h vs. IMC

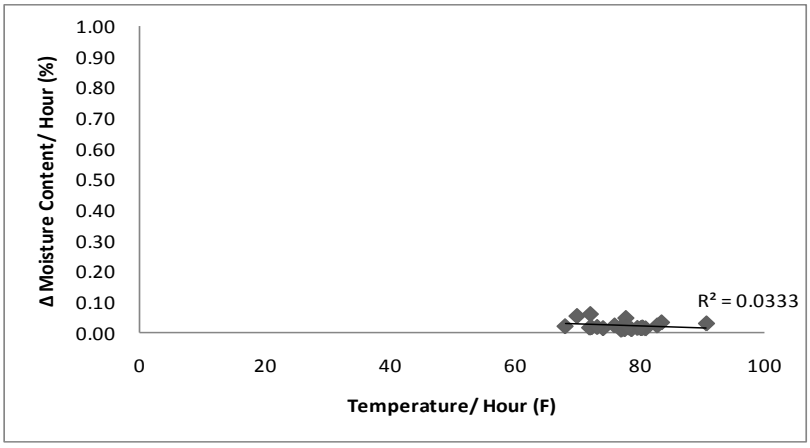

(b) ΔMC/hour vs. Temperature

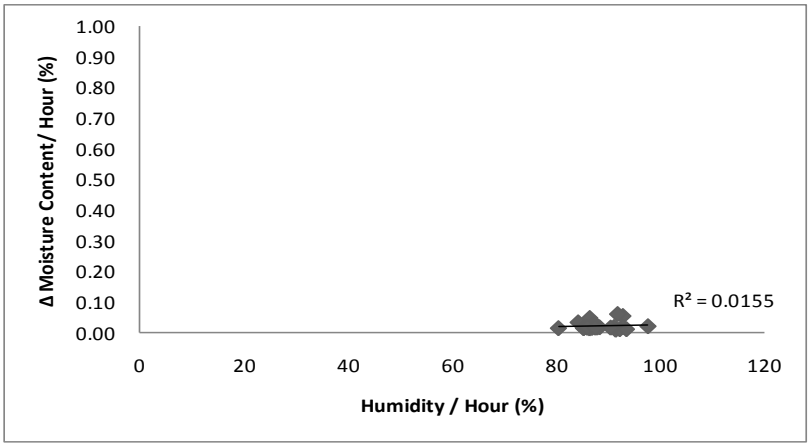

(c) ΔMC/h vs. Humidity

Figure 12-6. Plots of moisture change per hour against each of three independent variables at sensor C

12.3 CIR-foam Project Site in Benton County

Moisture contents and climatic data were collected from the CIR-foam layer in Benton County. After discarding the initial moisture contents above 12% (unusually high), eleven moisture content data sets from sensor A, thirty sets from sensor B, and twenty-five sets from sensor C were obtained.

Figure 12-7, Figure 12-8 and Figure 12-9 show plots of moisture content change per hour against three independent variables for sensor A, B and C. As can be seen from Figures 12-7, 12-8, 12-9 initial moisture content had the largest R-square value.

As shown in the regression equations below, Δmoisture content per hour in CIR-foam layer can be predicted as a function of the initial moisture content, the average CIR pavement temperature, the average humidity and the average wind speed.

$$\Delta MC/hr = -0.06951 + 0.01225\ IMC + 0.00125\ Temp \qquad (R\text{-square} = 19.0\%)$$

Overall, the R-square value for this project was reasonable, which suggests this equation can be used for predicting moisture level in a typical CIR-foam project. Overall R-square value was close to ones developed for individual sensors, which indicates that the data from three sensors are consistent among them.

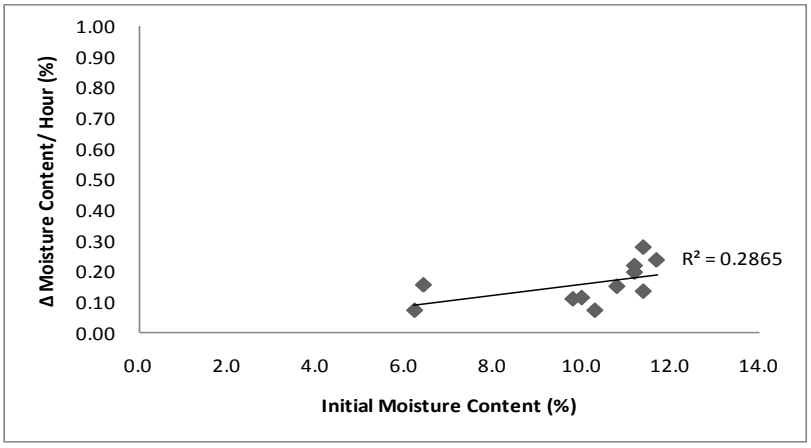

(a) ΔMC/h vs. IMC

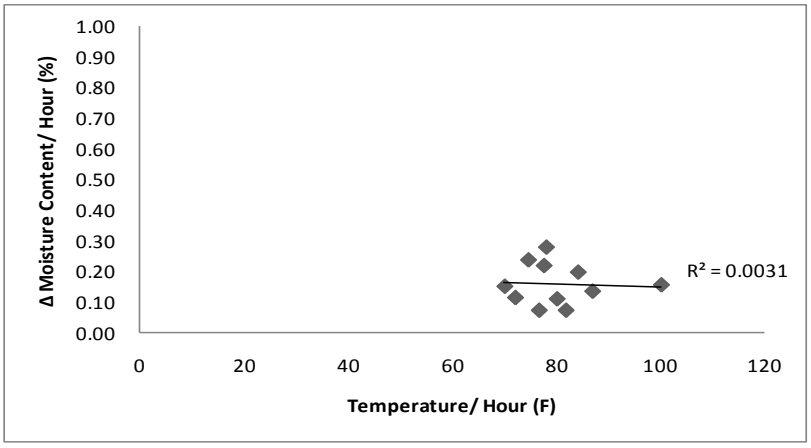

(b) ΔMC/hour vs. Temperature

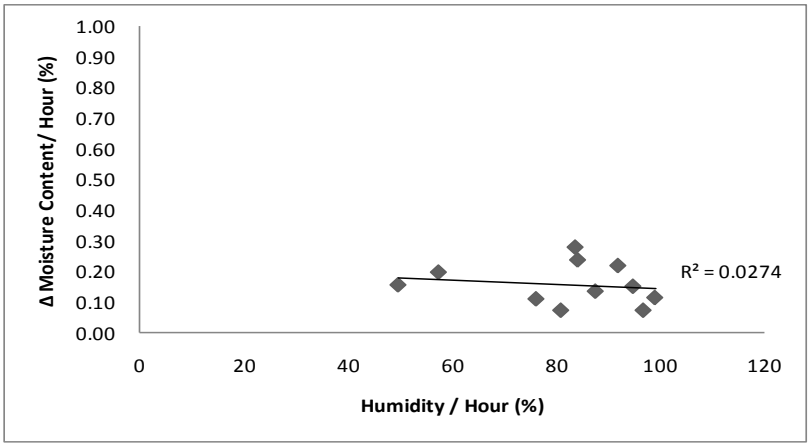

(c) ΔMC/h vs. Humidity

Figure 12-7. Plots of moisture change per hour against each of three independent variables at sensor A

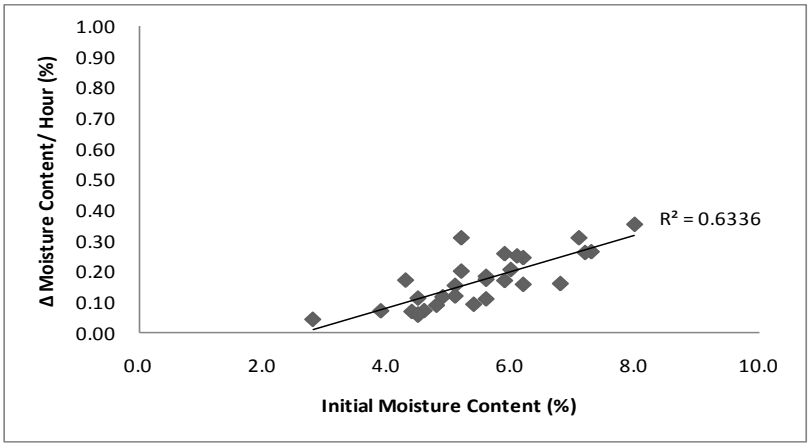

(a) ΔMC/h vs. IMC

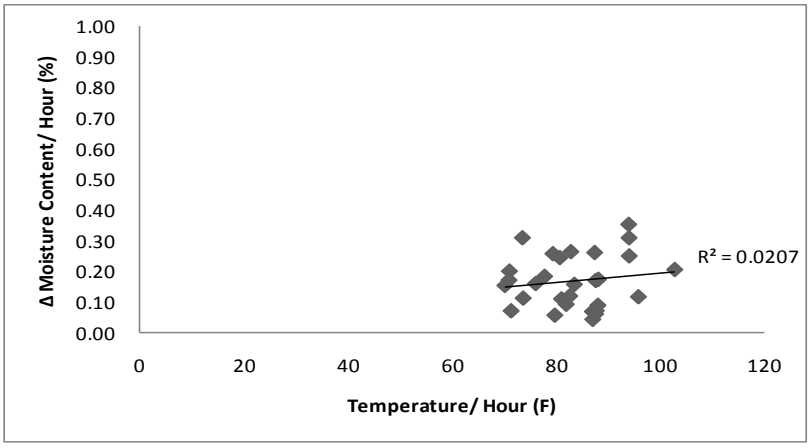

(b) ΔMC/hour vs. Temperature

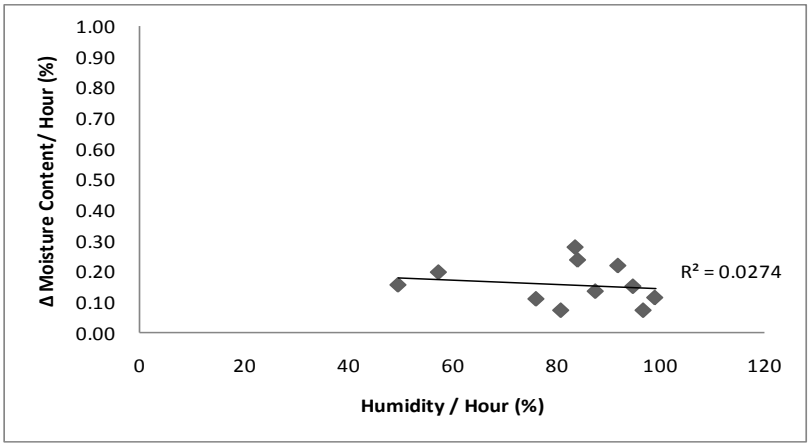

(c) ΔMC/h vs. Humidity

Figure 12-8. Plots of moisture change per hour against each of three independent variables at sensor B

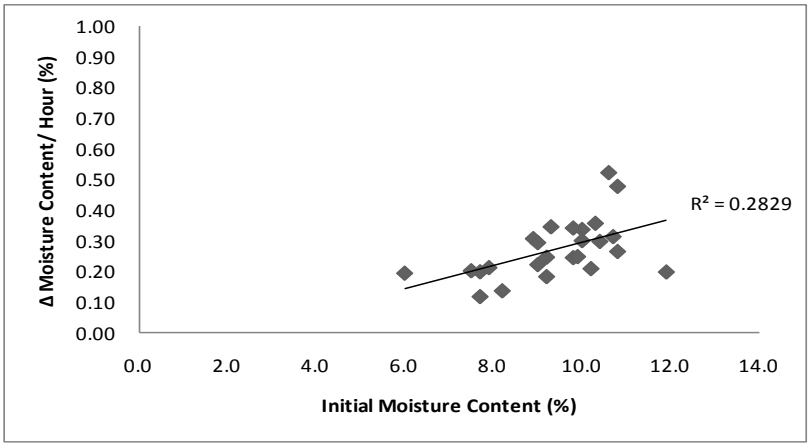

(a) ΔMC/h vs. IMC

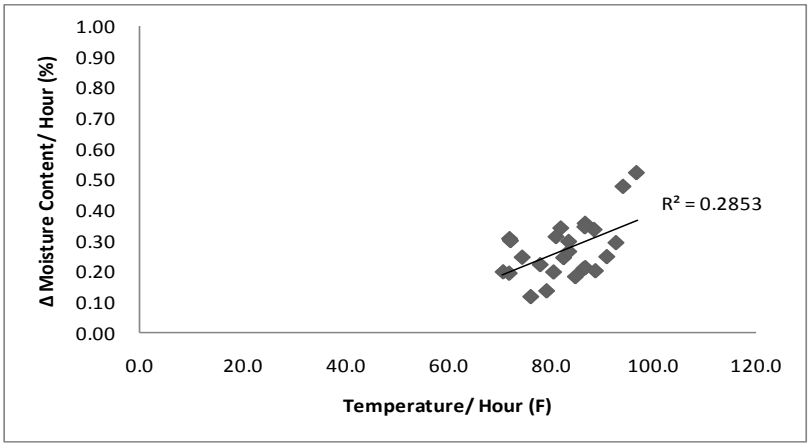

(b) ΔMC/hour vs. Temperature

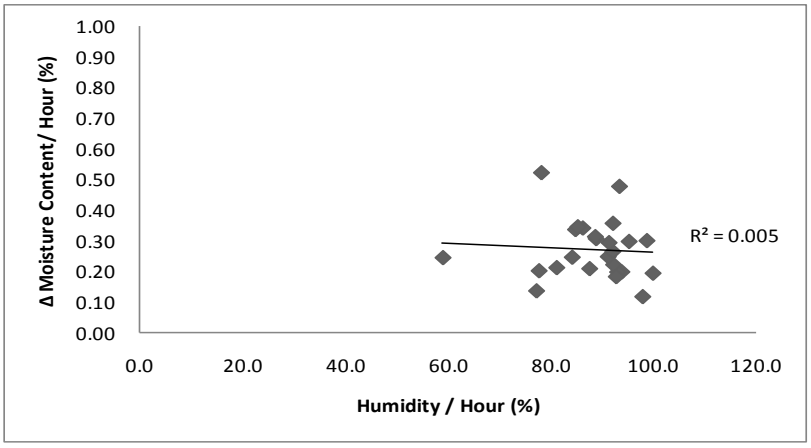

(c) ΔMC/h vs. Humidity

Figure 12-9. Plots of moisture change per hour against each of three independent variables at sensor C

12.4 CIR-foam Project Site in Marshall County

Moisture contents and climatic data were collected from the CIR-foam layer in Marshall County. After discarding the initial moisture contents above 12% (unusually high), twenty-six moisture content data sets from sensor A, and twenty-nine sets from sensor C were obtained.

Figure 12-10 and Figure 12-11 show plots of moisture content change per hour against three independent variables for sensor A and C. As can be seen from Figures 12-10 and 12-11 initial moisture content had the largest R-square value.

As shown in the regression equations below, Δmoisture content per hour in CIR-foam layer can be predicted as a function of the initial moisture content, the average CIR pavement temperature, the average humidity and the average wind speed.

$$\Delta MC/hr = 0.04261 + 0.04976\ IMC - 0.00059\ Temp \qquad (R\text{-square} = 39.7\%)$$

Overall, the R-square value for this project was relatively high, which suggests this equation is reliable for predicting moisture level in a typical CIR-foam project. Overall R-square value was lower than the ones developed for individual sensors, which indicates that the data from three sensors are variable.

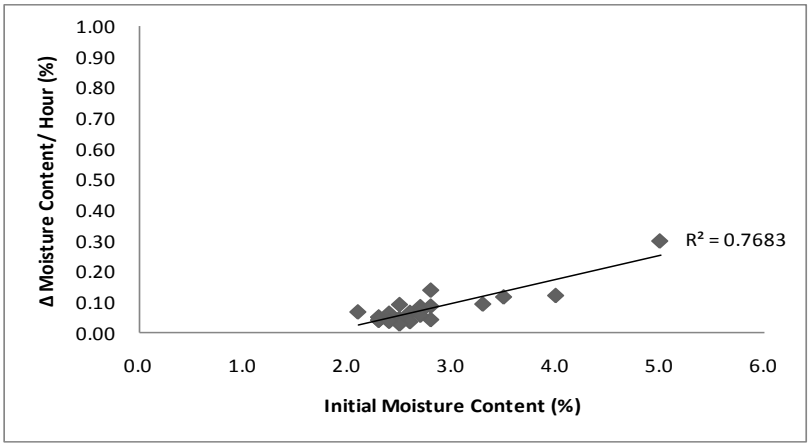

(a) ΔMC/h vs. IMC

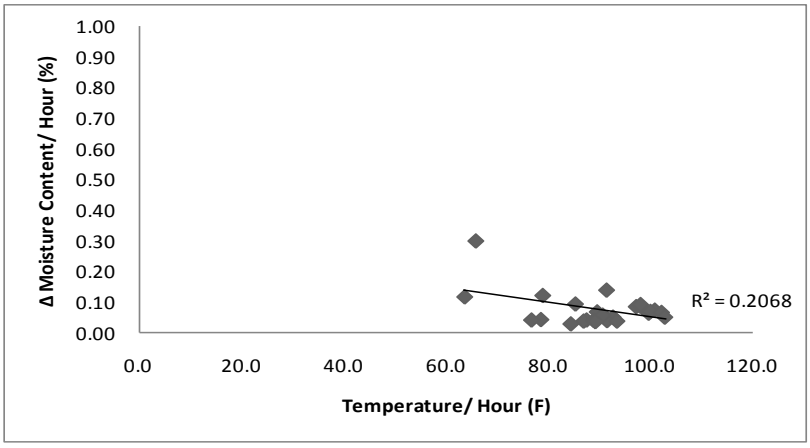

(b) ΔMC/hour vs. Temperature

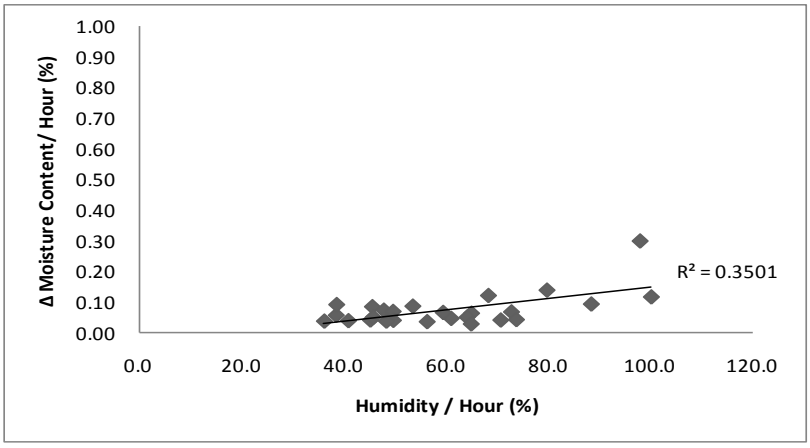

(c) ΔMC/h vs. Humidity

Figure 12-10. Plots of moisture change per hour against each of three independent variables at sensor A

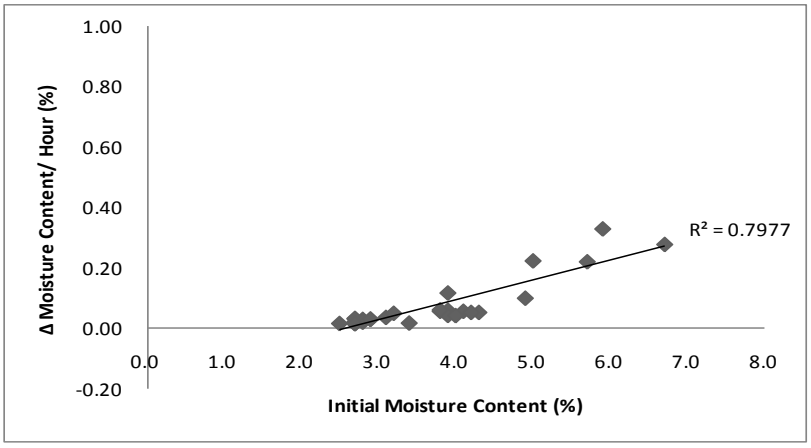

(a) ΔMC/h vs. IMC

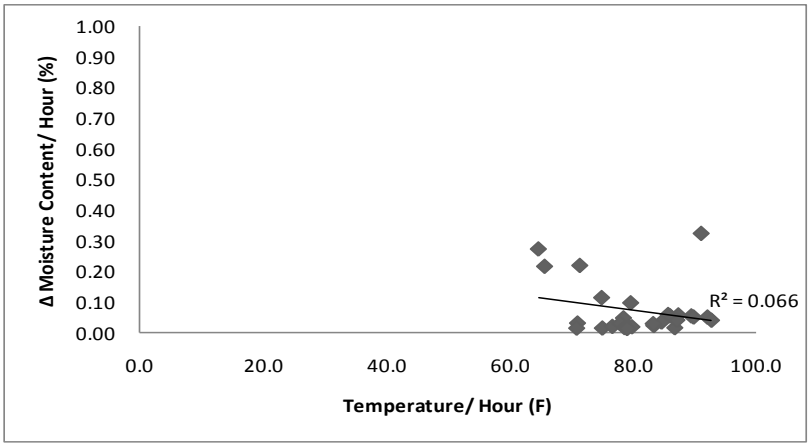

(b) ΔMC/hour vs. Temperature

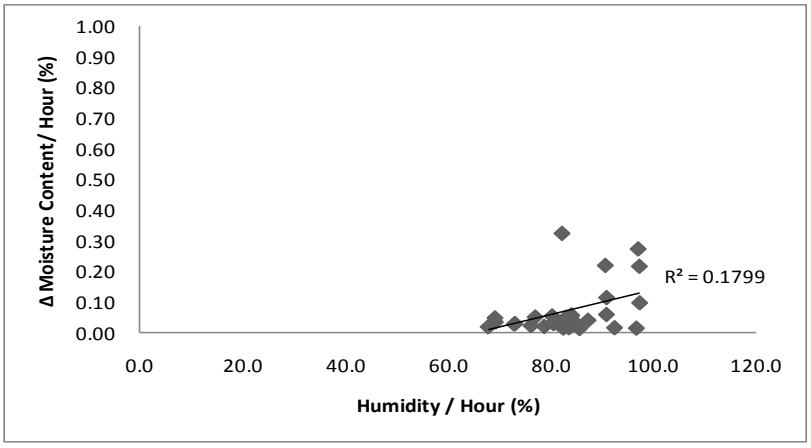

(c) ΔMC/h vs. Humidity

Figure 12-11. Plots of moisture change per hour against each of three independent variables at sensor C

12.5 CIR-foam Project Site in Delaware County 2010

Moisture contents and climatic data were collected from the CIR-foam layer in Iowa County. After discarding the initial moisture contents above 12% (unusually high), twenty-four moisture content data sets from sensor A, twenty-one sets from sensor B, and twenty-two sets from sensor C were obtained.

Figure 12-12, Figure 12-13 and Figure 12-14 show plots of moisture content change per hour against three independent variables for sensor A, B and C. As can be seen from Figures 12-12, 12-13, 12-14 initial moisture content had the largest R-square value.

As shown in the regression equations below, Δmoisture content per hour in CIR-foam layer can be predicted as a function of the initial moisture content, the average CIR pavement temperature, the average humidity and the average wind speed.

$$\Delta MC/hr = -0.05974 + 0.00691\ IMC + 0.00073\ Temp$$
$$(R\text{-square} = 36.6\%)$$

Overall, the R-square value for this project was low, which suggests this equation would not be reliable for predicting moisture level in a typical CIR-foam project. Overall R-square value was significantly lower than ones developed for individual sensors, which indicates that the data from three sensors are not consistent among them. It can be postulated that the low R-squared value was obtained because there was little moisture loss over the curing period.

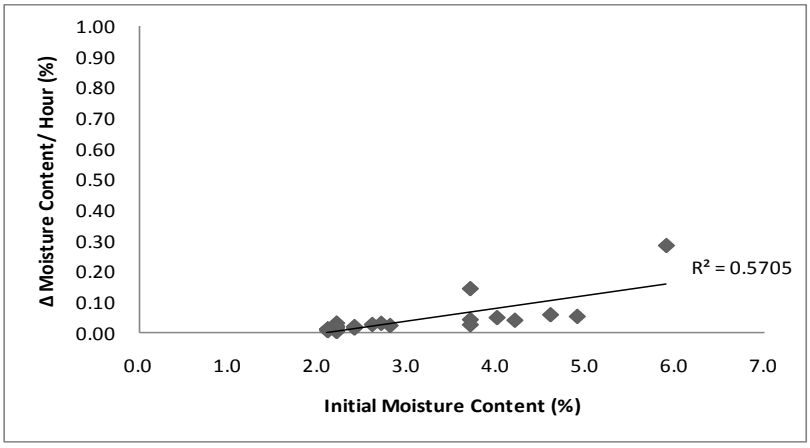

(a) ΔMC/h vs. IMC

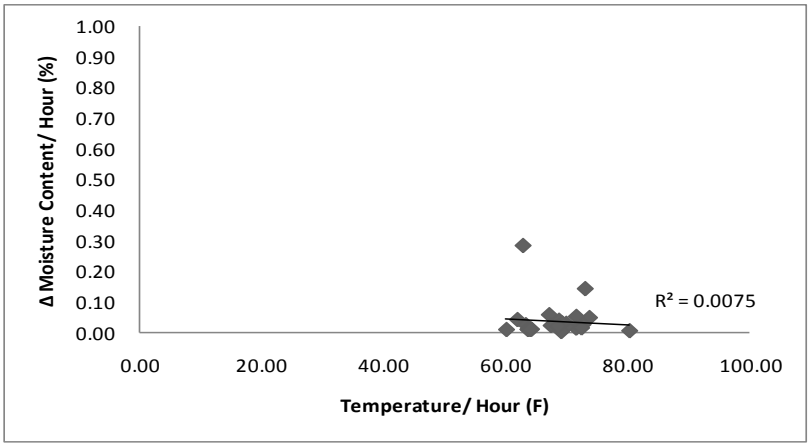

(b) ΔMC/hour vs. Temperature

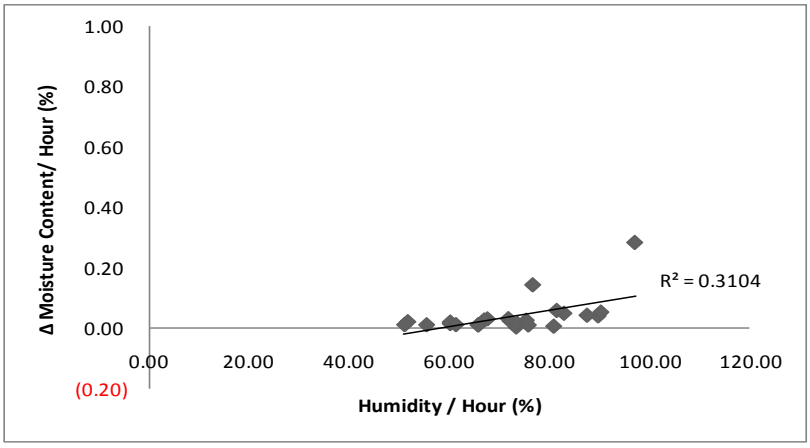

(c) ΔMC/h vs. Humidity

Figure 12-12. Plots of moisture change per hour against each of three independent variables at sensor A

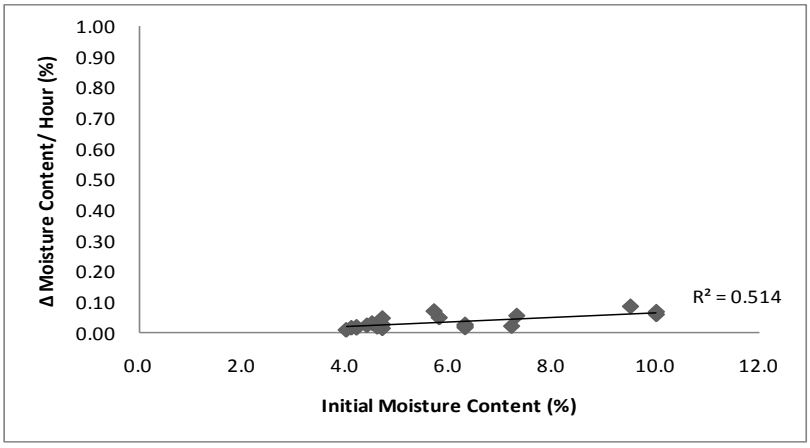

(a) ΔMC/h vs. IMC

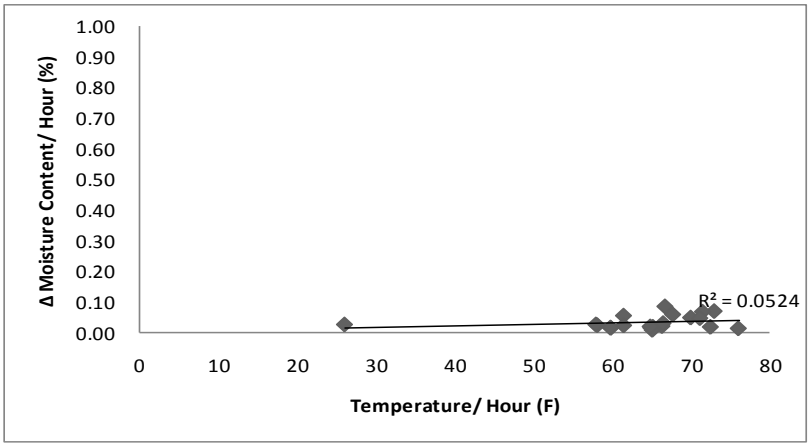

(b) ΔMC/hour vs. Temperature

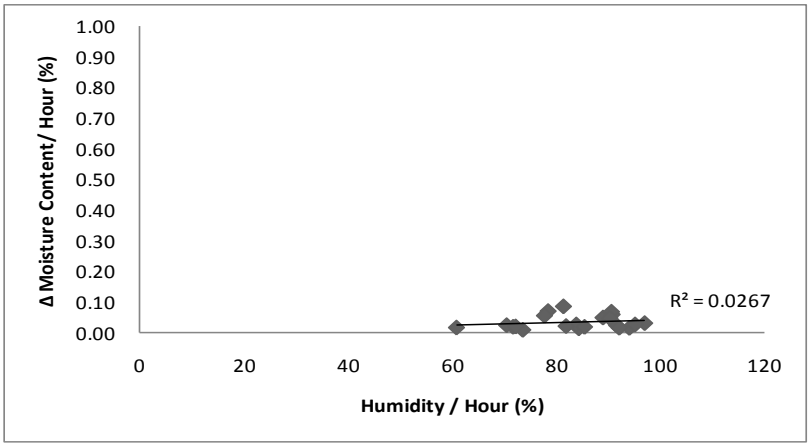

(c) ΔMC/h vs. Humidity

Figure 12-13. Plots of moisture change per hour against each of three independent variables at sensor B

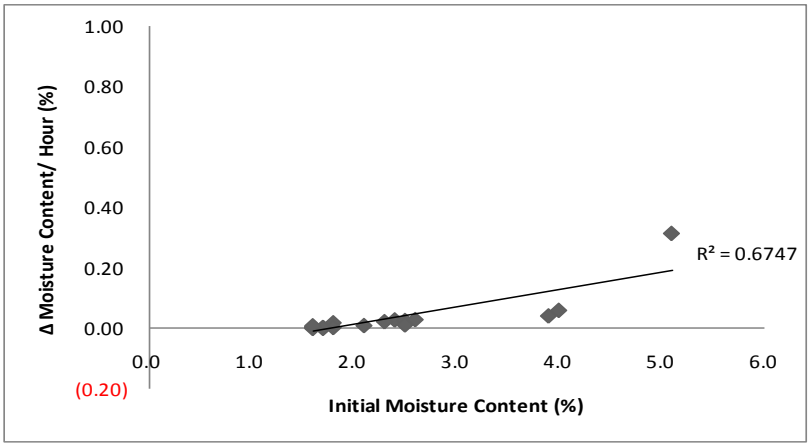

(a) ΔMC/h vs. IMC

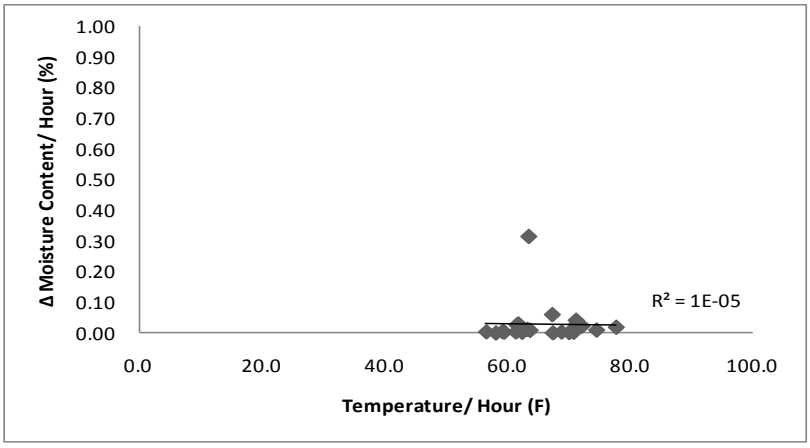

(b) ΔMC/hour vs. Temperature

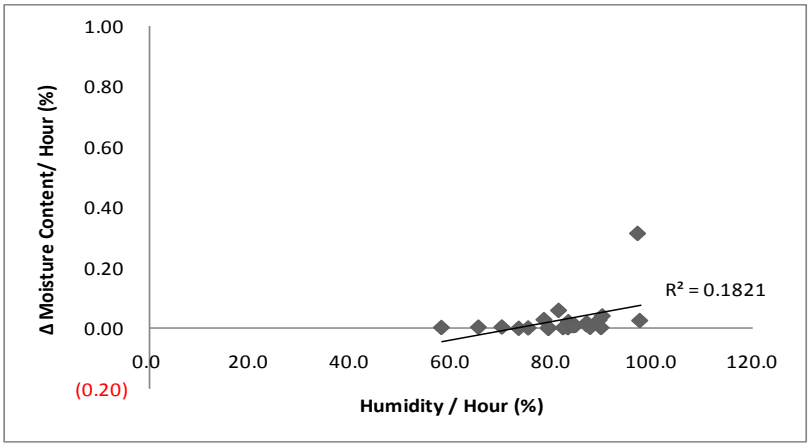

(c) ΔMC/h vs. Humidity

Figure 12-14. Plots of moisture change per hour against each of three independent variables at sensor C

12.6 CIR-foam Project Site in Delaware County 2011

Moisture contents and climatic data were collected from the CIR-foam layer in Delaware County. A new set of moisture content data was created when the rainfall had occurred. After discarding the initial moisture contents above 12% (unusually high), six moisture content data sets from sensor A, twenty six sets from sensor B, and eighteen sets from sensor C were obtained.

Figure 12-15, Figure 12-16 and Figure 12-17 show plots of moisture content change per hour against three independent variables for sensor A, B and C. As can be seen from Figures 12-15, 12-16, 12-17 initial moisture content had the largest R-square value.

As shown in the regression equations below, Δmoisture content per hour in the CIR-foam layer can be predicted as a function of the initial moisture content, the average CIR pavement temperature, the average humidity and the average wind speed.

$$\Delta MC/hr = -0.55394 + 0.022452\ IMC + 0.002608\ Temp \quad (R\text{-square} = 61.6\%)$$

Overall, the R-square value for this project was reasonable, which suggests this equation can be used for predicting moisture level in a typical CIR-foam project. The individual sensors offered higher R-square values than the overall equation because of a significant variation among moisture contents measured by three different sensors.

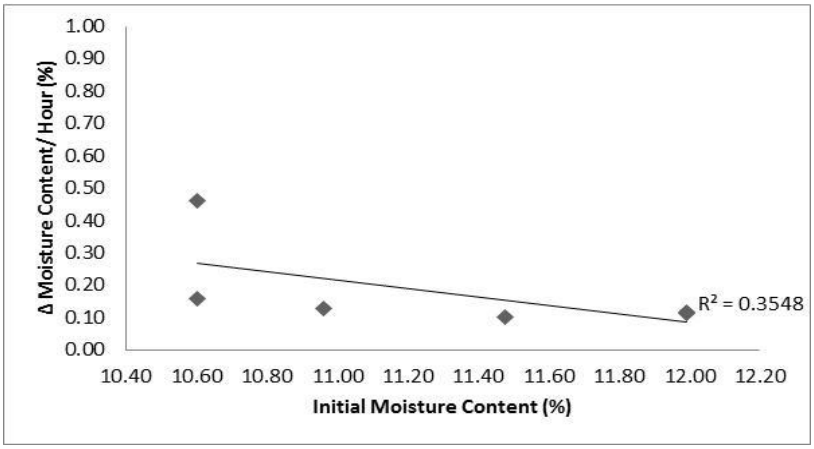

(a) ΔMC/h vs. IMC

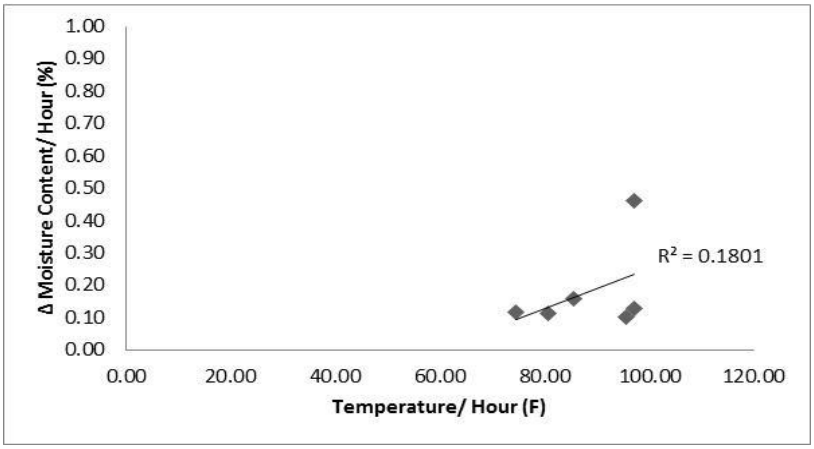

(b) ΔMC/hour vs. Temperature

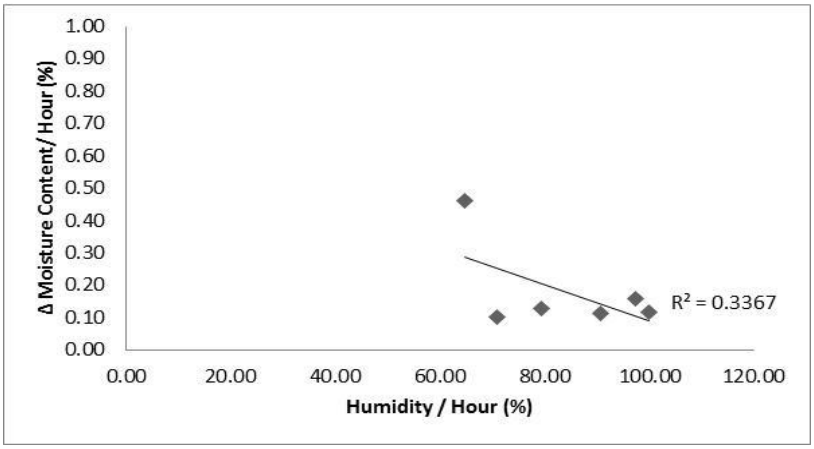

(c) ΔMC/h vs. Humidity

Figure 12-15. Plots of moisture change per hour against each of three independent variables at sensor A

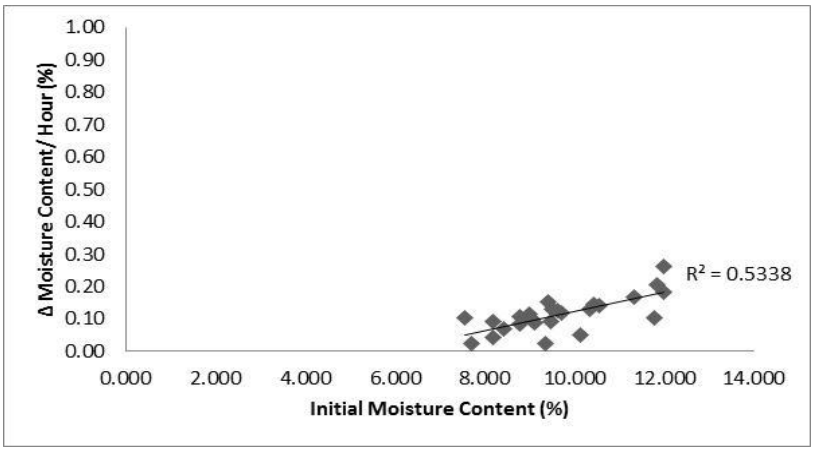

(a) ΔMC/h vs. IMC

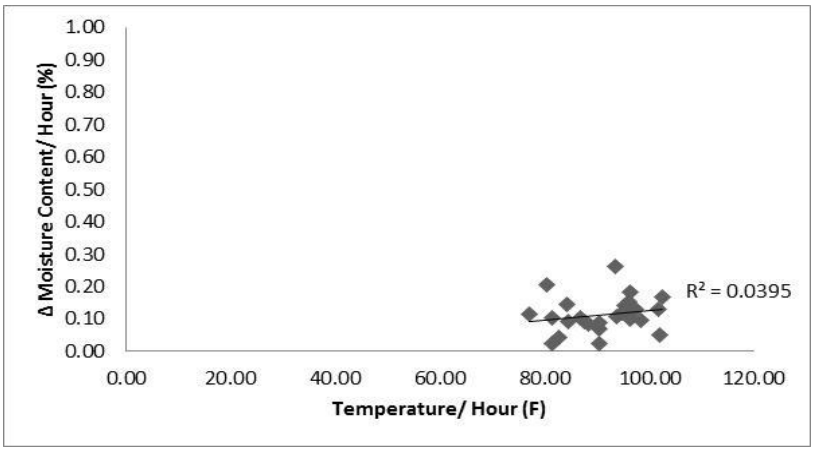

(b) ΔMC/hour vs. Temperature

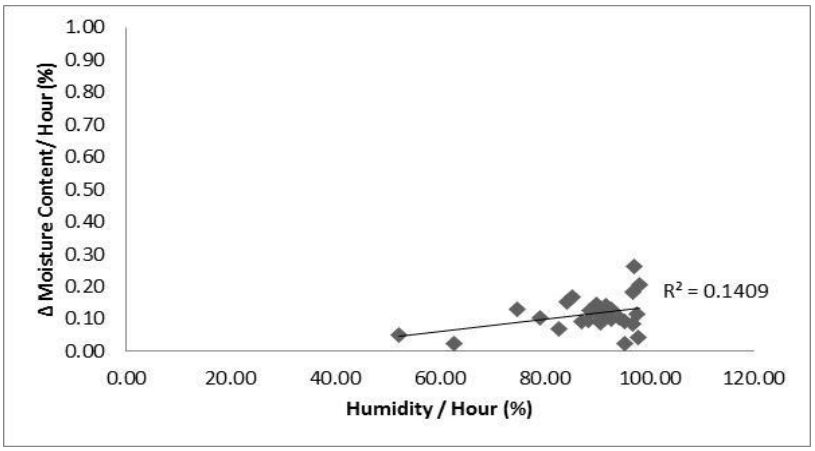

(c) ΔMC/h vs. Humidity

Figure 12-16. Plots of moisture change per hour against each of three independent variables at sensor B

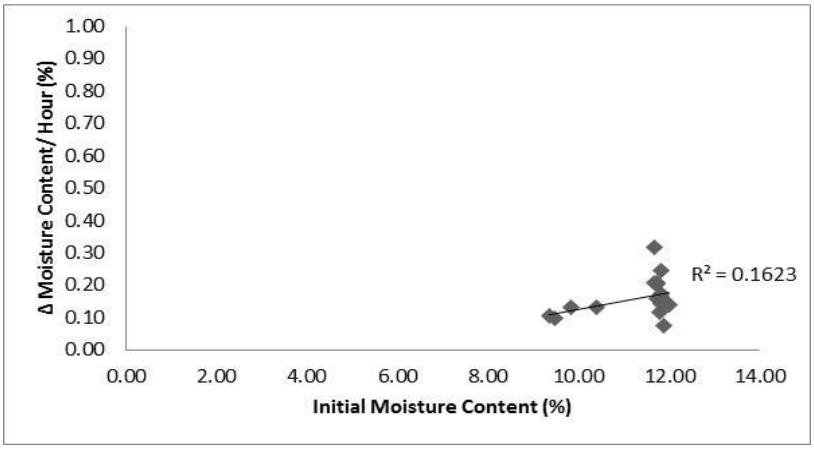

(a) ΔMC/h vs. IMC

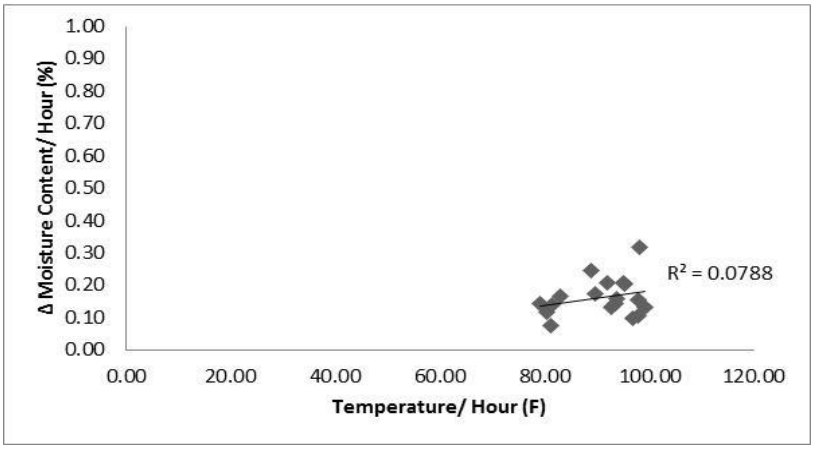

(b) ΔMC/hour vs. Temperature

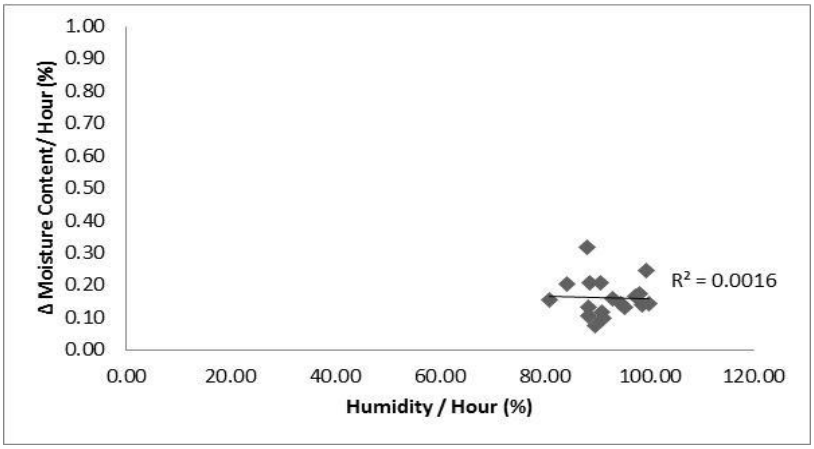

(c) ΔMC/h vs. Humidity

Figure 12-17. Plots of moisture change per hour against each of three independent variables at sensor C

12.7 CIR-foam Project Site in Black Hawk County

Moisture contents and climatic data were collected from the CIR-foam layer in Black Hawk County. A new set of moisture content data was created when the rainfall had occurred. After discarding the initial moisture contents above 12% (unusually high), thirty one moisture content data sets from sensor A, twenty five sets from sensor B, and thirty six sets from sensor C were obtained.

Figure 12-18, Figure 12-19 and Figure 12-20 show plots of moisture content change per hour against three independent variables for sensor A, B and C. As can be seen from Figures 12-18, 12-19, 12-20 initial moisture content had the largest R-square value.

As shown in the regression equations below, Δmoisture content per hour in the CIR-foam layer can be predicted as a function of the initial moisture content, the average CIR pavement temperature, the average humidity and the average wind speed.

$$\Delta MC/hr = -0.08778 + 0.026439\ IMC + 0.000582\ Temp \quad (R\text{-square} = 65.8\%)$$

Overall, the R-square value for this project was reasonable, which suggests this equation can be used for predicting moisture level in a typical CIR-foam project. The individual sensors offered higher R-square values than the overall equation because of a significant variation among moisture contents measured by three different sensors.

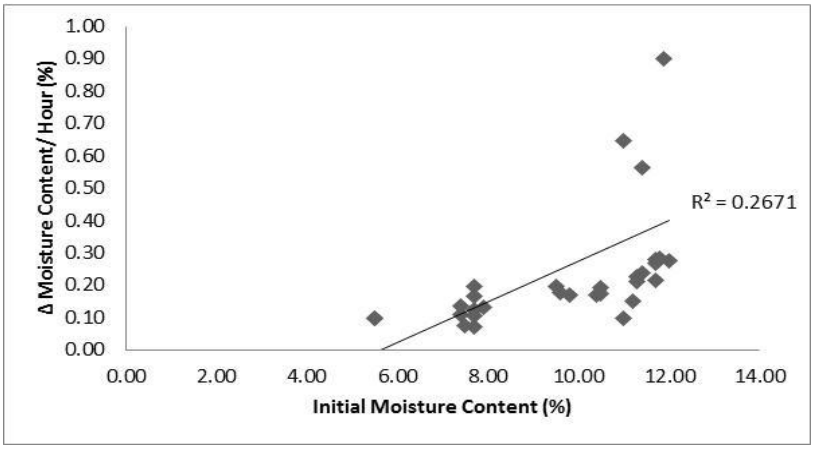

(a) ΔMC/h vs. IMC

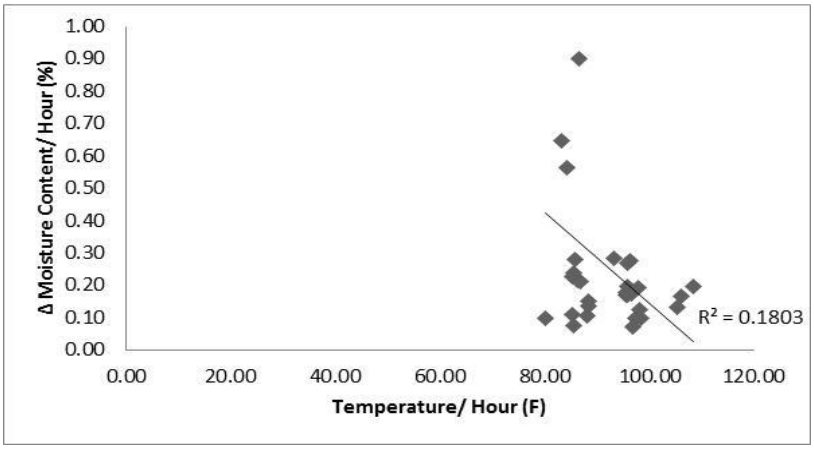

(b) ΔMC/hour vs. Temperature

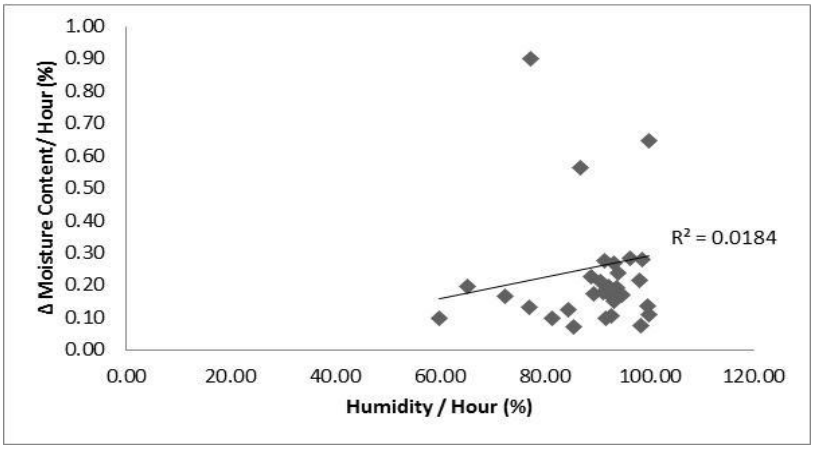

(c) ΔMC/h vs. Humidity

Figure 12-18. Plots of moisture change per hour against each of three independent variables at sensor A

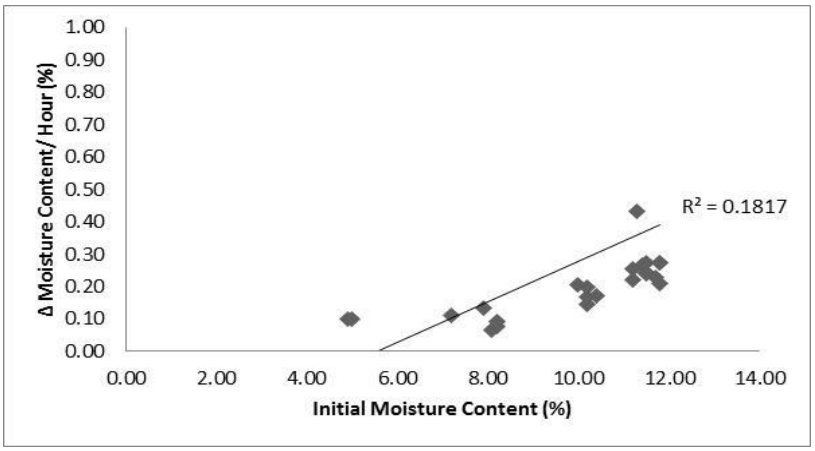

(a) ΔMC/h vs. IMC

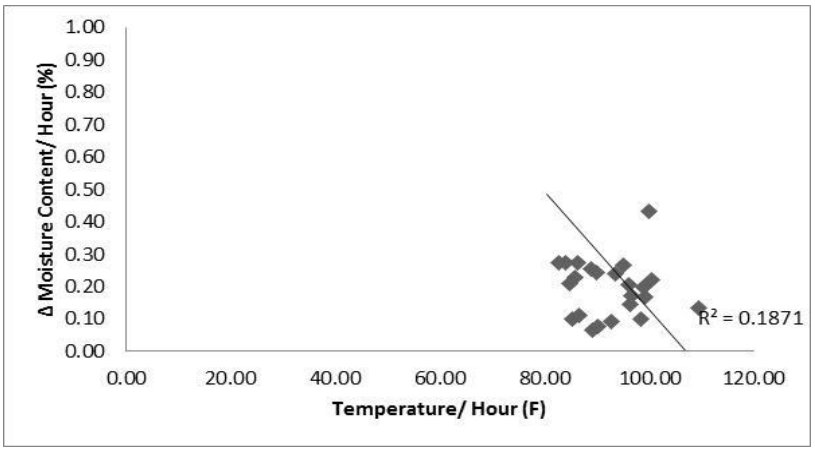

(b) ΔMC/hour vs. Temperature

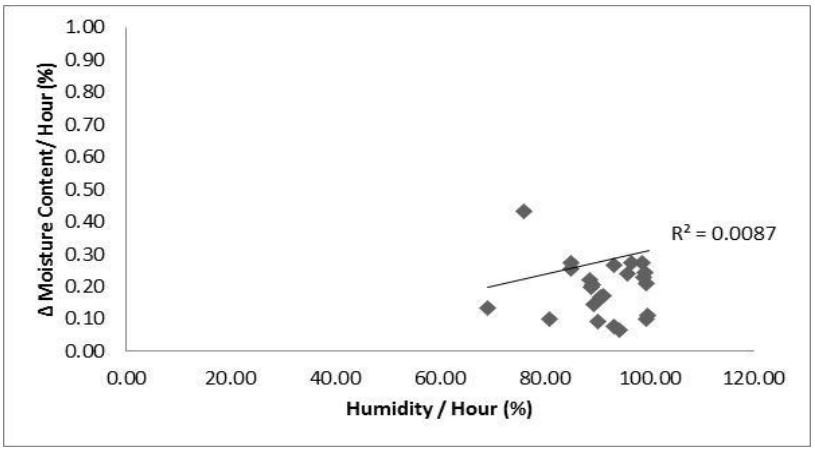

(c) ΔMC/h vs. Humidity

Figure 12-19. Plots of moisture change per hour against each of three independent variables at sensor B

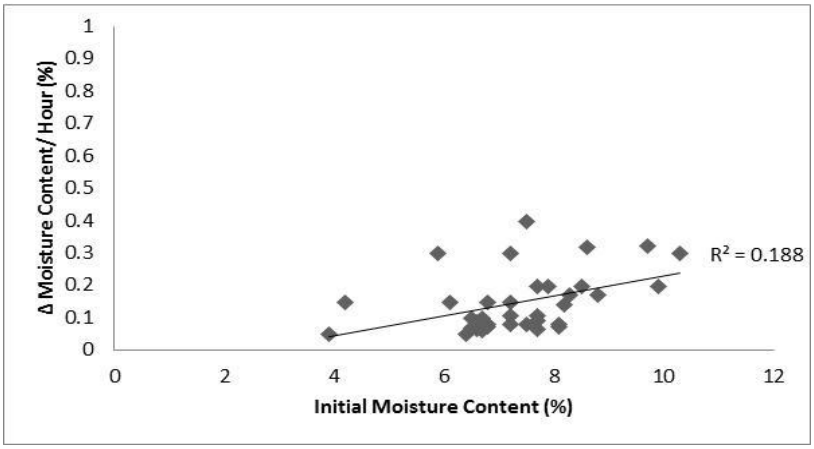

(a) ΔMC/h vs. IMC

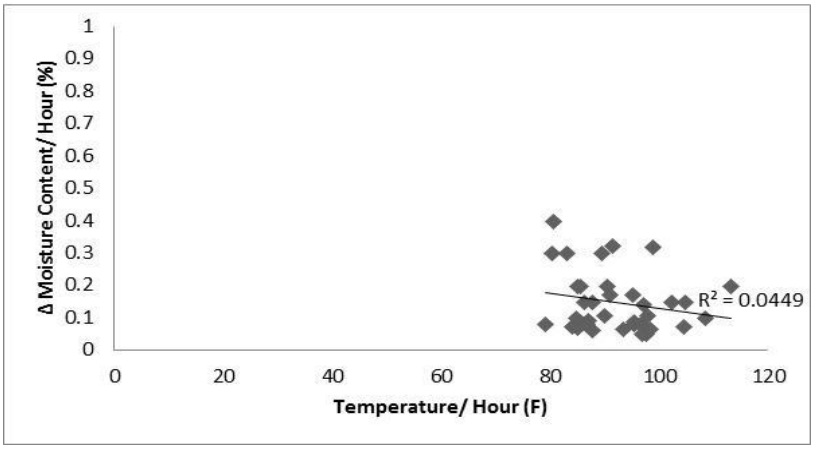

(b) ΔMC/hour vs. Temperature

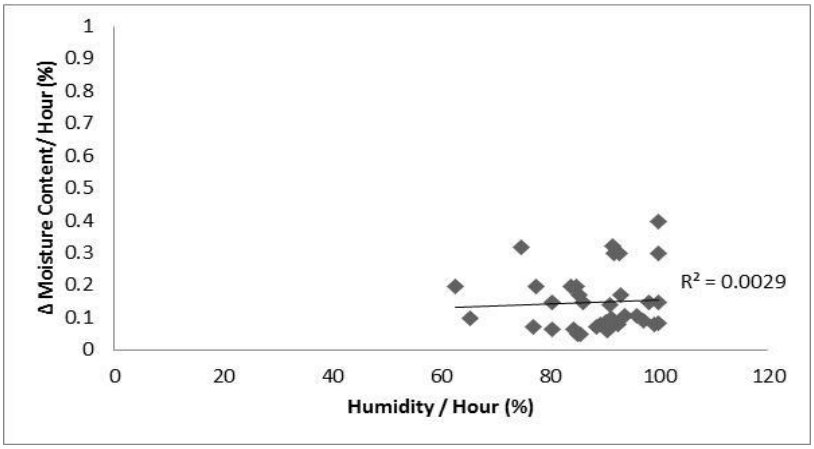

(c) ΔMC/h vs. Humidity

Figure 12-20. Plots of moisture change per hour against each of three independent variables at sensor C

12.8 Compilation of Moisture Data from all CIR-foam Sites

The moisture contents and climatic data from each CIR-foam project site were compiled in order to develop a typical regression equation for all CIR-foam projects. By using the larger amount of data points from multiple sites may increase a reliability of the developed equation. The CIR-foam projects ranged from being performed in early June to October, which would provide one typical equation for the entire construction season. In the regression equation below, Δmoisture content per hour in CIR-foam layer can be predicted as a function of the initial moisture content and the average CIR pavement temperature. Wind speed and relative humidity were found to have little impact on moisture loss and were left out of the equation. The moisture loss indices and R-square values for each project site are shown below in Table 12-1.

CIR-foam: $\Delta MC/hr = -0.0555 + 0.017924\ IMC + 0.000571\ Temp$

(R-square = 63.9%)

Table 12-1. Comparisons between moisture loss indices for each project site

Site	y-intercept	Initial Moisture Content (1/1000 %)	Average CIR Layer Temperature (1/1000 °F)	R-square Value
Clinton County	0.1726	30.17	-0.74	74.4%
Iowa County	-0.0166	21.15	0.27	82.3%
Benton County	-0.0695	12.25	1.25	19.0%
Marshall County	0.0426	49.76	-0.59	39.7%
Delaware County	-0.0597	6.91	0.73	36.6%
Delaware 2011	-0.5539	22.45	2.61	61.6%
Black Hawk	-0.0879	26.44	0.58	65.8%
Combined Sites (7)	-0.0555	17.92	0.57	63.9%

Overall, the R-square value for CIR-foam projects is good, which suggests this equation would be reliable for predicting moisture level in a typical CIR-foam project.

To determine the timing of the overlay on CIR-foam layer, first, the initial moisture

content along with air temperature should be entered into the moisture loss index developed from the combined sites. Data from Delaware County is used as an example to verify the accuracy of the equation.

$$\Delta MC/hr = -0.0555 + 0.017924\,(2.78) + 0.000571\,(33.8)$$
$$= 0.0136285$$

After one hour, the moisture content will become 2.76637% and it should be entered to the same moisture loss index formula with the new temperature for that hour. The rest of the recursive process is showed in Figure 12-21.

After 14 hours, the moisture content becomes 2.44%, which is very close to the actual moisture content measured of 2.47 measured for this example. The recursive process should be continued until the moisture level becomes 2.0%. Through this recursive operation, the time it takes for moisture content changes from 3.0% to 2.0% can be found.

				Initial Moisture Content			Temp		New Moisture Content
7:15 AM	-0.0555000	+	0.0179240	**2.7800000**	+	0.0005710	33.8	=	2.7663715
8:15 AM	-0.0555000	+	0.0179240	2.7663715	+	0.0005710	37.4	=	2.7509316
9:15 AM	-0.0555000	+	0.0179240	2.7509316	+	0.0005710	48.2	=	2.7296017
10:15 AM	-0.0555000	+	0.0179240	2.7296017	+	0.0005710	55.4	=	2.7045430
11:15 AM	-0.0555000	+	0.0179240	2.7045430	+	0.0005710	59	=	2.6778777
12:15 PM	-0.0555000	+	0.0179240	2.6778777	+	0.0005710	60.8	=	2.6506626
1:15 PM	-0.0555000	+	0.0179240	2.6506626	+	0.0005710	60.8	=	2.6239354
2:15 PM	-0.0555000	+	0.0179240	2.6239354	+	0.0005710	62.6	=	2.5966594
3:15 PM	-0.0555000	+	0.0179240	2.5966594	+	0.0005710	64.4	=	2.5688444
4:15 PM	-0.0555000	+	0.0179240	2.5688444	+	0.0005710	64.4	=	2.5415281
5:15 PM	-0.0555000	+	0.0179240	2.5415281	+	0.0005710	62.6	=	2.5157291
6:15 PM	-0.0555000	+	0.0179240	2.5157291	+	0.0005710	62.6	=	2.4903926
7:15 PM	-0.0555000	+	0.0179240	2.4903926	+	0.0005710	55.4	=	2.4696214
8:15 PM	-0.0555000	+	0.0179240	2.4696214	+	0.0005710	48.2	=	2.4533337
9:15 PM	-0.0555000	+	0.0179240	2.4533337	+	0.0005710	46.4	=	2.4383657

Figure 12-21. Moisture Loss Example

13. DEVELOPEMENT OF STIFFNESS CRITERIA

In order to supplement the moisture loss indices developed stiffness was measured and monitored at each project site during the curing period. Stiffness can be used to measure the resilient modulus of a pavement layer. States across the county are beginning to examine stiffness and its use in quality control of pavement layers. Previous studies of subgrade and base stiffness were examined in order to provide a comparison to this study's stiffness data and further create a criteria for curing.

13.1 Background and Other Studies

In a 2005 study by White et. al, subgrade/ subbase engineering properties at 12 Portland Concrete Cement project sites in Iowa were examined in order to evaluate the effect on pavement performance. One of the engineering properties examined was stiffness using the geogauge. Below, table 13-1 shows the stiffness values for each site as well as the subgrade/ subbase material used. Most values for the subgrade/ subbase were between the range of 2-8 MN/m. Projects 1, 11 and 12 had higher values around 15 MN/m. These projects with higher stiffness had fly ash and project 12 had a special granular subbase.

Table 13-1. Stiffness Results for 12 Portland Concrete Cement Projects in White et. al Study 2003

Project Number	Project Name	Subgrade/ Subbase Material	Number of Tests	Average Stiffness MN/m
1	Eddyville Bypass	Hydrated Fly Ash	33	14.82
2	Highway 330	Natural Soil	33	2.36
3	Knapp Street Subgrade	Natural Soil	51	1.60
4	Knapp Street Subbase	Granular Subbase	24	9.54
5	35th Street Subgrade	Granular Subbase	130	4.72
6	35th Street Subbase	Granular Subbase	24	5.88
7	Highway 34	Natural Soil	85	5.81
8	Highway 218	Natural Soil	85	7.22
9	Interstate 35	Natural Soil	85	4.68
10	Jack Trice Lot S1 Before Ash	Deteriorated Asphalt Pavement Subgrade	18	9.65
11	Jack Trice Lot S1 After Ash	Self-Cementing Fly Ash	18	16.30
12	University-Guthrie Avenue	Granular Subbase	30	15.72

In 2003, Mohammad et. al performed a study on the use of foam recycled asphalt pavement base materials. A test section was established on US Highway 190 in Louisiana to test the potential use of foamed asphalt treated RAP as a base course material in lieu of a crushed lime stone base for continuously reinforced concrete pavement. 3 base type sections , A, B and C, were established. Base A was a crushed limestone base, Base B was a foam asphalt treated base with 100% of RAP materials and Base C was a foam asphalt treated base with 75% of RAP and 25% of crushed concrete. The stiffness results from the test sections can be seen below in Table 13-2. Type B and C bases showed higher stiffness values than the crushed limestone. The difference in

stiffness from 100% RAP to 75% RAP was very small indicating 100% RAP would perform as well as 75%.

Table 13-2. Stiffness Results for 3 Test Sections in Mohammad et. al 2003 Study

Test Section	Base Type	Stiffness (MPa)	Stiffness (MN/m)
A	Crushed Limestone	155.9	17.98
B	Foam Asphalt Treated Base with 100% of RAP Materials	197.8	22.81
C	Foam Asphalt Treated Base with 75% of RAP and 25% of Crushed Concrete	193.4	22.31

Chen et. al performed an evaluation of In-Situ Resilient Modulus Testing Techniques. In this study approximately 100 field stiffness tests on different subgrade and base materials over 6 Texas Districts (Fort Worth, Pharr, Atlanta, Abilene, Austin and El Paso) were conducted. From this testing a ranking of base quality was established in regards to stiffness, as can be seen in Table 13-3. It was also concluded that density and stiffness showed a somewhat poor correlation with stiffness being 10 times more sensitive to the quality of a base than density. Based off of the rankings from this study the RAP bases from Mohammad et. al all are considered good bases.

Table 13-3. Base Rankings in regards to Stiffness from Chen et. al Study

Base Quality	Stiffness (MPa)	Stiffness (MN/m)
Weak	< 87	<10
Good	156-208	18-24
Excellent	>260	>30

13.2 Examination of Stiffness from Project Sites

The Geogauge was used to measure the stiffness of the CIR layer. Projects from 2009 and 2010, including sites in Clinton, Benton, Marshall, Iowa and Delaware 2010 counties, were tested roughly every 3-4 days for stiffness during the curing period. The results can be seen below in Figure 13-1. Stiffness reached a value of 20 MN/m at one point in every project. Stiffness trends were examined further previously in this report under

each project section. The overall trend from the 2009 and 2010 sites suggests that stiffness increased over time, with the maximum stiffness recorded around 30 MN/m. According to the Chen et. al rating system each base was overlaid with a good or excellent rating except for Benton County. The low stiffness values in Benton County could be a result of the frequent rainfalls that occurred during the curing period. The one question the data raised was the exact effect of rainfall on the stiffness. Benton and Marshall County both showed decreases in stiffness after significant rainfalls, however Iowa county showed steady increase despite a heavy rainfall on 8/28. In order to better understand the relationship between stiffness and rainfall it was decided that two more projects be examined and that stiffness measurements be taken every day, rather than 3-4 days, during the curing period.

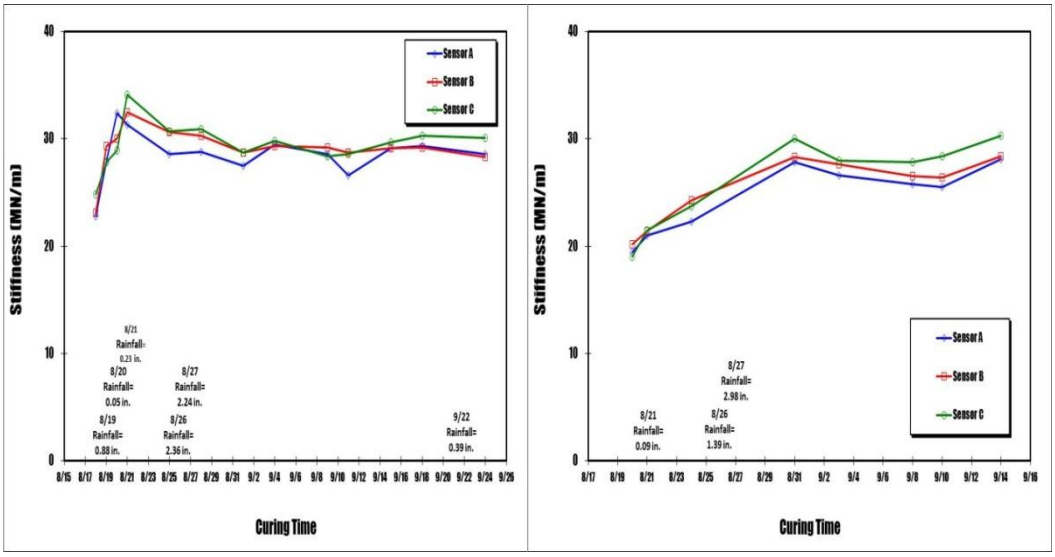

Clinton County *Iowa County*

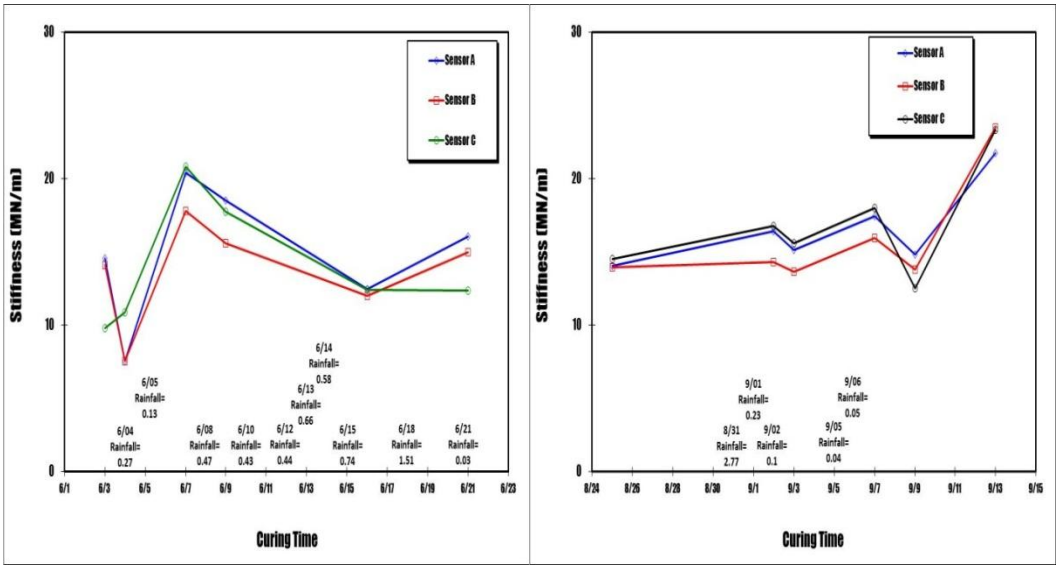

Benton County *Marshall County*

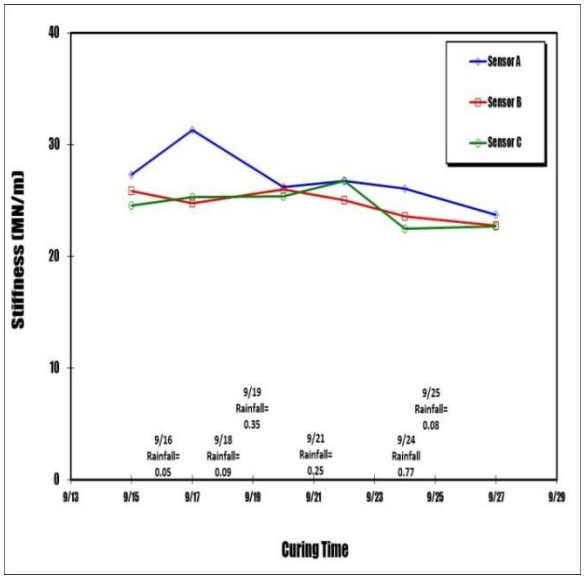

Delaware County

Figure 13-1. Plots of Stiffness Against the Curing Period for 2009 and 2010 Project Sites

In 2011 2 project sites were selected to examine. The projects occurred in Delaware and Black Hawk County. As previously stated, stiffness was measured every day in order to further examine the effect of rainfall on stiffness. The measurements can be seen in Figure 13-2 below. These plots show much more fluctuation than the previous year's mainly due to measurements being taken every day. For Delaware County it can be seen that there were decreases in stiffness around 7/15, 7/22 and 7/28. These dates all come after significant rainfalls. In each instance the stiffness began to recover after a

day or two. Using the ranking previously mentioned from Chen et. al Delaware County always qualified as a good base and reached an excellent qualification at times. Black Hawk County also showed fluctuations in stiffness. There were drops on 7/22, 7/29 and 8/8. Again, these all coincided with significant rainfalls and the stiffness began to rebound after a day or two. For much of the curing period Black Hawk County would be considered an excellent base. From these two project sites it can be concluded that rainfall does indeed have an impact on stiffness. The stiffness begins to increase again after a day or two. This is very important if looking at stiffness as criteria for curing. It is recommended that overlay only occur once the pavement has reached a predetermined value and that rainfall had not occurred within 24 hours of the measurement and that stiffness had shown increase for at least 2 days.

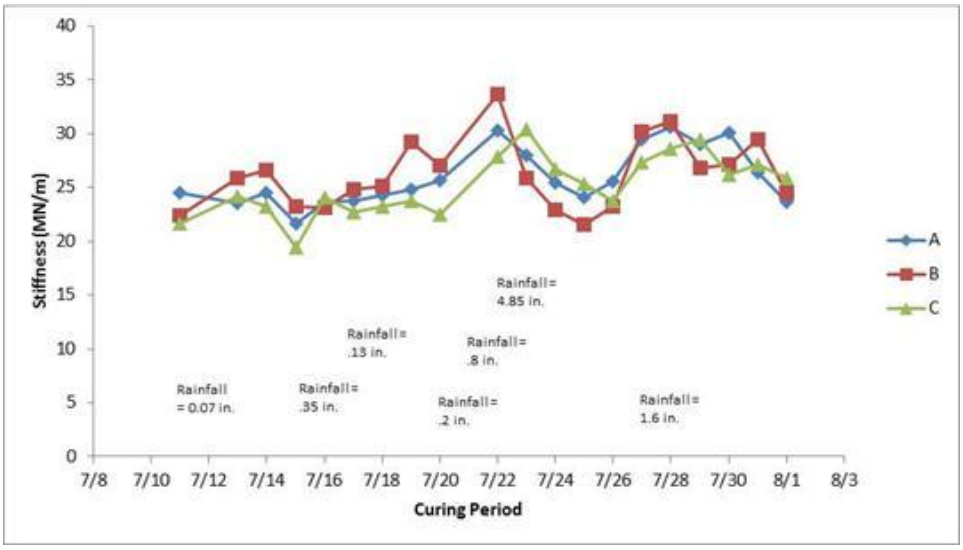

Delaware County 2011

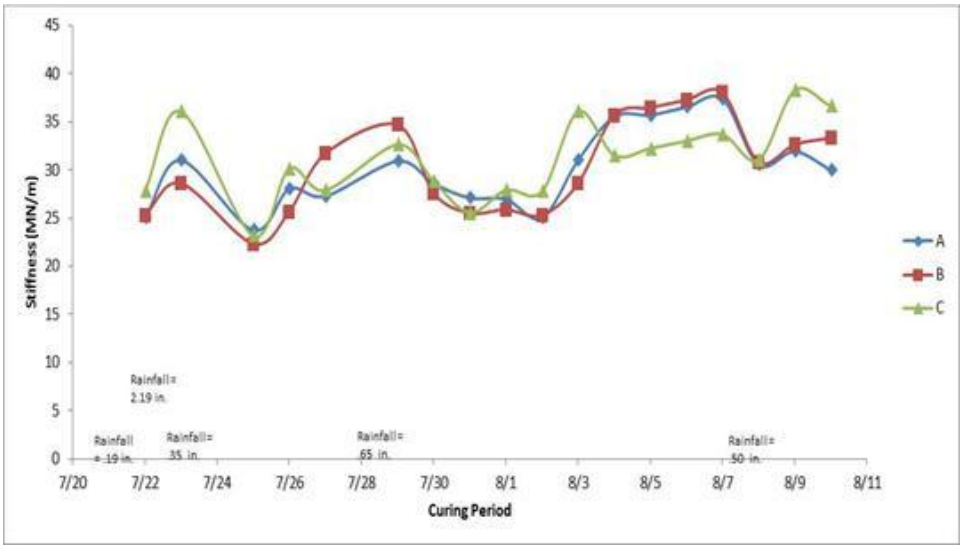

Black Hawk County

Figure 13-2. Plots of Stiffness Against the Curing Period for 2011 Project Sites

14. SUMMARY AND CONCLUSIONS

The current practice in Iowa simply controls the maximum moisture content in the cold in-place recycling (CIR) of 2.0 percent, whereas all CIR projects evaluated in this study, struggling with unfavorable climate, have been overlaid successfully with higher amounts of moisture. To develop a better analysis tool to monitor the CIR layer in preparation for a timely placement of the wearing surface, a set of moisture loss indices were developed based on the field measurements of moisture contents from both CIR-foam and CIR-emulsion construction sites.

Moisture loss indices were developed for each sensor of each site. Next, a single moisture loss index based on the data from the multiple sensors was developed for each site. Lastly, a typical moisture loss index based on all sites was developed for each of CIR-foam and DIR-HFMS-2S emulsion projects.

The moisture sensor was very consistent with the time and amount of rainfall and it is an accurate tool to monitor moisture in CIR layer. The Geo-gauge provided reasonable stiffness values steadily increasing over time. It was found that significant rainfall decreased stiffness. This decrease in stiffness due to rain was not usually instantaneous and it had taken 1-2 days for the CIR layer to reach the minimum stiffness before it began to increase again. The portable TDR device provided inconsistent result without a good correlation with an amount of rainfall and its use was later discarded.

Conclusions

Based on the field experiment the following conclusions are derived.

1. In some cases, the in-situ stiffness kept constant and, in other cases, despite some rainfalls, stiffness of the CIR layers steadily increased during the curing time.

2. The stiffness measured by geo-gauge was affected by a significant amount of rainfall. The stiffness would decrease for around 1-2 days after a significant rainfall before beginning to increase again.

3. The moisture indices developed for CIR-foam sites can be used for predicting moisture level in a typical CIR-foam project. The initial moisture content and the temperature were the most significant factors in predicting the future moisture content in the CIR layer.

4. The stiffness of a CIR layer is an extremely useful tool for contractors to use for timing their HMA overlay.

5. To determine the optimal timing of an HMA overlay, it is recommended that the moisture loss index should be used in conjunction with the stiffness of the CIR layer.

Recommendations/Future Studies

1. The long-term performance of the CIR pavement sections considered for this study should be monitored if the performance would be affected by the moisture condition when the overlay was applied.

2. A more in-depth study should be performed to determine if there is a direct correlation between stiffness and moisture content of the CIR layer.

3. To better understand the curing process of CIR-emulsion, more CIR-emulsion sites should be monitored.

4. To verify the moisture content requirement, the laboratory moisture sensitivity testing should be performed on the specimens with moisture contents below and above the threshold.

5. The effect of temperature on the stiffness gain should be further investigated.

6. The step-by-step implementation guideline of using the moisture loss index in conjunction with the stiffness of the CIR layer should be developed.

REFERENCES

Hanek, G. L., M. A. Truebe, M. A. Kestler. *Evaluation Moisture Sensors and Monitoring Seasonal Moisture Variation in Low-Volume Roads*. CD-ROM. Transportation Research Board of the National Academies, Washington D.C., 2001.

Jiang, Y. J., S. D. Tayabji. *Evaluation of In-Situ Moisture Content at Long-Term Pavement Performance Seasonal Monitoring Program Sites.* CD-ROM. Transportation Research Board of the National Academies, Washington D.C., 1999.

Kim, Y., S. Im, and H. Lee, "Impacts of Curing Time and Moisture Content on Engineering Properties of Cold In-place Recycling Mixtures Using Foamed or Emulsified Asphalt," Journal of Materials in Civil Engineering, Vol. 23, No. 5, ASCE, 2011, pp. 542-553.

Liang, R. Y., K. Al-Akhras, *Field Monitoring of Moisture Variations under Flexible Pavement*. CD-ROM. Transportation Research Board of the National Academies, Washington D.C., 2006.

Lee, S. I., D. G. Zollinger, R. L. Lytton, *Determination of Moisture Content of Soil Layers Using TDR Based on Micromechanics Approach*. CD-ROM. Transportation Research Board of the National Academies, Washington D.C., 2008.

Yu, X., N. Liu, J. Gonzalez, X. B. Yu. *New Instrument and Analysis Method for Accurate Freeze-Thaw Measurement*. CD-ROM. Transportation Research Board of the National Academies, Washington D.C., 2008.